# THE CONTRIBUTION OF SMALL – SCALE WIND AND PHOTOVOLTAIC RENEWABLE ENERGY SOURCES TO THE SCOTTISH ENERGY MIX

AILSA MHAIRI FOWLER

A thesis submitted in partial fulfilment of the requirements of
Robert Gordon University
for the degree of Doctor of Philosophy

April 2011

## ABSTRACT

Energy needs in the UK are currently met primarily through the use of finite resources, such as oil, coal and gas. The use of these fuels has led to an increase in greenhouse gas emissions. There is a need for a more localised and sustainable energy source to meet the demands of our cities. Renewable energy is now being considered as a realistic contributor to both our energy and environmental problems.

The contribution of small – scale distributed power generation from renewable sources to the Scottish energy mix is examined. The daily potential energy available from wind and solar resources will be modelled using spectral techniques such as Wavelets and Fourier analysis. From this, synthetic time series of the energy available will be created based on the characteristics of real life data. Along with this, a simple model for both the electricity and heating energy consumption of a typical domestic building is proposed. This allows for the approximation of daily domestic consumption values from monthly average energy values.

The potential energy available is then compared with the estimated domestic energy consumption. The loads best suited for, and met by PV generating systems and wind systems will also be assessed, along with the proportion of time that the domestic demand is met or exceeded. This work will be backed up with realistic examples from building integrated renewable systems based on typical data for Aberdeen. All this would allow for a potential statistical relationship between energy supply and demand to be developed in the future.

The results of the analysis allowed for the estimation of the potential wind and PV system sizes required to match either the typical summer or winter domestic demand. From these sizes, it was concluded that a combination of a $5m^2$ PV system and a 1.5kW wind turbine was required to match the typical domestic base load. Widespread implementation of these combined systems, on suitable dwellings, could provide a 16% contribution to the Scottish domestic electricity demand.

**ACKNOWLEDGEMENTS**

I would like to thank my academic supervisors Dr Alan Owen, Prof Ian Bryden, Prof Peter Robertson and Bruce Taylor, for their guidance in the completion of this project.

I am also grateful to the Department of Engineering, at Robert Gordon University, who have provided me with the support and facilities needed to produce and complete my thesis.

Finally I would like to thank my family for their unfailing support and assistance throughout the duration of my project.

## TABLE OF CONTENTS

## LIST OF TABLES AND FIGURES

## LIST OF TABLES



## LIST OF FIGURES

## LIST OF SYMBOLS AND ABBREVIATIONS

## LIST OF SYMBOLS

| | |
|---|---|
| A | Building element area ($m^2$) |
| A | Area of photovoltaic array ($m^2$) |
| A | Swept area of wind turbine ($m^2$) |
| $a_0$ | Fourier series coefficient representing the series mean |
| $A_g$ | Area of glazed building component ($m^2$) |
| $a_n$ | Fourier series coefficient – associated with sine terms |
| $A_n$ | Real coefficients of the Fast Fourier Transform |
| $A_N$ | Nth level Wavelet approximation function |
| $a_n$ | Nth level Wavelet approximation coefficients |
| $A_{new}$ | Modelled Wavelet approximation function |
| $A_O$ | Mean annual wind speed (m/s) |
| $b_a$ | Fourier series coefficient – associated with cosine terms |
| $B_n$ | Imaginary coefficient of the Fast Fourier Transform |
| c | Weibull scale parameter |
| C | Wavelet coefficients |
| $C_p$ | Power coefficient |
| D | Day of year |
| d | Temperature rise due to internal heat gains (°C) |
| D(i) | Number of days in month i |
| $D_N$ | Nth level Wavelet detail function |
| $d_n$ | Nth level Wavelet detail coefficients |
| $D_{new}$ | Modelled Wavelet detail function |
| E(t) | Total daily electricity consumption (kWh) |
| $\hat{E}(t)$ | Estimated deterministic component of daily electricity data (kWh) |
| $e_{app}(t)$ | Fourier approximated daily electricity values |
| $E_{ave}(i)$ | Average daily total electricity consumption per month (kWh) |
| ED(t) | Deterministic component of total daily electricity consumption (kWh) |
| $e_m(i)$ | Monthly error values |
| Err | Residual of daily energy consumption data series |
| ES(t) | Stochastic component of total daily electricity consumption (kWh) |
| $E_{solar}$ | Daily energy produced by solar photovoltaic system (kWh) |
| $E_{tot}(i)$ | Total monthly electricity consumption (kWh) |

| | |
|---|---|
| ew(t) | Modelled weekly electricity consumption |
| $F_1$, $F_2$ | Temperature ratios |
| $f_n$ | Significant harmonic frequency value |
| FS(t) | Fourier series approximation for daily wind speed values |
| G | Total solar radiation on tilted surface (kWh/m$^2$) |
| G(t) | Total daily gas consumption values (kWh) |
| $G_d(t)$ | Deterministic component of total daily gas consumption (kWh) |
| $G_s(t)$ | Stochastic component of total daily gas consumption (kWh) |
| H | Average design heat loss coefficient (W/°C) |
| H | Daily global solar radiation (kWh/m$^2$) |
| $H_d$ | Daily diffuse radiation on horizontal surface (kWh/m$^2$) |
| $H_T$ | Total daily radiation on tilted surface (kWh/m$^2$) |
| i | Hour of day |
| i | Month of year |
| $\bar{I}$ | Mean total solar radiation (kW/m$^2$) |
| k | Weibull shape parameter |
| $K_t$ | Daily clearness index |
| $K_T$ | Daily clearness index |
| n | Harmonic number |
| N | Period of series |
| N | Number of air change rates |
| N(t) | Data approximation using interpolation |
| P | Power extracted by wind turbine (W) |
| $P_R$ | Turbine rated power (W) |
| Q | Building heat loss (kW) |
| $Q_g$ | Internal heat gains (W) |
| $Q_{sg}$ | Average solar gain (W) |
| $R_b$ | Ratio of daily radiation on tilted surface to that on horizontal surface |
| $r_k$ | Autocorrelation coefficient, where k = time lag |
| $\bar{S}$ | Mean solar gain factor |
| S(m, t) | Individual year of daily total solar radiation, where m = year |
| S(t) | Total daily solar radiation |
| $S_{AVE}(t)$ | 4 year averaged daily total solar radiation |
| $S_{CORR}(t)$ | Corrected solar radiation on horizontal surface (modelled) |
| $S_d(t)$ | Deterministic component of the total daily solar radiation |
| $S_{day}(t)$ | Daily total global solar radiation (Wh/m$^2$) |

| | |
|---|---|
| $S_{hour}(i, t)$ | Hourly global solar radiation ($Wh/m^2$), where i = hour of day and t = day of year |
| $S_s(t)$ | Stochastic component of the total daily solar radiation |
| t | Time (day of year) |
| $t_{act}$ | Building base temperature based on actual data (°C) |
| $t_{ao}$ | Outdoor air temperature (°C) |
| $t_{app}$ | Building base temperature based on modelled data (°C) |
| $t_b$ | Building base temperature (°C) |
| $t_c$ | Dry resultant temperature (°C) |
| $t_i$ | Average indoor temperature (°C) |
| u | Wind speed value (m/s) |
| U | Thermal transmittance coefficient ($W/m^2K$) |
| U | Wind speed (m/s) |
| $U_{ci}$ | Cut-in wind speed (m/s) |
| $U_{co}$ | Cut-out wind speed (m/s) |
| $U_R$ | Rated wind speed (m/s) |
| V | Volume of building ($m^3$) |
| $W_{AR}$ | Daily wind speed values generated using AR model |
| $W_D$ | Daily averaged (hourly) wind speed (m/s) |
| $W_{daily}$ | Typical hourly wind speed (m/s) |
| $W_{model}$ | Fourier – Wavelet daily wind speed data |
| $W_N$ | Standardised normal wind speed values |
| $W_{new}$ | Non-normalised daily wind speed values |
| x | Original data series |
| $\bar{Y}$ | Mean value of data series |
| y(x) | Transformed data series |
| $\beta$ | Angle of tilted surface |
| $\delta$ | Declination |
| $\varepsilon(t)$ | White noise/Standardised normal variables |
| $\varepsilon_{WN}$ | White noise |
| $\eta$ | Efficiency |
| $\eta$ | Overall efficiency of photovoltaic system |
| $\lambda$ | Box-cox power transformation coefficient |
| $\mu$ | Annual mean value |
| $\mu_A$ | Annual mean wind speed |

| | |
|---|---|
| $\mu_{ES}(t)$ | Annual mean of stochastic electricity consumption data |
| $\mu_m$ | Monthly mean value, where m = month |
| $\mu_m$ | Monthly mean value |
| $\rho$ | Density of air |
| $\rho_g$ | Reflectance |
| $\sigma$ | Annual standard deviation value |
| $\sigma^2$ | Variance (total variance) |
| $\sigma_A$ | Annual wind standard deviation |
| $\sigma_{ES}(t)$ | Annual standard deviation of stochastic electricity consumption data |
| $\sigma_i^2$ | Variance associated with each harmonic frequency |
| $\sigma_m$ | Monthly standard deviation |
| $\sigma_m$ | Monthly standard deviation value |
| $\phi$ | Angle of latitude |
| $\phi$ (n) | Nth order autoregressive co-efficient |
| $\omega_s$ | Sunset hour angle for horizontal surface |
| $\omega_s$' | Sunset hour angle for tilted surface |

## LIST OF ABBREVIATIONS

| | |
|---|---|
| ACF | Autocorrelation function |
| AR | Autoregressive model |
| BRE | Building research establishment |
| CDA | Conditional demand analysis |
| $CO_2$ | Carbon dioxide |
| DWT | Discrete wavelet transform |
| FFT | Fast Fourier transform |
| GDP | Gross domestic product |
| $K_t$ | Daily clearness index |
| kW | Kilowatt ($10^3$) |
| kWh | Kilowatt-hour |

| | |
|---|---|
| MW | Megawatt ($10^6$) |
| MWh | Megawatt-hour |
| PACF | Partial autocorrelation function |
| PDF | Probability distribution function |
| PV | Photovoltaics |
| RLC | Representative load curves |
| S/D | Domestic energy surplus/deficit |
| TAF | Typical annual time function |
| TMY | Typical meteorological year |
| TRY | Test reference year |
| Wp | Watts-peak |

# CHAPTER 1

# INTRODUCTION

Due to the UK's finite hydrocarbon fuel resources and the changing UK political climate, there is a long term need for a more localised and sustainable energy mix to meet the energy demand of our cities. Renewable energy sources are now considered as a realistic and viable option to solving our energy and environmental problems. Investment in these types of energy sources would mean that the UK would be able to produce energy cleanly and locally, reducing our dependence on imported fuel supplies. Out of all the renewable resources, solar power and wind power are currently the most popular alternatives around the world for producing electricity. Over the past 10-15 years there has been growing interest, across Europe, in the use of photovoltaic (PV) panels for the production of electricity in urban environments. Current UK Government policy appears to concentrate on large-scale renewable energy production schemes, which often attract much public concern and frequently fail to achieve planning permission. By encouraging small-scale schemes, the public may feel more inclined to make a contribution to reduce emissions and could eventually contribute a significant amount of electricity into the energy market.

The aim of this project is to assess the possible contribution of small-scale distributed power generation from renewable sources to Scotland's energy mix. This assessment will focus on the contribution of renewable energy systems in the Aberdeen area, and will include the use of PV systems, small-scale wind systems and a combination of the two. Although more efficient solar energy conversion technologies are available, their contribution is not considered in this study for a number of reasons. These technologies produce heat energy which has an annual production profile that is the inverse of the typical heating demand. Based on this, these systems would require an element of energy storage on either a community or individual scale, to cope with the excess or shortfall in energy production over either the day or year. Focussing on renewable systems that can be incorporated with the grid system should provide a greater level of flexibility in utilising the energy produced by an individual system, and should reduce the number of additional elements that would need to sized and installed.

To assess the potential contribution of grid connected renewable systems, the daily potential energy available from wind and solar resources will be compared with the energy consumption of domestic buildings, allowing an estimate of the potential sizes of renewable systems required to match the domestic demand to be found. Using these system sizes, and considering practical

constraints, it will then be possible to assess what proportion of the domestic load of a typical dwelling will be met or exceeded; as well as which end-uses will be most suitable for using this renewable energy and how much additional energy would be required from non-renewable resources. In order to assess this contribution, the work to be carried out as part of this project can be divided into three key areas – wind and solar resource modelling, domestic energy modelling, and an analysis matching energy supply and demand.

As Aberdeen is the focus city of this project, an assessment of the local energy available for conversion by solar and wind systems needs to be made. Although the amount of usable energy available depends on a number of factors including: system size; conversion efficiencies; and rated power, the main variables affecting its magnitude are the wind speed and available solar radiation in Aberdeen. Resource data of this type is not commonly available on a daily basis for many locations. To obtain an accurate estimation of the energy available, this data could be obtained either through a long-term monitoring campaign, which would be time consuming and costly, or from a detailed statistical model. Based on this a number of techniques for modelling the available solar radiation and wind speed for Aberdeen are proposed (Chapter 4). These models will be developed with the aim of producing synthetic time series of the resources data, which are used as an input to assess the potential energy production of the wind and PV systems. Three models are proposed to generate this data, and include the use of time series techniques, Fourier analysis and Wavelet analysis. Each model procedure can be used repeatedly, producing a number of statistically typical years of data.

For an accurate comparison of energy supply and demand, a method for estimating daily energy consumption values will also be proposed (Chapter 5). As this type of data is not usually available on a time scale to match that of the modelled solar radiation or wind speed data, a method for obtaining daily consumption values from monthly mean energy values will be proposed for a typical UK dwelling. The technique outlined will be applied to both the dwelling's electricity and heating consumption, allowing for two sets of energy data to be generated. The modelled electricity consumption data will be used for a direct comparison with the electricity produced by small-scale renewable systems, allowing for the estimation of the system sizes. The modelled heating consumption data will be useful for a number of reasons – it may be possible to match some of this demand, electrically, by either a PV or wind system thus offsetting the amount of conventional energy required; and the available modelled data could also be used for a comparison with technologies more suitable for direct heat generation. As both these proposed energy models will not be dependent on the physical properties of the dwelling, and will only rely on monthly parameters, they should be suitably generalised to be used to obtain an estimate of the daily energy consumption profile for a range of dwelling types

and sizes. The modelling procedure described could also be expanded to estimate the energy consumption of office and commercial buildings.

Comparing both the modelled resource data sets and the modelled energy consumption values, it should now be possible to assess the potential level of load matching that could be obtained using small-scale renewable systems (Chapter 6). This comparison between the energy supply and demand should allow for ideal system sizes to be estimated matching a desired proportion of demand. This ideal system production will then be compared with that of practically installable system sizes. Based on the practical system sizes, it should then be possible to quantify which of the domestic end-uses is best matched to the available renewable energy; how much of the chosen load is matched and for how long, on either an annual or daily basis. This comparison will allow for a detailed assessment of the suitability and energy production of certain small-scale renewable systems for selected buildings and locations. The level of energy matching will be assessed for PV systems and small wind systems individually, and for a combination of both allowing for optimal combined system sizes to be obtained. As some of these proposed renewable systems could be installed directly on urban residences, the electricity generated, but not used at the point of production, could be fed directly into the grid system offsetting the energy that is produced by conventional means.

The analysis of the practical systems energy supply and demand matching will show that only a proportion of the total domestic electricity demand can be met per day, due to the variability in the solar and wind resources, and practical system sizing constraints. The analysis will demonstrate that the load best met by either a PV or small wind system is the constant daily base load attributed to the cold appliances present in the dwelling. Taking this into consideration, an analysis of the individual resources will be carried out to estimate the sizes of systems required to meet this demand. The results of this analysis will demonstrate that a PV array of 5.5m$^2$ is required to match the cold appliance base load, whereas a 6kW wind turbine will be required to match this same constant load over the day. The PV array predominantly will match the cold appliance demand over the summer months, with an average of 60% of this demand being met over the remaining months of the year. Alternatively the 6kW turbine will match the base load over a typical day and over the year will match the load 60% of the time. To provide a better level of load matching, a combined system of a 5m$^2$ array and a 1.5kW turbine will be estimated as the optimal size of renewable system for a typical dwelling. For a domestic installation in Aberdeen, this system is anticipated to produce around 1900kWh of electricity per year, and will potentially result in a combined income and energy saving cost of £755 for the dwelling, if an appropriate feed-in tariff is applied. The energy supply and demand analysis will demonstrate that a combined PV and small wind system will provide a more

constant level of energy matching, and will result in a reduction in sizes of the individual renewable components.

As the modelling procedures described in this project would be generalised and applied to different locations and different dwelling types, the comparison of energy supply and demand would be obtained for a range of property types. Using a breakdown of housing statistics, and average energy availability, it would be possible to assess the total potential contribution of small-scale renewable systems, within a city on a more detailed time basis. This would allow for the feasibility of widespread distributed generation schemes to be estimated. The implementation of such networks would help to alleviate some of the UK's energy security and supply problems, and help to minimise some of the environmental issues associated with conventional hydrocarbon or nuclear energy production. Allowing the building's residents to become 'energy providers', should potentially heighten their awareness in terms of energy consumption, and could aid in the reduction of one of the largest sectors of energy use. The procedures outlined could also be used to encourage the introduction of widespread demand side management schemes, allowing for a better management of the current UK generation resources.

# CHAPTER 2

# RESOURCE MODELLING LITERATURE REVIEW

## 2.1 INTRODUCTION

The majority of energy used in the UK is produced from finite resources such as oil, coal, gas, and nuclear fuels. At current rates of consumption, it is estimated that oil and gas supplies will be exhausted within the next 40 – 60 years [1]. As these fuel sources decline the UK will become increasingly dependent on other countries to supply more of its energy needs and it is estimated that the UK will be importing more than 80% of its oil and gas by 2020 [2]. The continued use of these fossil fuels has led to an increase in the production of greenhouse gases, especially carbon dioxide ($CO_2$). Currently the UK emissions of $CO_2$ contribute about 2% to the global man-made total [3]. Increased emissions of greenhouse gases can contribute to climate change [4]. The effects of global warming require the level of $CO_2$ emissions be greatly lowered, which includes reducing the UK's consumption of fossil fuels. The UK government is aiming to reduce $CO_2$ emissions by about 60% by 2050, with significant progress made by 2020 [2].

Renewable energy sources, such as solar and wind power, are one option to solve our energy and environmental problems. Investments in equipment to harvest these energy sources would allow the UK to produce energy cleanly and locally, reducing our dependence on imported fuels and ensuring a more diverse energy supply. The UK government aims to use renewable sources to generate 10% of electricity supplies by 2010 [2], whilst the Scottish government aims to generate 50% of electricity from renewable sources by 2020 [5]. However, in 2007 renewables only accounted for 5% of the electricity generated in the UK [6]. The proportion of electricity generated from renewables is significantly higher for Scotland, representing 20.2% in 2007 [7]. The UK percentage has doubled since 2003, partly due to an increase in the quantity and installed capacity of wind turbines, which now account for 33% of electricity generated from renewables. At the end of 2008, the total installed capacity of wind turbines was 3287.9MW [8]. This capacity is mainly from large wind turbines and is equivalent to 1.8% of the UK's current electricity supply. Considering that the UK has the largest wind resource in Europe, this is a very small contribution.

Small-scale wind turbines are used for providing power for homes and businesses, usually in remote areas. Recently there has been renewed interest in wind turbines for urban environments,

including building integrated turbines and roof mounted turbines developed by organisations such as ' Renewable Devices' and 'Eclectic'. Small wind turbines cover devices with a rating of less than 50kW [9] and can be subdivided based on power rating for example, micro turbines have ratings less than 3kW. These systems usually have a cut-in wind speed of around 2.5-4m/s, with a rated speed of 10-12m/s [10]. The installed UK capacity of small turbines is about 7.24MW, with the majority in the range of 0 to 10kW [9]. A complete system for a household could cost between £1500, for a micro turbine, and £19,000 depending on if the system is roof mounted or free standing, its application and size. It is estimated that a typical system of around 2.5kW can save about £530 in annual electricity costs, depending on its location [11].

Solar photovoltaics (PV) are an alternative to wind turbines for producing electricity in urban environments. These systems are typically integrated into the building fabric either as a roof-mounted system or as part of the building façade. The installation options would depend on the type of building and the available space. It is estimated that solar PV systems could be installed on about 25 million properties in the UK [12]. Solar PV systems are typically subdivided into two categories – (1) grid connected installations where the system interacts with the local electricity network, and (2) off grid installations where the system is supported by a generator or battery back up. At the end of 2007 there was an installed PV capacity of 3.81kWp, with about 96% of these systems being connected to the grid [13]. Based on the average UK solar energy availability, it is estimated that a typical household system of size 2kWp, covering approximately 16m$^2$ of roof area, would provide about 40% of a household's annual electricity consumption [14], depending on location and choice of PV module, and would cost between £7000-£18,000 [13].

The energy output of a wind turbine depends on a number of factors including the turbine swept area, its performance characteristics and the wind speed at its installation location. The energy output from a PV system is primarily dependent on the available conversion efficiency of the system, and the available solar radiation.

## 2.2 REVIEW OF RESOURCE MODELLING TECHNIQUES

Based on the expression for the power available in the wind, it is the wind speed characteristics that produce the greatest variation in power and energy outputs. To assess whether a location is suitable for the installation of a wind turbine, knowledge about the proposed site's long-term wind speed is required. Ideally this data would be obtained from long-term hourly measurements, which can be costly and time consuming to obtain. Some statistical information

is available for Europe [15] but for most locations the only data available is long-term average wind speed values. Hourly wind speed data is very variable and wind patterns can vary significantly from one year to another. To compensate for this variability and limited available data, it is often proposed that synthetic wind speed sequences be generated for different locations to provide a means for assessing the potential for wind energy production. There has been much discussion about the potential methods that could be used to generate such sequences of wind speed data [16, 17, 18].

For solar photovoltaic systems, the amount of energy available depends on the conversion efficiency of the chosen PV module type, the area of panels, and the amount of solar radiation present at the chosen location. The first two parameters are subject to design considerations and can be considered as fixed, whereas the solar radiation availability is much more variable. To estimate the energy produced by such a PV system, detailed information about the amount of solar radiation is necessary. Most solar data commonly available is in the form of monthly means of global radiation or sunshine hours [19]. Typical long-term monthly diurnal solar radiation profiles are also available for some key cities within the UK [20], however neither of these data forms are suitable for the accurate estimation of the daily energy production, over the year, from solar conversion systems. Long-term solar radiation data on an hourly basis is often very difficult to obtain for some locations. This has led to the development of techniques for generating synthetic sequences of solar radiation data. Due to the strong seasonal and annual variation expected in the solar radiation, theses techniques are not as wide ranging as those used for generating wind speed data.

The techniques used for modelling wind and solar data include the use of probability functions, harmonic analysis, time series models and wavelet analysis. Six main methods have been identified and each will be discussed in turn in the following sections.

- **Probability/Weibull Distribution Function**

The variation in wind speed data is most often described using the Weibull distribution [21]. This distribution function estimates the hourly frequency of different wind speeds over the year based on the average wind speed value and the Weibull shape and scale parameters. This distribution function along with the power curve can provide an estimate of the energy production over the year. However, this method does not provide any information about when during the year each wind speed occurs. This factor is important when assessing the time of year, and duration, that an electricity load can be met by the available wind resource. It is possible to generate a series of hourly or daily wind speed values from the Weibull distribution

by applying the inverse transform method [22]. Again this would require knowledge of the site's long-term values for the shape and scale parameters.

There are a number of issues associated with this technique. Firstly, if the Weibull scale and shape parameters were not known, they would have to be calculated from long-term data. There are a number of methods available for calculating these parameters including the method of moments and the linear least squares regression [23]. Celik [24] conducted a comparison between the estimated energy produced using Weibull distribution functions and actual long-term data. He concluded that on average the Weibull data estimated the energy output very well, with an annual error of 2.79%. The other main issue with generating a Weibull series of wind speed data is that it ignores the correlation between sequential hourly or daily values and does not maintain any underlying structure present in the wind speed data [25,26]. Using the Weibull distribution function directly is useful if you want to estimate the total monthly energy production for a specific turbine [21, 23], and have the available data, but does not allow for a detailed estimation of when consumer loads are best matched.

- **Test Reference Year/Typical Meteorological Year**

To obtain sequences of various types of climatic/meteorological data, methods for generating so-called 'Typical Meteorological Year' (TMY) or 'Test Reference Year's' (TRY) are often implemented. These techniques involve selecting 12 months of data, from a series of long-term measured data, each representing characteristics that are considered as 'typical' of the actual meteorological data for the chosen location. Each chosen month is selected based on its closeness in certain statistical parameters to those of the individual month's actual long-term measured data. For example, some techniques make the selection based on how similar each month's cumulative distribution function is to the long-term data's cumulative distribution function [27]. Each typical year of data generated should maintain the same properties of the long-term data, e.g. the monthly means and standard deviations of the new data should be similar to those of the actual data. This would allow a TMY/TRY to be used in estimating the typical energy production of a solar or wind system.

Numerous methods are available for generating TMY/TRY but they have tended to focus on synthetic sequences of solar radiation and temperature data, rather than on wind speed data [27, 28]. Argiriou et al [27] conducted a comparison of the available methodologies for generating TMY/TRY, to use in the simulation of solar energy systems. Some of the methodologies performed better for solar heating systems than they did for solar photovoltaic systems, though no reasons were proposed in this paper as to why this was so. Therefore, it is better to know

what type of system the data is to be used for before selecting a TMY/TRY methodology. This might ensure a more accurate/representative result.

Regardless of which methodology is used, the generation of a Test Reference Year requires a high level of input data. Miguel and Bilbou [29] recommend that at least 25 years of historical solar radiation data is required to generate a TMY successfully, and that the methodology chosen will depend on whether hourly or daily data is available. The results obtained from the different TMY/TRY methodologies may also vary on location. This level of variability may also affect which methodology is more appropriate for generating a TMY of wind speed data. In terms of energy supply calculations, long-term solar or wind data may not be available for the location chosen by the system designer. A high level of statistical analysis must be carried out on the historical data before the synthetic data series is obtained. This would be very time consuming computationally, and the results are still subjected to some of the variation experienced in some months of the actual data. This may introduce errors in estimating the amount of energy produced by a renewable system.

- **Harmonic Analysis/Fourier Analysis**

For data that exhibits a strong annual or seasonal variation (like solar radiation or wind speed) harmonic or Fourier analysis techniques can be used to generate a time dependent sequence of data. These techniques have been frequently applied to solar radiation [30-35] data to obtain a typical annual sequence of either daily or hourly values. Fourier/Harmonic analysis splits the original data into a number of frequency components representing the important cycles, or predictable variations in the data. Once each frequency component has been obtained, its contribution to the overall variance in the data is assessed to see how many components are required to adequately represent the original data set [30, 31]. The most significant components are recombined using a Fourier series, to calculate the value of solar radiation that is most likely to be present on each day of the year.

Phillips [30] used harmonic analysis on 20 years of hourly solar radiation data and found that the significant information in the data can be represented by 75 Fourier coefficients. Their analysis identified the key components on both an annual and daily basis for three locations in the United States. Balling [31] carried out a similar procedure and found that the annual component was the most important, representing between 92.9 - 99.95% of the total variance in the data. This result depended upon the location of the measured solar radiation data. The advantage of using harmonic analysis techniques is that the known average variability in some meteorological variables can be represented by a small number of parameters. This has been

shown to be the case for a number of other locations around the world [32, 33]. Another advantage of this technique is that it can be used to generate synthetic data series on a time scale specified by the user, for example on either a monthly or daily basis [33]. The technique can be applied to either a full set of historical data to obtain the average long-term annual functions, or it can be applied to each individual year separately. Both methods ensure that a high percentage of the variance is represented by a small number of parameters.

The use of harmonic analysis could be problematic for locations where a long historic range of detailed data is not known. However, it can be applied with some degree of success if only the monthly averages of the solar radiation data are known [34]. Without knowledge of the typical hourly cycles present in the data, it would be difficult to use a Fourier series to generate hourly data. It is in general a simple technique that can provide a good estimate of the variation in the energy provided by solar renewable conversion systems. Better accuracy could be obtained by adding a model capable of estimating the short-term variations in the data [36].

Although there is some underlying periodicity in wind speed data [25, 26], only one study has been found discussing the harmonic content of daily wind speed data [37]. This study used five years of daily wind speeds and examined the harmonic content for four separate months, representing the seasonal variation. The results of the analysis were obtained for ten stations and it was concluded that 90% of the variance could be represented by just seven harmonic components – the most significant being the first component representing the monthly cycle. However, despite these results no effort was made to generalise the results to obtain an annual function for the wind speed variation. This would have been useful as it would have allowed for an estimation of the wind energy at different times of the year as a function of day of the year. There is also no discussion as to whether the same seven components are significant for all months, which could result in a generalised model for wind speed as a function of monthly mean value. As only five years of data were used for the study, consideration should be given as to what the fundamental cycle for the variation in wind speed data is. More data may have provided a better explanation of the fluctuations in the data.

- **Markov Chains**

Markov chains are also commonly used to generate synthetic series of wind speed data [38,39,40]. This process requires actual wind speed data to be divided into a number of states. A transitional probability matrix can then be built for the Markov chain, consisting of the probabilities of the transition of a wind speed from one defined state to another state. For example, at time t, the hourly wind speed can be described as being in state i. From this state

there is a fixed probability $P_{ij}$ that this wind speed will next be in state j. Therefore the present wind speed is only dependent on the previous wind speed state. [22]. The order of Markov chain used in the modelling process gives an indication of the number of previous time steps/states used to determine the present wind speed state, i.e. a 1st order Markov chain for hourly wind speeds only uses the previous hour's wind speed state in its model. This technique implies a form of memory for the data, possibly allowing for part of the wind speed structure to be maintained. Once the transitional matrix has been constructed, the probabilities within it are generated in a two stage process. Initially the cumulative transitional matrix is calculated, and then a uniform random number generator is used to produce a new value which when compared with the cumulative matrix, determines the next state of the wind speed.

One of the key issues when using Markov chains is the size of the transitional probability matrix. This size depends on the number of states that the original wind speed data is divided into (for example if there are 5 different states the matrix size is 5x5, for a 1st order process). Therefore the more states the larger the number of parameters to be estimated. Shamshad et al [38] divided their original data into 1m/s wind speed states producing a 12x12 probability matrix, whereas Sahin and Sen [39] based the sizes of their wind speed states on the mean and standard deviation of the actual data. The number of parameters to be estimated increases if a 2nd order Markov chain is used. Although this procedure can be quite time consuming computationally, it has been demonstrated that it accurately maintains the main statistical properties of the long-term data used to build the model [40]. None of the papers mention whether these parameters are compared on an annual or monthly basis. This would create some doubt as to how well the model maintains the expected annual and seasonal patterns. The modelling process appears to generate suitable wind speed data on an hourly basis, however none of the structure of the data is maintained. Shamshad [38] et al state that both 1st and 2nd order Markov chains fail to match the autocorrelation and the power spectrum of the original data used in developing the transitional matrix. This conclusion seems to be repeated for most other papers demonstrating the use of Markov chains for wind speed modelling. This makes the technique less suitable for generating wind speed sequences for use in processes estimating the time of best energy availability, e.g. matching wind speeds generating potential with electricity demand.

The Markov chain process may be more useful if applied to hourly data after the diurnal and seasonal patterns have been removed. However, this would require knowledge of even more model parameters and would result in a more complex technique. The process may be more suitable for generating daily average wind speed values, as there is less of a deterministic component to be maintained.

- **Time Series Techniques**

In an attempt to maintain the autocorrelation structure of hourly wind speed data, time series techniques have been applied [41-44]. Out of these modelling techniques, autoregressive models (AR) are of particular interest. AR models estimate the present value of a variable based on a summation of sequential previous time values of the same variable plus some white noise, where white noise is defined as a set of uncorrelated random variables with mean of 0 and a finite variance [45]. A generalised nth order AR model is described by equation (2.1) [45]:

$$Z(t) = \phi(1)Z(t-1) + \phi(2)Z(t-2) + \ldots\phi(n)Z(t-n) + \varepsilon(t) \qquad (2.1)$$

Where $\phi(1)$, $\phi(2)$, …, are the autoregressive parameters calculated from the autocorrelation function, and $\varepsilon(t)$ is the white noise. The higher the order of the AR model, the greater the number of previous values required, e.g. an AR(2) model requires two previous wind speed values to estimate the current wind speed value.

To apply time series techniques to any data set, the data must be stationary and have a Gaussian distribution [45]. Therefore, before a model can be fitted to hourly wind speed data a power transformation must first be applied to change the Weibull distribution to a Gaussian one, and the diurnal non-stationarity is removed by converting the data to a standardised normal variable [41,42]. The seasonal non-stationarity is taken into consideration by fitting an AR model for each month of available data, resulting eventually in twelve sets of modelling parameters for just one year of synthetic hourly wind speeds.

Brown et al [41] was one of the first to demonstrate the applicability of such a time series model. However, their input data was limited to one month, which resulted in the development of an AR (2) process. Although their model matched the structure of the original data, no conclusions were stated as to how accurate this model would be for long-term average data. The procedure is accurate but the confidence in their results is low due to the limited data available for model building.

The same procedure was applied to hourly wind speed data covering periods of 12 years to 31 years [44]. This increased the confidence in the model orders and made the model parameters more reliable. Poggi et al [43] used 3-hourly average data as their input and concluded that an AR(2) model was suitable for all months of the year for Corsica. To test the accuracy of their model they compared the models monthly statistical parameters (mean, standard deviation etc.)

with those of their original data. They found a close correlation between the two data sets indicating that the AR models are capable of maintaining the statistical properties of hourly wind speeds as well as the autocorrelation function.

Although wind speed measurements are strongly location dependent, the AR(2) model appears to be consistently used for modelling monthly wind speed data for a number of different locations. However, the parameter values will differ for each location. It is also generally accepted that the use of time series models is an accurate way to simulate hourly wind speed data [42,43].

The main drawback in using these techniques is the number of parameters required. Firstly, for 12 months, there will be 12 sets of AR(2) parameters. Second, to add back in the non-stationarity, the model data produced needs to be multiplied by each day's mean and standard deviation values. Third, the data then needs to be transformed to have a Weibull distribution function. This is a long computational process to go through and requires a significant level of information about the chosen wind site. However, Torres et al [44] state that the daily mean and standard deviation values can also be modelled using periodic functions but they do not state whether this is on a monthly or annual time basis. Either way, using this technique along with time series, will reduce the number of parameters required.

The other main issue involves the power transformation to be applied to the data. There do not appear to be any statements in the studies as to whether one power coefficient is required for the annual data, or if twelve monthly values are needed. This would make a difference to the computational complexity of the data. It is widely accepted that each month of wind speed data has different scale and shape parameter [15] – this factor does not seem to have been included in any of the time series models. The number of power factors required would also impact on the Weibull parameters for each month of wind speed data.

Finally, no discussion, in any of the papers reviewed, is included as to how the random ($1^{st}$) seed value is selected for each model. It might be chosen at random for each month or once a month of data has been generated, the last value simulated may be used as the input to the following month's model, and so on. This is important in case there is any correlation between values at the end and beginning of consecutive months.

It can therefore be concluded that although time series models require significant input data to reliably estimate the model parameters, the techniques are an accurate method for both

simulating and forecasting data. It is also a technique that is simple to run repeatedly, adding further reliability to data generated.

Time series techniques have also been widely used for generating sequences of solar radiation data [46,47]. Much of the work done in this area can be divided into two approaches. The first approach uses time series techniques to model the stochastic, short-term variations in daily solar radiation data, and then adds this to a predetermined trend function. This was demonstrated by Amato et al [46], who analysed 20 years of solar radiation data to obtain a model using a Fourier series and a first order autoregressive process. Although their technique required a significant amount of input data, representing the seasonal trends, in the form of monthly mean and standard deviation values, Fourier series coefficients and autocorrelation coefficients, their output data series appeared to maintain all the key statistical parameters expected in the solar radiation data. They also suggested that some of the input values to their modelling procedure could be generalised for the different locations across Italy. This could remove any possibility of location dependency in their actual modelling procedure.

A similar procedure was demonstrated by Zeroual and Ankirm [36]. Their procedure was based on three years of daily global solar radiation data, allowing for the main trends to be estimated by a Fourier series containing seven harmonic components. After this trend was removed, the remaining data was analysed to assess the applicability of time series models. Based on this analysis, instead of generating the random fluctuations in one step, the data was divided into three 4-monthly sections. Each section was then modelled using three time series models ranging from an AR(1) to an AR(3). This technique was not tested for any other solar data within the same country, so may be very specific to the actual location chosen. However, these papers do demonstrate that only autoregressive models are required to generate the stochastic component in daily solar radiation data.

Time series techniques were also used to directly generate sequences of the daily clearness index, $K_t$. The daily clearness index is defined for horizontal surfaces as the ratio between the global solar radiation on the surface to the global extraterrestrial radiation on the same surface [48]. This variable is often used to reduce the dependence on the location of the chosen solar site on any of the trend components [47]. Knight et al [49] demonstrated this technique for generating hourly solar radiation values. Their procedure can be divided into two steps. The first involved obtaining values of the daily clearness index from a cumulative distribution function. These values were then arranged sequentially to maintain the autocorrelation structure of the solar radiation data. A first order autoregressive model is then used to obtain hourly solar radiation data.

- **Wavelet Analysis**

Wavelet techniques have also recently been used for generating random data series [50,51,52]. This technique, is similar to that of harmonic analysis, in that it is used to break down a time series into a number of standard wave functions e.g. the Haar or Debauchies wavelet, that can then be randomised in such a way that, when recombined, a new data series is formed.

Wavelet analysis is generally a technique used for examining both the time and frequency content of a signal or data series. The discrete wavelet transform is used to decompose a signal into a number of components that can be reconstructed back into the original signal. The signal decomposition is carried out in two steps. Firstly, the signal/data series is passed through a number of high pass and low pass filters producing 'Approximation Functions', i.e. high scale or low frequency components, and 'Detail Functions' i.e. low scale or high frequency components, where 'scale' is calculated as the inverse of the frequency. The filter outputs are then sub-sampled by removing every other sample. This process is carried out repeatedly on the outputs of each of these low pass filters until there is a single sample left. More simply, the approximations are equivalent to taking the averages of the input data, and the detail functions are the equivalent to the differences between the original data and the approximations. For wavelet analysis to be applied the data set in question must satisfy two criteria. The first is that the data must have a normal distribution function, and the second is that the data series length must equal $2^N$, where N is a positive integer [53]

Aksoy et al [52] used the wavelet technique to generate new time series of hourly wind speed data. Their techniques can be summarised by a number of steps. Firstly, a power transformation was applied to the data to ensure that it had a normal distribution. This new data was then decomposed to obtain the approximation and detail functions. The approximation and detail functions were then re-ordered, in pairs, to maintain the hourly persistence in the original data – this produced new approximation and detail functions. These new functions were recombined using wavelet techniques to obtain a new time series of data that when the inverse power transformation was applied represented a new series of hourly wind speed data. The technique is relatively straightforward and produced data that was statistically representative of the original data series used. However, no analysis was carried out on the new data in terms of frequency analysis to ensure that the actual structure of the wind speed data was maintained. The paper does not describe a modelling procedure as such; instead it allows the original data to be randomised to produce many outputs that could represent actual long-term hourly wind speed data. For the technique to be applicable a large number of years of historical wind speed data (or climate data) must be available as an input.

Other issues that should be considered involve the power transformation discussed in the paper. The method selected to normalise the wind speed data, along with the randomisation process, could lead to the generation of negative wind speed values. This is not something discussed in the paper. Also as stated earlier the data must be normally distributed, therefore the use of the power transformation is dependent upon the location and time scale of the data used. For example, if the data was transformed as one year only one power coefficient would be required. However, if the data was treated on a monthly basis a number of different coefficients would be required. Therefore the model is not completely non-parametric. It also adds to the level of computation involved. The accuracy of the results could also be affected by the choice of wavelet base used to decompose and reconstruct the data. Aksoy et al [52] demonstrated the process using the Haar wavelet, but a different shape might better resemble the short-term fluctuations in the data. Finally the data series must be of the correct length, $2^N$, for perfect decomposition. This limits the applicability of the process, as it would not be simple to use for exactly one year's hourly wind speed values.

# CHAPTER 3

# ENERGY MODELLING LITERATURE REVIEW

## 3.1 INTRODUCTION

The analysis of energy consumption within buildings is focussed on the domestic and commercial sectors. The total amount of energy used within these areas has increased over the past number of years. Total domestic energy use has increased partly due to the higher proportion of people living on their own and partly due to increased levels of income, producing an increase in appliances [1]. However, the domestic energy consumption per household has remained relatively constant since the 90's. Although the efficiency of appliances has increased [2], the number of appliances in both the domestic and commercial sectors has increased. This has had a greater impact on the energy consumption in the commercial sector. However, in the commercial sector, the main reason for the increase in consumption is the increase in floor space, resulting in an increase in air conditioning, lighting and IT energy consumption.

Domestic sector energy is defined as the energy used in dwellings and accounted for 27.5% of final energy consumption in 2008 [3]. By 2001 more than 80% of UK households had gas central heating [4] and 85% of households heated their hot water using their central heating system. Assuming that every household uses electricity, the energy consumption in the domestic sector can be subdivided into heating or gas consumption, and electricity consumption. A breakdown of household energy use is shown in Figure 3.1. This implies that gas consumption accounts for about 82% of the overall domestic energy consumption.

Domestic electricity consumption has increased by 50% in the last 30 years due to an increase in the number of households and the number of household appliances, and a 63% increase in lighting load [2]. The increase in Scotland could also be attributed to the high proportion of flats using electricity for heating [2]. On average a UK household consumes approximately 22MWh of energy per year in total [5].

Out of all dwellings with gas central heating the average gas consumption per year is about 19800kWh. The average electricity consumption of all households is around 5300kWh per year [5]. The combined total domestic consumption for Scottish dwellings is higher than the UK average due to a longer heating period, and the dwellings typically having a lower standard of insulation [6]. Whilst annual total electricity consumption is relatively constant for different sizes and type of dwellings, gas (heating) consumption is more variable. The heating

consumption requirement of a building depends upon a number of variables including the physical construction of the building, the age, type and size of the dwelling, the external temperatures, the useful heat gains and occupancy periods, the geographical location, and the available funds of the occupants [7]. The actual amount of fuel consumed within a dwelling depends upon the heat losses of the dwelling and on the efficiency of the heating system or boiler. There is also a difference in demand during the week – with weekday consumption typically being lower than that of the weekend.

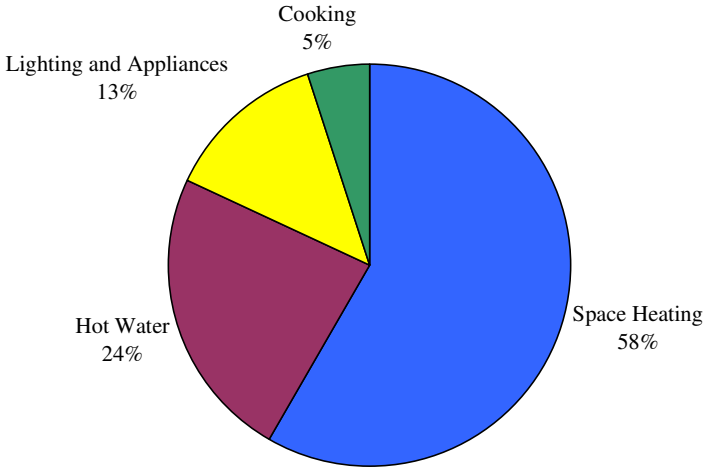


Figure 3.1: Breakdown of Domestic Energy Consumption by End-use [2]

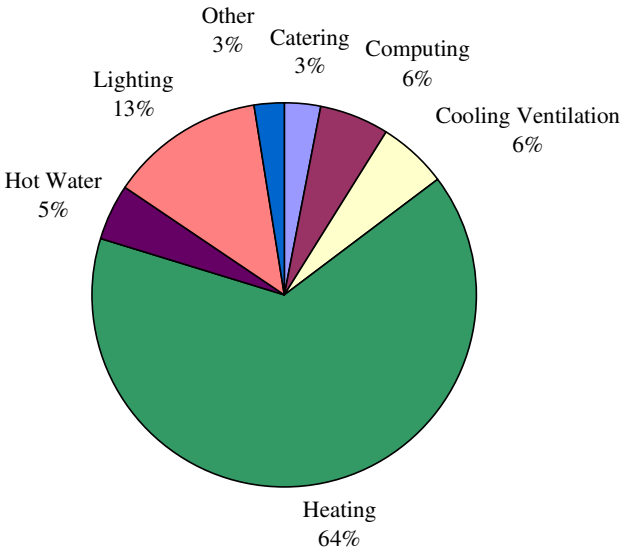


Figure 3.2: Breakdown of Commercial Energy Consumption by End-use

In the commercial sector energy consumption has increased by more than 65% since 1973 [8]. Energy consumption in the commercial sector will be examined mainly as the consumption within offices as they offer the greatest opportunity for energy savings. The energy use within offices has increased not just because of changes in floor area but also due to the increase in energy intensive appliances such as IT equipment, air-conditioning and lighting. A percentage breakdown of office end use energy consumption is shown in Figure 3.2. Again the space heating and hot water load consumptions are the most significant. Office energy consumption can be subdivided into four office types, depending upon their combination of size, construction and whether they are naturally ventilated or use air conditioning [9]. Based on measured data, the typical annual energy consumption for these four office types ranges from 205kWh/$m^2$ to 560kWh/$m^2$ of treated floor area. The overall electricity consumption per square metre increases significantly as the floor area of the office increases, but the heating and hot water consumption is still the largest single end use [9].

## 3.2 REVIEW OF ENERGY MODELLING TECHNIQUES

To assess the potential energy contribution of small-scale renewable systems for buildings, detailed information on the actual energy consumption within domestic and commercial buildings is required. For the domestic sector, most of the available energy data is in the form of annual totals of gas and electricity consumption by region in the UK [10]. Some more detailed information may be available from actual utility bills, but this may be only available quarterly or monthly. For a detailed comparison between energy supply and demand, a higher resolution of energy consumption data is required. Initially data on a daily basis would be useful in terms of estimating the annual proportion of domestic load that can be bet by either solar or wind energy systems. This would provide details on the long term potential of such small-scale renewable systems, and would provide an estimate of the level of energy savings achievable. Ideally the energy consumption data should be available on a hourly basis as this would provide an estimate of the best size of renewable system required, and the individual domestic loads that could potentially be met. To obtain this level of detail, the energy consumption of domestic buildings would have to be obtained using metering equipment. This process can be very costly and the data would not be available for analysis for some time after the installation of the metering equipment (i.e. 6 months – 1 year). Another consideration for the metering of energy consumption data is whether the total energy consumption is sufficient, or if detailed information about specific end uses is required. Although the National Grid publishes detailed electricity data [11], this data relates to the total electricity demand for the UK/England and Wales, and is not subdivided by sector (i.e. domestic, commercial, industry etc).

Due to the limited data available, numerous techniques have been proposed for either modelling or forecasting the energy consumption within buildings for both electric and gas end-uses. Energy modelling techniques are useful for the planning of new power generation and transmission systems [12], and give an assessment of the potential consumption costs. These same factors can be considered on a smaller scale, to assess if small distributed renewable energy systems can help to solve some of the UK's energy supply issues, and if they are cost-effective in terms of energy production.

The techniques used for modelling or forecasting energy demand depend on the level of detail required in the demand data. Some techniques focus on the short-term, requiring data on an hourly basis, generally in the form of a 'typical' load profile. Other techniques focus on a longer time basis, from months to years, and try to estimate the underlying trends in the electricity and gas data. Both approaches are valid, but consideration must be made in relation to the resource data availability, and the level of energy matching required.

Numerous studies have tried to estimate the monthly total energy demand using weather variables or economic factors, or a combination of both [13,14,15]. Hor et al [13] used multiple regression techniques to establish a mathematical relationship between total monthly electricity demand in England and Wales and a number of weather variables. These variables included average monthly temperature, heating degree-days, cooling degree-days, enthalpy latent days (relating humidity to air conditioning loads), rainfall and humidity. Out of these, temperature appeared to have the greatest affect on electricity demand. This was attributed to the use of electricity for heating and air conditioning systems. As most domestic residences in the UK do not use electric heating, or possess a/c systems, the importance of this result may be lessened when trying to estimate domestic electricity demand. The same assumption could be made regarding the importance of heating degree-days, cooling degree-days and enthalpy latent days. The authors also tried to incorporate some social- economic factors into their models, including the gross domestic product (GDP), and population. Overall they found that their modelled results matched very well with actual electricity demand.

A similar process was carried out by Ranjan and Jain [14] on electricity consumption data in Delhi. However, due to the annual variation in the electricity consumption data, they developed four regression models – one for each season of the year. They focused their analysis on weather variables, including temperature, sunshine hours, rainfall and humidity, as well as population. Out of the four models developed, they found that over the winter and summer periods, 97 – 99% of the variation in electricity consumption could be explained by temperature

and population variables. The models for the remaining two seasons were more variable, incorporating the remaining three weather factors mentioned.

Multiple linear regression was also used on both electricity and gas consumption data in the USA [15]. Again, weather variables were used for predicting the total residential and commercial energy consumption for eight states. In terms of electricity consumption, they developed two regression models, one for the summer and one for winter whose input variables were combinations of temperature, wind speed and humidity. The relative significance of each of these variables could be due to the difference in end-uses, in particular a higher use of air conditioning systems in the USA. As expected, the model developed for gas consumption was based on temperature.

Multiple linear regression is a straight forward technique for modelling energy demand, in particular electricity consumption. All of the models described require a large number of independent variables in order to construct the mathematical model for electricity demand/consumption. This level of input data required may not be available for all locations, or on the required time scale. The models have tended to focus on large regions or countries in terms of energy demand and have not made any statement as to the applicability of their models for more specific locations within the regions/countries. Due to the limited relationship between weather and energy demand care should be taken to ensure that all the data used to build the model are available over the same time range and scale. The models using social or economic input variables tend to use nationwide/state-wide average parameters, limiting their applicability for different locations.

Due to the generalisation of the data in terms of total energy/electricity consumption, it is difficult to assess whether such models are actually applicable for modelling domestic energy consumption at the individual level. Their applicability will also be affected by the specific end-use differences between commercial and domestic buildings. Most of the models using linear regression techniques use a monthly time scale for their data. However, no information is readily available in the papers reviewed as to whether these models could be used on a daily or even hourly basis if the input data were readily available. This could be due to the averaging of the data on a monthly basis smoothing out the fluctuations in the actual energy consumption data, and on the selected weather variables.

A number of studies have been carried out to assess the potential of energy models primarily based on variations in daily or hourly temperature [16-18]. Valor et al [16] focused on the strength of the relationship between daily temperature values and total daily electricity demand.

Due to the variation in the data, and the typical electricity end uses in Spain, they were able to characterise their electricity consumption in terms of heating and cooling degree-days.

Similar to this analysis, Magnano and Boland [17] used temperature data to generate synthetic time series of total electricity consumption on a half-hourly basis. Their analysis of three years of electricity consumption data, and temperature data, enabled them to develop a two-stage model. Firstly the annual, weekly, and daily cycles were estimated using a Fourier series model. This explained the key underlying trends in the electricity consumptions. The second stage of the model involved two steps – the first used a model of temperature data to explain some of the additional variation in the data, and the second step used time series techniques to explain the random effects left in the electricity data. Dhar, Claridge et al [18] also investigated the use of a temperature based Fourier series to model the electricity consumption in commercial buildings.

The key advantage of these models is the availability of location specific data, as temperature data is generally measured for most large cities on some time scale. The other main advantage is that they allow the generation of consumption data that can represent any significant changes in climate, e.g. a particularly warm or cold season. This is very practical from a planning perspective ensuring an adequate match between electricity supply and demand. The main disadvantage of these models relates to how each country/location uses its electricity. For example, both these previous studies represent hot temperature climates that probably use significant amounts of electricity for air-conditioning. Although there is a strong relationship between temperature and total electricity in the UK this relationship has not been demonstrated as significant on a sector-by-sector basis. This may reduce the applicability of these modelling procedures for the estimation of domestic electricity consumption.

A more detailed alternative statistical regression technique for modelling energy consumption is conditional demand analysis (CDA). This technique focuses on estimating the energy consumption of specific end uses in the domestic sector. CDA is also a regression technique but uses economic variables and household characteristics as the independent variables. The main variable of interest is whether each household under consideration contains a certain appliance/end use [19]. To be able to estimate the actual consumption of each end use, detailed information on appliance ownership statistics and monthly energy consumption totals are required to build the CDA model. Other variables of interest when calculating the regression equations are weather data. However, this will depend on whether the electricity consumption at the chosen site/location is weather dependent. These weather variables may be little or no use in calculating the UK domestic electricity end uses. If monthly, average or total end use consumption is to be estimated, this technique (CDA) would require the development of

monthly regression equations i.e. twelve equations for one year. A shorter energy estimation time scale would result in the development of more equations.

There are a number of advantages to using CDA to estimate domestic energy consumption. Firstly, the technique can be applied to dwellings/households in any location, provided that appropriate information is available on appliance ownership etc. Secondly, if an energy production system (small-scale renewable) is to be installed to match a certain proportion of the domestic load, CDA allows detailed information on each end use without the need for sub-system metering.

The main disadvantages of this technique relate primarily to the availability of the data required to generate the regression equations. Also, to provide detailed energy consumption data, on a daily basis, a significant number of parameters and equations would be required, making the techniques both time consuming and mathematically complex.

On a shorter, hourly time scale, a number of bottom-up models have been developed to generate domestic load profiles [20,21]. These load profiles give a description of how the magnitude of the domestic electricity load varies over a 24-hour period, and of the diurnal variation in specific appliance end uses. Ideally these techniques will provide a description of the energy consumption per household that can then be used to build up a picture of the regional or countrywide energy consumption.

Capasso et al [20] developed such a model using information on the socio-economic and demographic variables affecting energy consumption in Italy. These variables were described using probability functions. As well as information on population statistics, occupancy patterns and appliance ownership data, the model also required detailed technical data about common domestic appliances, including their operation cycles and power consumption in order to obtain an accurate load profile. No consideration seems to be given for the age of the domestic appliances in relation to their power consumption. The technique could only be applied for a typical household within a known country or region, based on the statistical inputs. As such, it may prove less than accurate for detailed load matching at specific sites. Also, the generation of load profiles may be limited to producing either a typical seasonal profile or a weekend/weekday profile. This may prove limiting in estimating what proportion of annual variation in electricity consumption can be met by a renewable energy producing system.

Yao and Steemers [21] developed a methodology for simulating both electricity and heating consumption load profiles for the UK. They developed five load profiles for both consumption

profiles based on five occupancy patterns. The load profiles could also be subdivided by dwelling type. Each of these profiles was then combined and averaged to obtain a typical load profile of electricity and heating consumption. To generate the load profiles of electricity, detailed data about the appliance ratings and usage patterns, and statistical information about the ownership of appliances were required. These were obtained from national averages for the UK. Random profiles for each appliance were generated and summed to give the load profiles matching each occupancy patterns. This method will generate profiles for a typical dwelling type, and will not allow for any variation due to location – e.g. temperature difference between Scotland and England.

To allow for some of the seasonal variation in electricity demand, Balachandra et al [22] developed the technique of representative load curves (RLC). Representative load curves are typical load profiles based on groups (of data) with similar load curves. The technique was based on the measured total electricity demand for Bangalore, India and grouped the daily load curves into nine key categories representing the summer, winter and monsoon seasons. The only key difference in the nine load profiles is the magnitude of the electricity load at any time. Some caution should be taken with the results produced as only one year of energy data was used to obtain the RLC's. Although the authors now have typical load curves to help with the planning of new potential energy/power generation sources, the curves provided do not distinguish between the weekend and the weekdays variation. This variation is very important when considering the energy consumption within buildings. Each load curve follows the same basic shape. The paper also does not try to equate the load curves in a series of representative equations. Therefore the paper is more a description of data analysis than a full modelling technique.

Riddell and Manson [23] quantified domestic electricity load profiles in New Zealand using a nine parameter Fourier series approximation. The results obtained were compared with those of time series and polynomial techniques, and were found to give a better approximation to actual load data. The authors also found that the magnitudes of the Fourier coefficients indicated whether the peak consumption occurred predominately during the day or night. They also attempted to generalise their technique by normalising all the Fourier series coefficients by the mean coefficient, or total daily power consumption. This enabled them to scale their values up for an increase in the number of households.

Although they used nine parameters, the procedure outlined is very simple and would allow estimation of the hourly electricity consumption based on information about the estimated daily total load. As the daily load varies seasonally, this would ensure some variation in the

magnitude of hourly electricity data. They do not make any distinction between different load profiles for different day-types (e.g. weekend or weekdays), or for any seasonal variation. However, they estimate that occupants in the same close location are more likely to have similar load profiles making their technique very applicable for energy matching on a community scale.

The Building Research Establishment (BRE) [24] developed a model for calculating the energy demand of a domestic building on an annual basis. The main focus of their model is estimating the dwelling's demand for space heating and hot water. It is referred to as an engineering/technical model as it requires a high level of knowledge about the dwelling, its local environment and the behaviour of the occupants. The input data required is based on these three categories and includes specific information on the physical description of the dwelling and its heating system (e.g. U-values), the outdoor temperature, or degree-days and the amount of solar radiation at its location and the buildings heating patterns. Based on this level of input data, the estimated energy demand should be very accurate for the dwelling in question. The advantage of the BRE's model is that the procedure is very generic allowing it to be used for any type of domestic building and any location. The main disadvantage of this model, and other engineering/technically-based models is the high level of detailed input data required. Also the model is primarily used for estimating/calculating the annual heating demand. This would prevent it from being used directly for the comparison or matching of energy demand and supply on a daily basis. However, the technique may be generalised/modified to allow for an estimation of the energy consumption on a monthly basis.

Larsen and Nesbakken [25] assessed the potential of using the Norwegian engineering model ERAD, for estimating the domestic load for a number of end-uses including space heating. Again this model requires a significant amount of information about the physical construction of the house and any other variables that might have an impact on the total energy demand, e.g. temperature, occupancy, efficiency of equipment etc. Some of this input data may also be difficult to obtain.

Although the key techniques identified for modelling energy consumption cover a wide range of techniques and timescales, they all exhibit the same drawback over the level of model information required. To produce a detailed estimation of energy demand, each of the techniques summarised require a significant number of input parameters including, but not limited to, details of the physical characteristics of the dwelling and its local climate, the dwellings occupancy patterns, and information on the number of appliances and their operation.

Even though the focus of this work is on developing a technique for modelling the energy consumption in domestic buildings, many of the techniques summarised could be applied to commercial or office buildings.

# CHAPTER 4

# RESOURCE MODELLNG

## 4.1 INTRODUCTION

In order to design a solar energy system and assess its potential contribution to energy consumption, it is necessary to have knowledge of the amount of solar radiation available at the chosen location. As the energy output depends most significantly on the solar radiation, the input variable to be modelled must be the daily solar radiation available in Aberdeen. The modelling procedure described allows the average total daily solar radiation on a horizontal surface to be estimated.

To make an assessment of the potential power production of a wind system, it is important to have detailed, accurate information about the wind speed profile at the chosen location. Although the power produced depends on the swept area of the turbine, the only generalised input data required is the wind speed – the area will depend on the selected specific turbine. Therefore to obtain a generalised method of estimating the wind energy available a model of the daily wind speed must be developed.

This chapter will consider the requirements for building solar and wind resource models in turn. The data used in the development of these models will be analysed to obtain daily and monthly average values of solar radiation and wind speed; identifying any trends in the data over these time scales using visual inspection; Fourier analysis; and the use of autocorrelation. The distribution and statistical parameters of the wind and solar data will also be analysed.

## 4.2 SOLAR ENERGY DATA ANALYSIS

The first data set considered is comprised of four years of hourly global horizontal solar radiation for the chosen location of Aberdeen. The data set was provided by an academic organisation with a proven track record in the analysis of solar energy, and covers the period from 1$^{st}$ January 1975 to 31$^{st}$ December 1978 [1].

To allow for a direct comparison between the available solar energy and the daily domestic energy consumption, the hourly solar data must be converted to daily solar radiation. The hourly values were summed for each day using the expression:

$$S_{\text{day}}(t) = \sum_{i=1}^{24} S_{\text{hour}}(i,\ t) \tag{4.1}$$

where $S_{day}(t)$ is the daily total global radiation ($Wh/m^2$), $S_{hour}(i,t)$ is the hourly global radiation, i is the hour and t is the day of the year.

The total daily radiation for all four years was plotted against time, and is shown in Figure 4.1. This figure shows that there is a clear annual cycle, showing that the available solar energy is higher during the summer months. There are also time varying fluctuations about this annual cycle. The annual variation results from the position of the sun relative to the earth, which is dependent upon the movement of the earth around the sun and the rotation of the earth about it's own axis [2]. The daily fluctuations are due to the local atmospheric conditions and the amount of cloud cover.

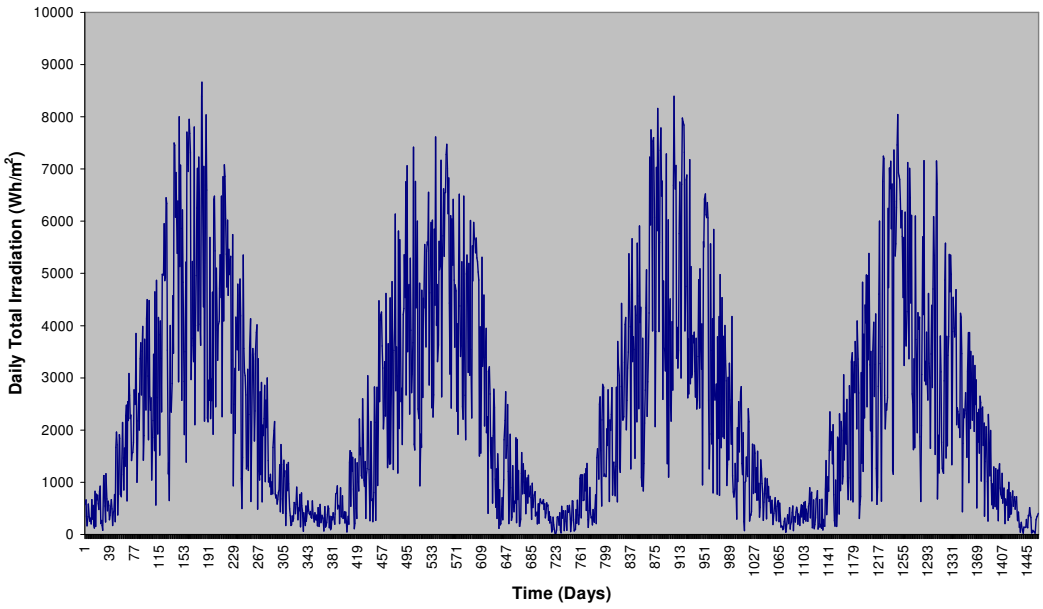


Figure 4.1: Four Years of Variation in Global Solar Radiation for Aberdeen

A Fourier Transform was used to identify the cyclic content of the hourly and daily irradiation data by splitting a periodic time series into its harmonic components. Each component is

represented by an amplitude and cosine waveforms at differing frequencies. When these harmonic components are added together, they form a Fourier series of the form:

$$y(t) = a_0 + \sum \left[ a_n \cos \frac{2\pi n t}{N} + b_n \sin \frac{2\pi n t}{N} \right] \tag{4.2}$$

Where $a_0$ is the overall mean of the data series, n is the harmonic number, t is time, N is the period or number of data points in the time series i.e. N =365, and $a_n$ and $b_n$ are the Fourier coefficients of the form:

$$a_n = \frac{2}{N} \int_{-N/2}^{N/2} y(t) \cos \frac{2\pi n t}{N} \tag{4.3a}$$

$$b_n = \frac{2}{N} \int_{-N/2}^{N/2} y(t) \sin \frac{2\pi n t}{N} \tag{4.3b}$$

Estimates of these Fourier coefficients are obtained by using the Fast Fourier Transform (FFT) to calculate the real and imaginary parts of the Fourier transform. The number of pairs of coefficients is determined as half the length of the data set. For example, for a year of daily data there will be 182 pairs of coefficients. The FFT of the solar radiation produces two vectors of data – $A_n$, the real coefficients, and $B_n$ the imaginary coefficients. In order to use these values in the Fourier series, each value should be multiplied by two. Therefore, the Fourier Series in terms of the FFT coefficients would be expressed as:

$$y(t) = 2 \sum \left[ A_n \cos \frac{2\pi n t}{N} + B_n \sin \frac{2\pi n t}{N} \right] \tag{4.4}$$

The value of the average component from the FFT can be used directly [3,4].

The FFT was taken for a combination of the four years of hourly irradiation data. The results of this are in Figure 4.2, which shows that other than the annual average values, there are four easily identifiable peaks at certain frequencies. These frequencies correspond to a yearly cycle of 365.25 days – the same time period as one solar year, and cycles of 1, 2 and 3 cycles/day –

accounting for the diurnal variation in the solar radiation. These cycles are also present in each individual year of hourly data. The magnitudes of the frequencies greater than 2000cycles/year are not shown in Figure 4.2 as their contribution is considered insignificant in comparison to those up to 2000cycles/year.

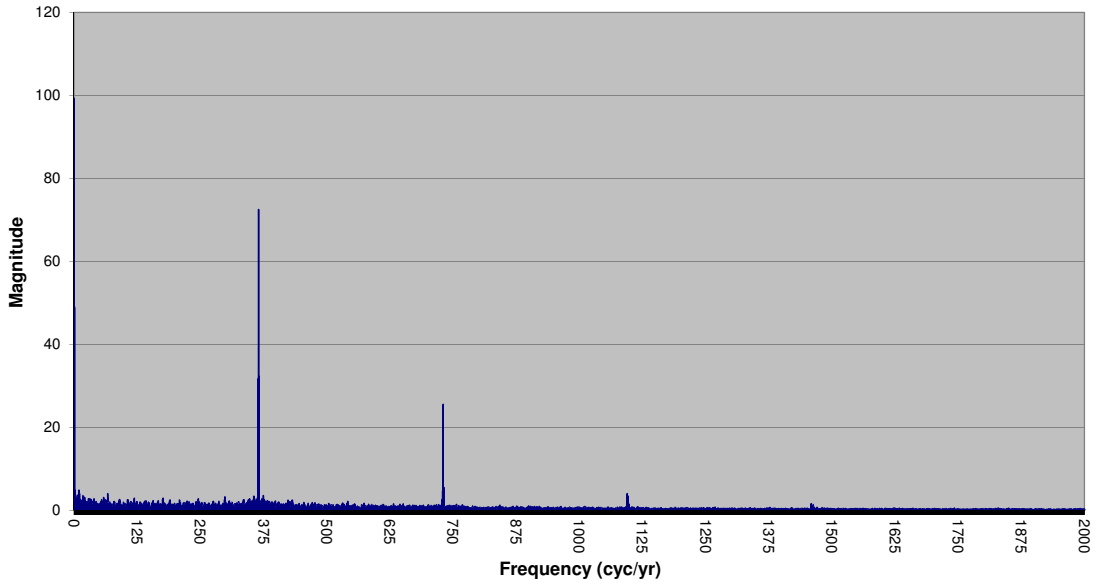


Figure 4.2: FFT Of Four Years of Hourly Global Radiation Data for Aberdeen

The FFT was also used to analyse the harmonic content of the daily data, as shown individually for each year in Figure 4.3. The results for the series of four years of data shows that there is only one cycle clearly present - this is the annual cycle, and this was to be expected due to the conversion in the data being analysed from hourly to daily. Based on this result, the harmonic content can only be used to estimate the daily total radiation. To estimate the diurnal variation, the contents of the hourly FFT would be required. Figure 4.1 also indicated a strong annual cycle.

The actual amount of available solar radiation depends on location, the time of year, and on the local weather conditions and cloud cover. When using the data to design a PV system the use of solar radiation data averaged over a period of time will provide a more accurate and reliable estimate of the performance of the system. Therefore, the four years of daily data will be averaged, by summing each year's daily values and dividing by the number of years, to obtain a typical year of solar radiation data that can then be used as an input for the PV system analysis.

## 4.3 SOLAR ENERGY MODELLING

From the analysis of the solar radiation data, as demonstrated in Figure 4.1, it can be seen that the daily data is made up from a trend component and a random or stochastic component such that:

$$S(t) = S_d(t) + S_s(t) \tag{4.5}$$

where S(t) is the total daily solar radiation on a horizontal surface, t is the day of the year, $S_d(t)$ is the trend or deterministic component, and $S_s(t)$ is the stochastic component of the solar data. Therefore the solar radiation data can be modelled in two steps.

It is widely accepted that the deterministic part of the solar radiation data is strongly periodic and can be modelled using the Fourier series [5,6,7], and the Fourier Transform.

The FFT was calculated for each year of daily radiation data to find estimates for the coefficients required for a Fourier series approximation of the data. The results for all years of data are shown in Figure 4.3. From this it can be seen that there is only one significant peak at a frequency of 1 cycle/year. This is the fundamental frequency contained within the daily solar data. The remaining cycles, greater than 40 cycles/year are very small in comparison to these clear peaks and are therefore considered to be less significant to the overall data. Figure 4.3 also shows that this frequency is the most important frequency for all the years of data analysed.

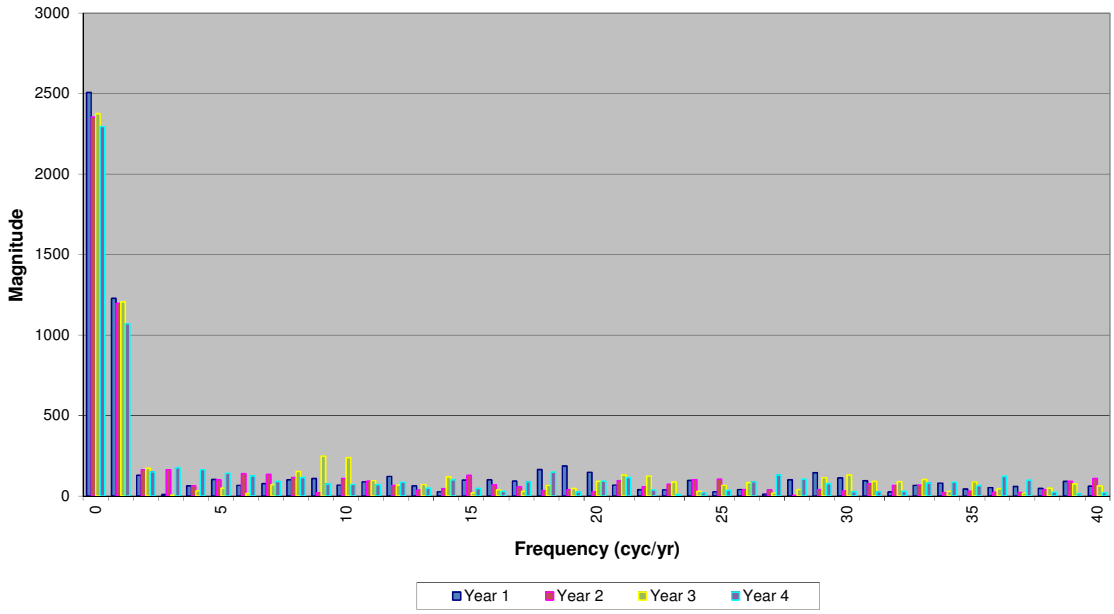


Figure 4.3: FFT of All Years of Daily Solar Radiation Data

The significance of these cycles/frequencies is found by calculating their individual contributions to the overall variance of the data. For each harmonic frequency, its significance can be found from the squares of its amplitudes $a_n$, and $b_n$. The total variance is found by summing these contributions and dividing by two [4] i.e:

$$\sigma^2 = \frac{\sum (a_n^2 + b_n^2)}{2} \tag{4.6}$$

And the percentage contribution of each harmonic is found from:

$$\% = \frac{\sigma_i^2}{2\,\sigma^2} \times 100 \tag{4.7}$$

where $\sigma^2$ is the total variance, and $\sigma_i^2$ the variance of each harmonic frequency. All harmonics except that of the dc or average component are included in the above calculations.

The percentage contribution to variance for a frequency of 1 cycle/year was calculated for each of the years in the data set. These values, along with the harmonic amplitudes for each year are shown in Table 4.1.

| Year | Frequency | $a_n$ coefficient | $b_n$ coefficient | Percent of Variance |
|---|---|---|---|---|
| 1 | 1 cycle/yr | -1207.37 | 228.21 | 65.72% |
| 2 | 1 cycle/yr | -1181.82 | 189.26 | 67.83% |
| 3 | 1 cycle/yr | -1174.74 | 272.51 | 63.49% |
| 4 | 1 cycle/yr | -1039.68 | 255.72 | 58.57% |

Table 4.1: Annual Harmonic Coefficients

Using the data in Table 4.1 and the annual average daily solar radiation for each year, a Fourier series can be used to model the deterministic component, or 'Typical Annual Time Function' (TAF) of each year [6,8,9]. A 'TAF' estimates the most likely value of solar radiation for a given day of the year.

Based on the information in Table 4.1 the fundamental frequency contributes on average 64% to the overall variance in the daily solar radiation data. By averaging the coefficients in Table 4.1

the overall average deterministic part of all the solar radiation data in the series can be found from the following Fourier series:

$$S_d(t) = 2382.78 - 1150.92 \cos\left(\frac{2\pi t}{365}\right) + 236.43 \sin\left(\frac{2\pi t}{365}\right) \quad (4.8)$$

Where 2382.78Wh/m$^2$ is the 4-year annual average value for Aberdeen. This average TAF is the same as the numerical average of all the individual year's typical annual time functions, and represents the average annual cycle. The monthly average values were calculated for each year's typical annual time function. The annual variation in mean values follows the same pattern for each year and for the average typical function, being higher over the summer and lower over the winter. The monthly magnitudes are also similar for each year. The monthly mean values were also calculated for the 4-year average typical time function and were compared with those calculated for each year. These monthly parameters are shown in Appendix A1. The monthly values for the averaged time function are approximately the same as the numerical average of each month's mean value over all four years. This is also true of the monthly standard deviation values. This was to be expected as the average typical time function (Equation 4.8) is just the numerical average of all four years TAF's.

A comparison between this average annual cycle and one year of actual data is shown in Figure 4.4. This shows that the overall shape of the data is maintained, but there are still fluctuations about this component over the whole year. These fluctuations could be due to either the environmental conditions on each day, or due to the accuracy of the instrumentation used to obtain the hourly solar radiation values.

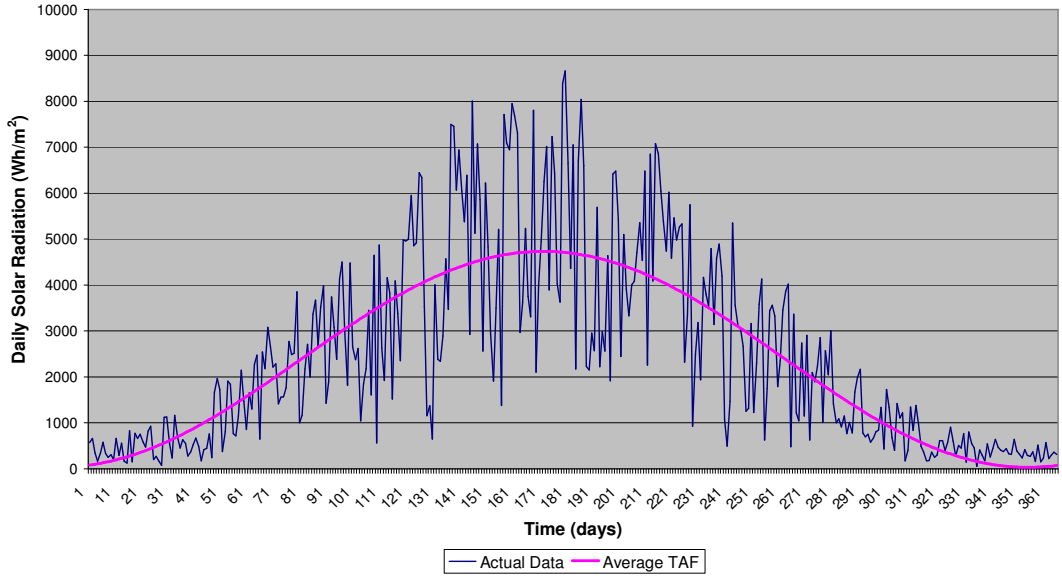


Figure 4.4: Comparison between One Year of Actual Data and The Average Deterministic Component

These fluctuations represent the stochastic component of the daily solar radiation data. Their values can be found in two ways. Firstly, all four years of data can be averaged to obtain a 'typical' solar year i.e.:

$$S_{\mathrm{AVE}}(t) = \frac{1}{m}\sum S(m,\ t) \tag{4.9}$$

where $S_{AVE}(t)$ is the 4-year average solar radiation, t is the day of the year, m is the year number, and S(m,t) represents each years solar radiation. Then the stochastic component would be the difference between the average solar data and the deterministic component given in equation (4.8) [10], such that:

$$S_s(t) = S_{\mathrm{AVE}}(t) - S_d(t) \tag{4.10}$$

However, by averaging the solar radiation data using equation (4.10), the magnitudes of the 'high' solar radiation days will have decreased, thereby reducing the estimated energy output on those days. The averaging process will also have increased the values of 'low' solar radiation days, causing an overestimation of the energy available on some days. This would prevent an accurate assessment of the output of a photovoltaic system being obtained.

The second method for obtaining the stochastic components is to find the difference between each year of actual data and its corresponding typical annual function such that:

$$S_s(t) = S(t) - S_d(t) \tag{4.11}$$

where S(t) represents the individual year of solar radiation data and $S_d(t)$ represents its corresponding TAF or deterministic component. This method will provide four years of stochastic data. A comparison between the stochastic outcomes from the two methods is shown in Figure 4.5.

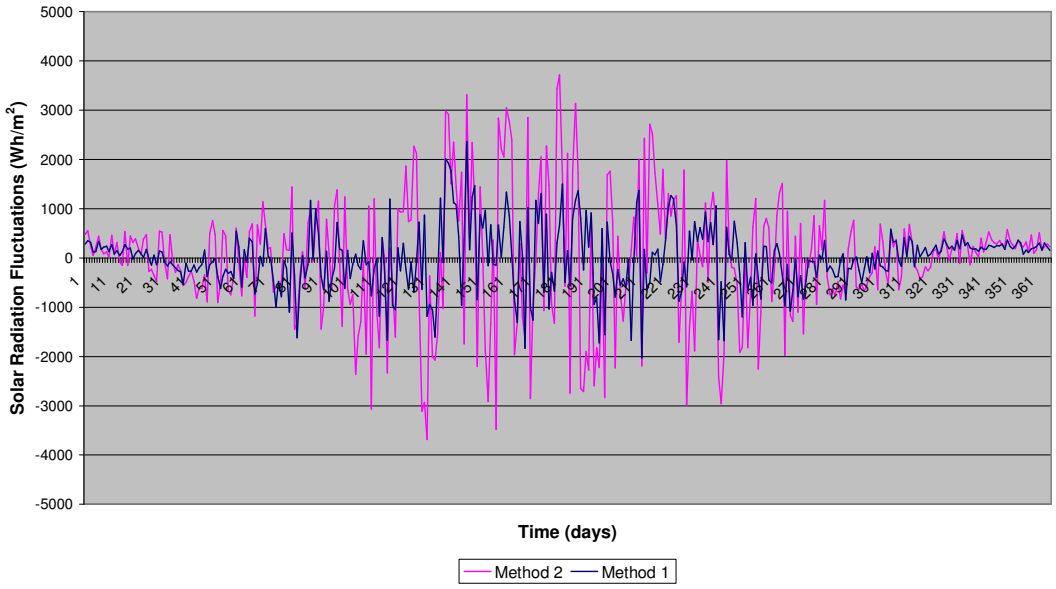


Figure 4.5: Comparison Between Average Stochastic Component (Method 1) and One Year's Stochastic Component (Method 2)

Figure 4.5 shows the annual variation in both stochastic components and that the magnitudes of the individual fluctuations are dependent upon the time of year. The magnitudes of both increase over the summer months and decrease again towards the end of the year. Over the start and end of the year the stochastic component is positive and relatively small in magnitude compared with the remainder of the year's values. This is most likely due to the lower mean values at this time of year, and the daily fluctuations being much closer in size to these mean values than those during the rest of the year. This is true for both data sets obtained using Method 1 and Method 2. However, there is a difference in the overall minimum and maximum values of the fluctuations. The averaged data (Method 1) varies between –2000Wh/m$^2$ and

2500Wh/m$^2$ whereas the four individual years of stochastic data (Method 2) ranges between ±4000Wh/m$^2$. As stated previously the difference between the two methods is the result of the averaging process (equation (4.9)), which either underestimates the output on a day with high solar radiation or overestimates a day with low radiation levels. Based on the shape of both stochastic components it can be assumed that the monthly mean and standard deviation values vary over the year.

The distribution of the averaged data (Method 1) is approximately normal with a mean value of 1.25 and a standard deviation of 634.15. The distributions of each of the four individual years, obtained from Method 2, are also approximately normal but with a tendency towards a left hand skew. On average the mean value is about 0 and the standard deviation is about 1200. The majority of the data contained within this averaged data's distribution lie within the limits of ±4σ, backing up the minimum and maximum values observed from Figure 4.5.

The monthly mean and standard deviation values were also calculated for both methods of stochastic data analysis. The monthly mean values for each year were compared with those of the averaged stochastic component and are shown in Figure 4.6, where the bars represent the data obtained from Method 2 and the smooth line the data from Method 1. A comparison of the monthly standard deviation values for all the stochastic data are shown in Figure 4.7.

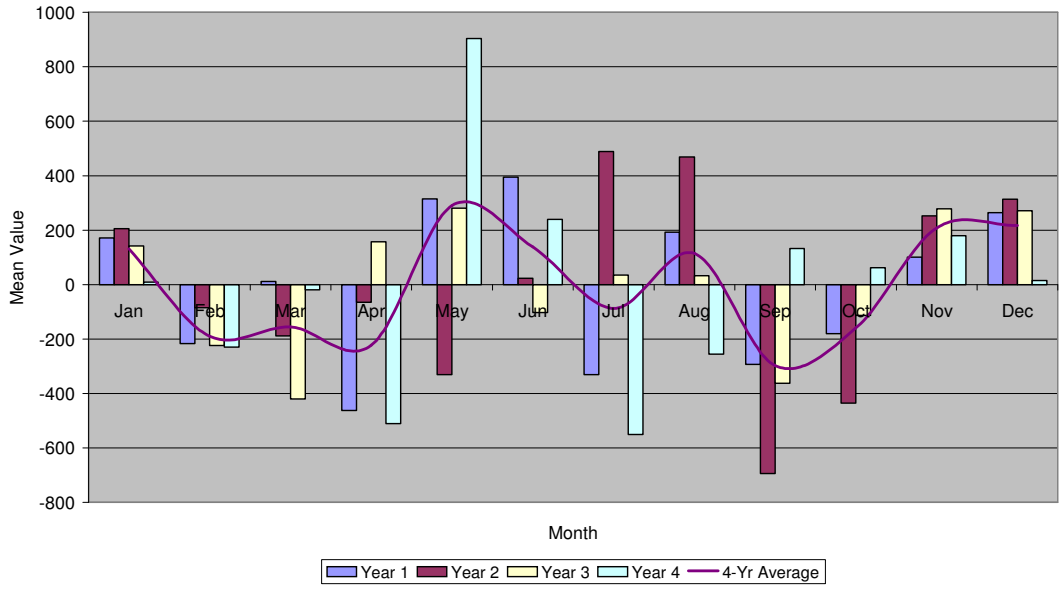


Figure 4.6: Comparison of Monthly Mean Values for Both the Stochastic Data Sets

Figure 4.6 shows that there is no obvious pattern to the annual variation in monthly means. However, the monthly mean values for the averaged stochastic data (equation (4.10)) are approximately the same as the numerical averages of the monthly means obtained from the four years of stochastic data.

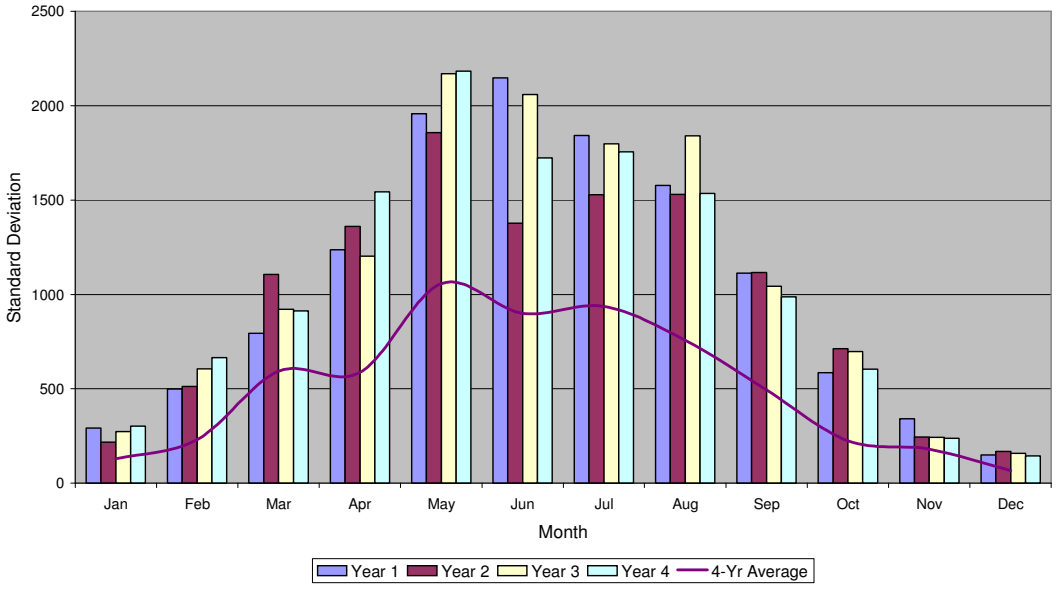


Figure 4.7: Comparison of Monthly Standard Deviation Values for Both Stochastic Data Sets

Figure 4.7 shows that there is an annual cycle present in all the data but that the magnitudes of the standard deviation values for the 4-year averaged data (Method 1) are approximately half that of each of the annual standard deviation values (Method 2). Therefore using the 4-year averaged (Method 1) standard deviation values will significantly affect the magnitudes of the overall fluctuations. Since the average annual time function monthly mean and standard deviation values are approximately the same as the numerical averages of each years monthly mean and standard variation (Method 2), it would make sense to assume that the stochastic standard deviation values should also be the same as the numerical average. By doing this the overall magnitudes of the fluctuations will be more representative of those within a typical year of daily solar radiation data. Based on this, Method 2 will be used to estimate the stochastic component of the solar radiation data. Table 4.2 shows the averaged standard deviation values (Method 1) and the numerical averages of the monthly deviation values for each year (Method 2). This table also shows the monthly mean values for the stochastic data.

| Month | Averaged Standard Deviation **Method 1** | Numerical Standard Deviation **Method 2** | Mean |
|---|---|---|---|
| Jan | 127.934 | 271.285 | 131.983 |
| Feb | 230.019 | 570.838 | -188.626 |
| Mar | 593.331 | 933.108 | -153.546 |
| Apr | 585.206 | 1335.697 | -219.838 |
| May | 1056.897 | 2042.228 | 292.670 |
| Jun | 899.851 | 1826.546 | 139.115 |
| Jul | 936.462 | 1730.910 | -89.024 |
| Aug | 757.247 | 1620.027 | 109.572 |
| Sep | 493.002 | 1064.945 | -303.866 |
| Oct | 224.118 | 650.281 | -166.433 |
| Nov | 179.863 | 266.607 | 203.088 |
| Dec | 66.424 | 155.231 | 216.367 |

Table 4.2: Monthly Mean and Standard Deviation Values of Stochastic Data

The stochastic components, obtained from each year of data, are assumed to be stationary as the 'trend' or annual cycle has been removed using the deterministic model. To test for stationarity the data needs to be transformed, by month, into a set of standardised normal variables such that:

$$\varepsilon(t) = \frac{S_s(t) - \mu_m}{\sigma_m} \tag{4.12}$$

where $\varepsilon(t)$ is the normalised data, $S_s(t)$ is the original stochastic data, $\mu_m$ is the monthly mean value, $\sigma_m$ is the monthly standard deviation value and m is the month number. The normalised data is then tested for stationarity and is found to satisfy the two conditions required – (1) the mean function is constant over time, and (2) the covariance function is zero for all time lags greater than one [11].

In order to examine the structure of the stochastic data, obtained from Method 2, and to assess if it can be modelled as white noise, the autocorrelation function and the partial autocorrelation function were calculated annually and for each month. The autocorrelation function is often used to identify whether a data series is random or non-random. It gives an indication of the

structure of the data as the autocorrelation coefficient, r, calculates the dependence within the series as the time lag k, increases. The autocorrelation coefficient is calculated from:

$$r_k = \frac{\sum_{t=1}^{N-k} \left(Y_t - \bar{Y}\right)\left(Y_{t+k} - \bar{Y}\right)}{\sum_{t=1}^{N} \left(Y_t - \bar{Y}\right)^2} \tag{4.13}$$

where k is the time lag in days, $\bar{Y}$ is the mean value of the data series, t is the time in days, Y is the actual time series and N is the number of data points in the series [12, 13].

The annual autocorrelation plot of the stochastic component for one year is shown in Figure 4.8, and shows that the majority of values, except $r_0$, lie within ±90% confidence limits. The same conclusion is reached for each month of the stochastic data. The partial autocorrelation function (PACF) gives an indication of the order of model required, and was calculated for each month of stochastic data. The output values of the PACF were all within the values of the 90% confidence limits calculated by $\pm 2/\sqrt{N}$ limits, where N is the number of data points. This result indicates that there is no defined structure to the data indicating that each month can be modelled as white noise [11].

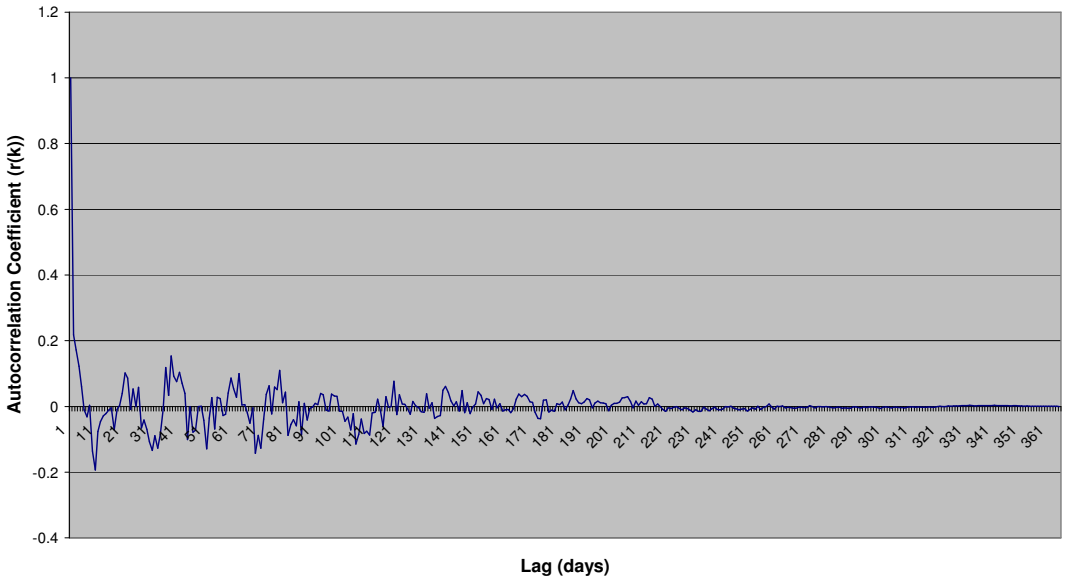


Figure 4.8: Annual Autocorrelation Plot of One Year of Stochastic Data

Based on this conclusion twelve sets of white noise, $\varepsilon_{WN}$, are generated. Each set of white noise has a mean of zero and a standard deviation of 1, the same properties as the standardised normal variable, and is transformed to give a 365-point data set using equation (4.12) in the following form [19,26]:

$$S_s(t) = \sigma_m \varepsilon_{WN}(t) + \mu_m \tag{4.14}$$

where $S_s(t)$ is the estimated stochastic data, $\varepsilon_{WN}$ is the monthly white noise, $\sigma_m$ the monthly standard deviation value and $\mu_m$ the monthly mean value, ( as shown in Table 4.2) and ,t is the day of year.

This data series $S_s(t)$ is added to the deterministic component $S_d(t)$, obtained from equation (4.8), to obtain an estimate of the daily variation in solar radiation for Aberdeen. The magnitudes of the fluctuations are similar in scale to those of the actual solar radiation data. However, a number of values within the estimated data are negative, which cannot exist in real life, and there are no occurrences of zero solar radiation values within the measured data. Therefore a correction value needs to be applied in order to remove the negative values from the modelled data. Each negative value within a month is replaced with the four-year monthly average value making the data values comparable with the long-term monthly average. The value of each long-term monthly average depends upon the number of years of data within the overall modelling procedure. A comparison between the corrected modelled data, $S_{CORR}(t)$, and a typical year of data is shown in Figure 4.9. This shows that the overall pattern of the daily solar radiation data is maintained and that the magnitudes of the fluctuations are comparable with those present in each month of actual daily radiation data.

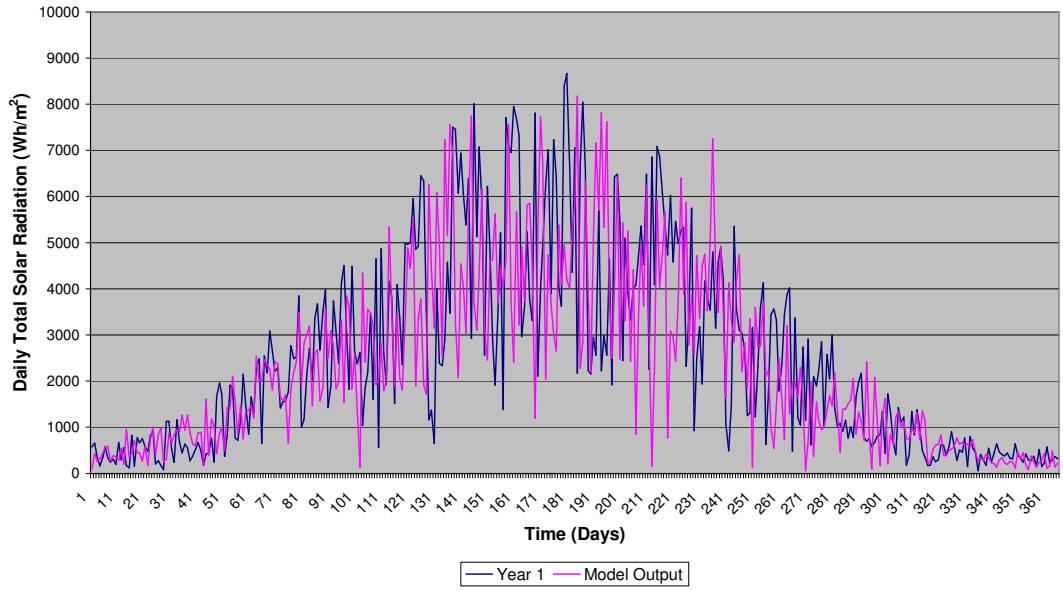


Figure 4.9: Comparison Between One Year of Actual Solar Radiation Data and the Corrected Modelled Solar Data

This modelled data can be compared with the actual data in a number of ways. The overall annual autocorrelation plot of the modelled data is shown in Figure 4.10 along with the autocorrelation of the original four years of solar radiation data. The overall shape of the autocorrelation function for the modelled data is the same as most of the actual data. If the stochastic data was modelled based on the mean and standard deviation values from the first method outlined for the stochastic data, the shape of the autocorrelation plot would be significantly different to those shown in Figure 4.10. The minimum and maximum peak values would be increased, and there would be no dip in autocorrelation values at low lag values.

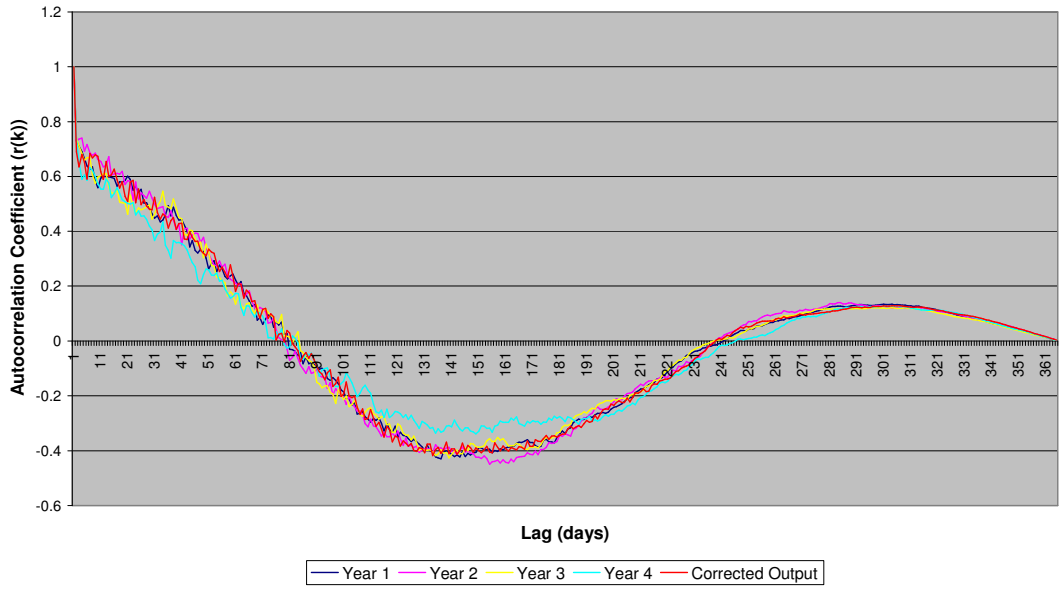


Figure 4.10: Annual Autocorrelation Comparison of Daily Solar Radiation Data

The statistical parameters of the modelled data and the four input years of solar irradiation data are also compared and are shown in Table 4.3. The mean value of the modelled data lies well within the range of mean values for the original data, however the standard deviation of the modelled data is probably too low. The modelled data's skew value is comparable with those from the four years of actual data, indicating that the probability distribution functions of the data are all very similar. The coefficient of variation values of all five data sets are within ±10% of 0.8 – making the modelled data very comparable with the actual data.

| Statistical Parameter | Year 1 | Year 2 | Year 3 | Year 4 | Modelled Data |
|---|---|---|---|---|---|
| Mean | 2506.416 | 2354.352 | 2375.580 | 2294.786 | 2328.844 |
| Standard Deviation | 2146.446 | 2058.094 | 2143.606 | 1981.122 | 1918.800 |
| Skew | 0.876 | 0.729 | 0.979 | 0.907 | 0.909 |
| Minimum | 58 | 26 | 42 | 23 | 59 |
| Maximum | 8663 | 7616 | 8395 | 8044 | 8174 |
| Coefficient of Variation | 0.856 | 0.874 | 0.902 | 0.863 | 0.824 |

Table 4.3: Comparison of Annual Statistical Parameters

Overall, the procedure outlined for estimating daily solar radiation data provides an accurate and reliable model. Although the model is only based on four years of data, the same procedure could be used for a larger number of input years, providing greater reliability in the model outcome. Although the output magnitudes used in the model are only suitable for Aberdeen the actual modelling procedure could be used for any location provided there were a number of years of daily solar radiation data available.

## 4.4 WIND ENERGY DATA ANALYSIS

The wind resource data set comprises of hourly (average) wind speed measurements for a period of five years from January 1975 to December 1979 [14]. The data was recorded at Dyce, Aberdeen at a height of 10 metres above mean sea level, and at 10-minute intervals, averaged to obtain hourly data. Five years of data was used to account for the variability of the data in any one year and to provide a more typical data set. It is generally recommended that a minimum of five years of data is required to obtain an accurate annual average wind speed for any location [15]. The hourly data for each year was averaged over each day to obtain the average wind speed per day. This was done using the following expression

$$W_D = \frac{1}{24}\sum_{i=1}^{24} W_{i,D} \tag{4.15}$$

where $W_{i,D}$ is the hourly wind speed (m/s), i is the hour of day, D is the day of the year and $W_D$ is the daily average wind speed value (m/s). A similar process was applied to the data to obtain the monthly average wind speeds for each year.

The analysis of the daily wind speed values indicated that there are no occurrences of zero wind speeds throughout the five years. There is no obvious annual pattern to the data although it can be seen that in general the wind speeds are lower over the summer months than the values over the winter months. The variation in monthly mean wind speeds over the five years shown in Figure 4.11 also demonstrates that there is no clear pattern as to which month has either the highest or lowest wind speed value.

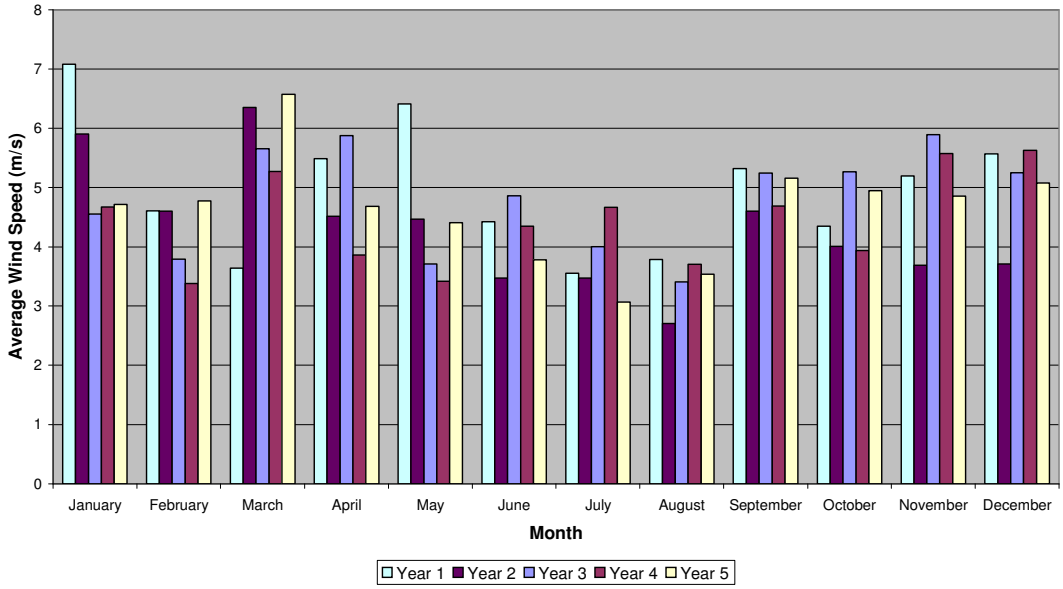


Figure 4.11: Annual Variation in Monthly Mean Wind Speeds

The variation in wind speed values over a set time period i.e. a month or a year, is commonly described by the probability distribution function (PDF). The annual distribution function was calculated for each of the five years of hourly wind speed data and is shown in Figure 4.12. The wind speed values range from about 1m/s to 16m/s with an overall average of 4.65m/s. The shape of the distribution is right skewed and is the same shape for all five years. The shape of the distribution is similar to that of the Weibull distribution, which is commonly used in estimating the available wind resource at different locations [16,17]. The Weibull distribution function is given by:

$$f(u) = \frac{k}{c}\left(\frac{u}{c}\right)^{k-1} \exp\left[-\left(\frac{u}{c}\right)^{k}\right] \tag{4.16}$$

where u is the wind speed, c is the scale parameter and k is the shape parameter. The values of c and k vary for different locations, and can alter the overall shape of the distribution function. The annual values of c and k for the location are found using the least squares approximation to a straight-line method [18]. For the five years of hourly data the average Weibull parameters are c = 5.519, and k = 1.988. The estimated Weibull distribution using these values is also shown in Figure 4.12 for comparison. Overall the Weibull distribution fits the data well, but it

underestimates the occurrences of wind speeds of about 2 m/s for each year. This is not a significant problem as most commercial wind turbines have cut-in speeds greater than this.

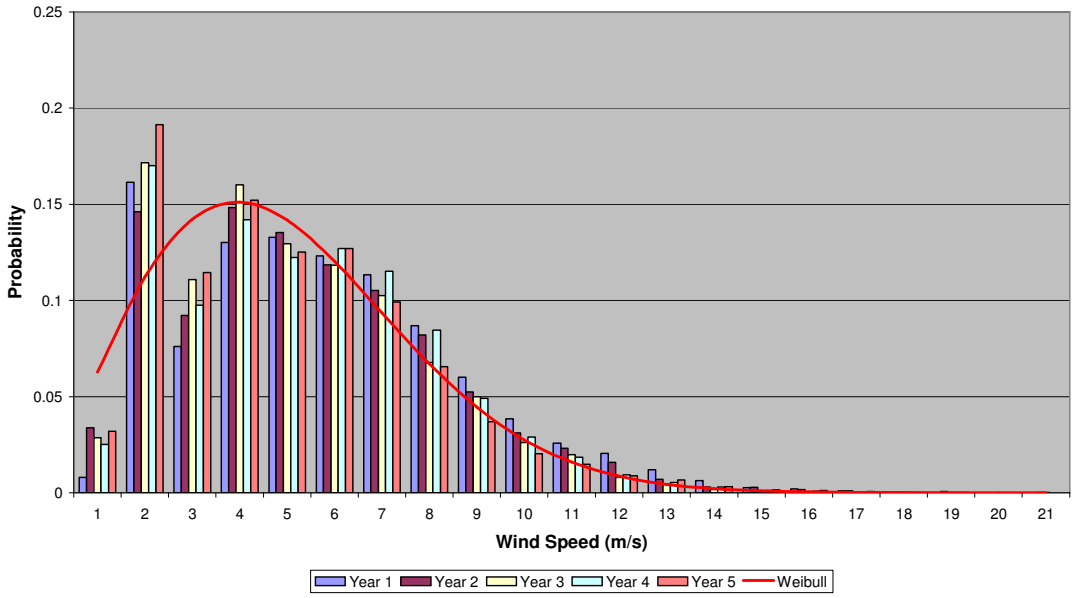


Figure 4.12: PDF of Hourly Wind Speed Data For Each Year

The wind speed distribution function can also be estimated for each month, using the hourly data set. The shape of each month's distribution is similar to that of the annual distribution. The Weibull parameters, c and k, are found for each month using the same method as before. The monthly values of c and k vary over the year, with more significant variation occurring in the values of the scale parameter. The Weibull distribution was calculated for the highest and lowest values of c, and their corresponding values of k, and the results for one year are shown in Figure 4.13.

The lowest scale value occurs during the month of August and the corresponding distribution indicates that there is higher proportion of low wind speeds during this month. In other words, the distribution function is narrower and the peak is closer to the y-axis. The highest scale value occurs in March, indicating that the majority of wind speeds are equal to or greater than the annual average wind speed.

The monthly Weibull parameters were also calculated for each year to see if there was a pattern as to when the highest and lowest scale parameters occur. These results are shown in Appendix A2. The variation in monthly scale values is very similar to the variation in monthly mean wind

speed. The highest value usually occurs over the winter months, and tends to coincide with the highest monthly wind speed. There is no obvious trend for the low c values. This is also backed up by Figure 4.11, which showed a comparison of the monthly average wind speeds for each year

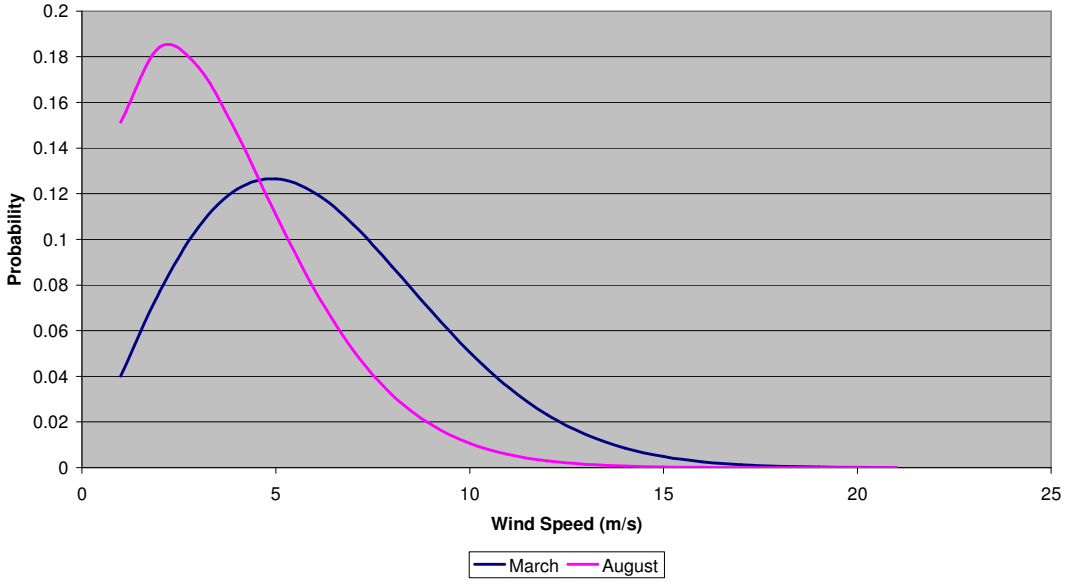


Figure 4.13: Comparison of PDFs with High and Low c Values

The 24-hour daily wind speed profiles of the hourly data were also averaged to obtain typical diurnal profiles for each month and an annual diurnal variation. The typical annual diurnal variation is shown in Figure 4.14. The wind speeds are lower in the morning, with a peak around noon, and then decrease over night. This pattern is the same for all months of the year, with the peak value depending on the monthly wind speed value. The diurnal variation of the wind speed is similar in shape to that of the 24-hour temperature profile (also shown in Figure 4.14). This strong relationship between the two variables shows that the temperature variation over land surfaces, due to heating from the daily solar radiation profile, greatly affects the wind speed [15]. This regular shape in diurnal variation indicates that there is some predictable, deterministic component in the hourly wind speed data.

The FFT was calculated for the hourly and daily data sets to find the frequency content and structure of the wind speed data. The Fourier transform of all five years of hourly data was taken and is shown in Figure 4.15. The annual average (or dc component) is the most significant value within the data set, but to illustrate the remaining significant frequencies, this value is not

shown in Figure 4.15. Apart from this annual average, the most significant frequencies occur at 1, 2 and 3 cycles/day. Based on the assessment of the contribution to the overall variance of each of the other cycles present, the most significant peaks occur at frequencies equal to 365.2 days, 91.25 days and about 60 days. The first time value represents the annual variation in the data, the second represents a cycle of ¼ of a year, which could be indicative of a seasonal cycle, and the last value represents a cycle every two months. All the significant frequencies, along with their contributions to the total variance are shown in Table 4.4.

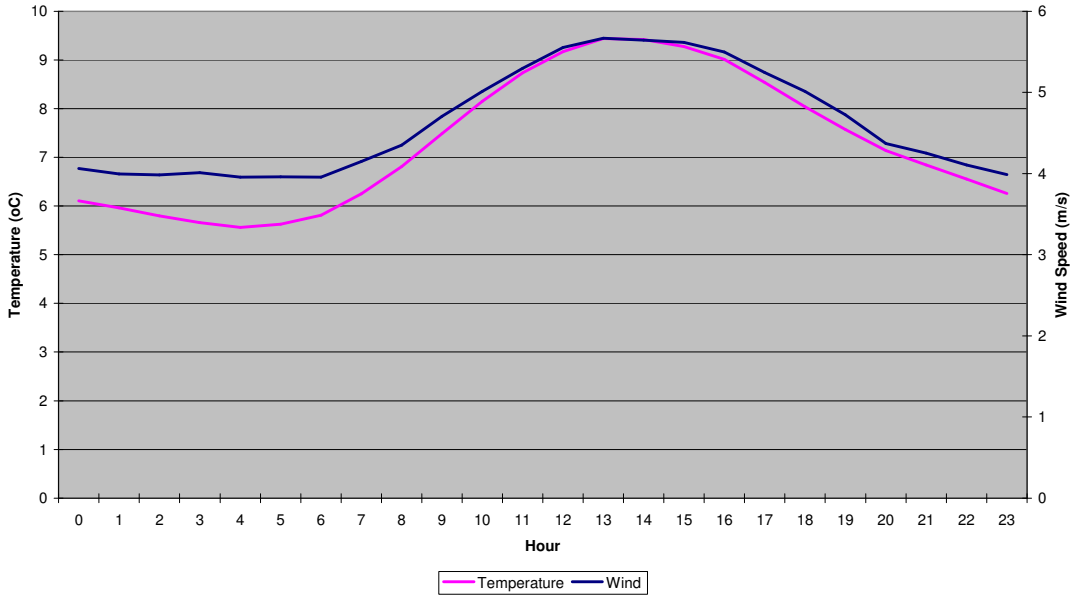


Figure 4.14: Average Annual Diurnal Variation in Wind Speed and Temperature

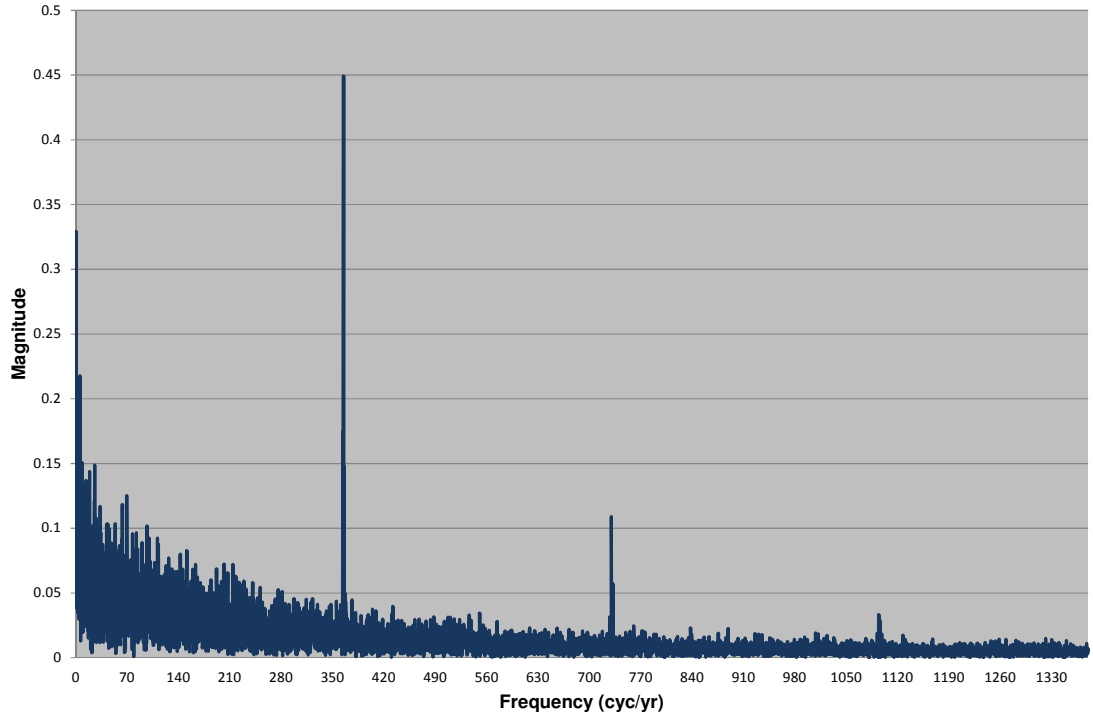


Figure 4.15: FFT of Five Years of Hourly Wind Speed Data

| Frequency | $a_n$ coefficient | $b_n$ coefficient | Percent of Variance |
|---|---|---|---|
| 0.8 cycle/yr | 0.1648 | 0.0655 | 0.76% |
| 1 cycle/yr | 0.3010 | 0.1328 | 2.62% |
| 2 cycles/yr | -0.1596 | -0.0810 | 0.77% |
| 4 cycles/yr | 0.1530 | -0.0998 | 0.81% |
| 6 cycles/yr | -0.0345 | 0.2148 | 1.15% |
| 365.2 cycles/yr | -0.4000 | -0.2040 | 4.89% |
| 730.4 cycles/yr | 0.0789 | 0.0750 | 0.28% |

Table 4.4: Significant Harmonic Components of Hourly Wind Speed Data

Apart from the daily cycle, all the other significant frequencies in Table 4.4 are present in the Fourier Transform of the daily wind speed data over five years. Within the analysis of the daily data, two other frequencies are highlighted. The first occurs at 228 days and the second at 39.6 days. On a daily basis the contribution of all these cycles is not that significant overall, as the sum of their contribution to the variance of the data accounts for about 12%. However, not all these cycles are present in each individual year of daily wind speed data. Analysis of each

individual year showed that between 30 – 42% of the variance in any year can be represented by between 10 to 15+ significant frequencies. Also, with those cycles common to all years, their individual contribution to variance differs significantly from year to year. This implies that the importance of some cycles varies annually. Due to this variation in each year, it would be difficult to use a generalised Fourier series to represent any underlying trend in any one year of daily wind speed data.

The FFT of the hourly wind speed data also provides information about the cyclic content of wind speeds over a 24-hour period. Based on this information, it was found that only the average annual mean wind speed and components at 1 and 2 cycles/day were needed to estimate a typical 24-hour profile of wind speed variation in Aberdeen. As these cycles are present in all the years of wind speed data, a generalised Fourier series, as shown in equation (4.17), could be used to estimate this typical diurnal profile based on any mean wind value.

$$W_{daily} = A_o\left[1 - 0.1719\cos\frac{2\pi t}{24} - 0.0877\sin\frac{2\pi t}{24} + 0.03389\cos\frac{4\pi t}{24} + 0.0327\sin\frac{4\pi t}{24}\right] \tag{4.17}$$

where $W_{daily}$ is the hourly wind speed value, t is the hour, and $A_o$ is the mean annual wind speed. The value of $A_o$ can be varied to generate different diurnal profiles depending upon the mean wind speed value for Aberdeen.

## 4.5 WIND ENERGY MODELLING

### 4.5.1 Proposed Wind Model (1)

From the analysis of the wind speed data, it can be seen that there is no clear, repeatable underlying trend in either the monthly or daily data sets of wind speed data. Therefore it is assumed that the daily wind speed data set can be treated as a random/stochastic time series. Based on this, the applicability of fitting standard time series models to the data will be assessed.

As stated previously, these techniques can only be applied to data that is stationary and has a Normal distribution function. Firstly the distribution function of the daily wind speed data needs

to be transformed from that of a Weibull distribution. This is done by applying a Box-Cox power transformation [11] to the daily data set. These transformations are defined as:

$$y(x) = \begin{cases} \dfrac{x^{\lambda} - 1}{\lambda} & \text{for } \lambda \neq 0 \\ \ln(x) & \text{for } \lambda = 0 \end{cases} \tag{4.18}$$

Where x is the original data set, λ is the power, and y(x) is the transformed data set. The value of the parameter λ is found by selecting the values of λ that maximises the logarithm of the likelihood function [11,19]. The power coefficient was calculated for each individual year of wind speed data. Although each year has a Weibull distribution function originally, the value of the power coefficient varies for each year of data, and ranges from 0.3 to 0.45. There does not appear to be any relationship between the power coefficient for any year and the same year's Weibull parameters. There is also no pattern/relationship between the power coefficient and the annual mean. Figure 4.16 shows a comparison between the original distribution function and the new transformed distribution function for one year.

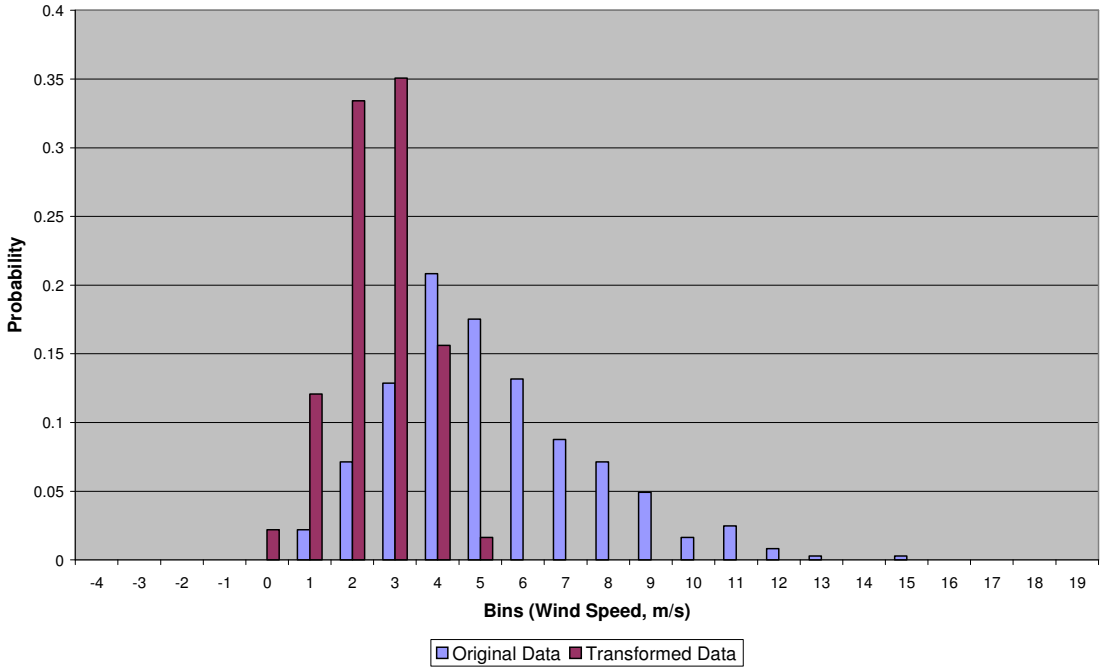


Figure 4.16: Probability Distribution Comparison For One Year

Secondly, the non-stationarity in the daily wind speed data needs to be removed. The simplest method for doing this is to convert the transformed data set to a set of standardised normal variables using:

$$W_N = \frac{y_i - \mu}{\sigma} \tag{4.19}$$

Where $y_i$ is the new wind speed data series, $\mu$ is the annual mean, and $\sigma$ is the annual standard deviation. Table 4.5 shows a comparison of the mean and standard deviation values for each year of transformed wind speed values. This table also shows the power transformation coefficients for each year of data. Normalising the data on an annual basis instead of a monthly basis was selected due to the results of the FFT analysis of the daily data, indicating a weak seasonality in the data. Each year's normalised data, $W_N$, was then tested for stationarity and was found to satisfy the two required criteria specified earlier in the chapter.

| Year | Mean | Standard Deviation | Power Coefficient, $\lambda$ |
|---|---|---|---|
| 1 | 2.0000 | 0.7621 | 0.3075 |
| 2 | 1.7000 | 0.7595 | 0.3018 |
| 3 | 2.0710 | 0.9449 | 0.4145 |
| 4 | 1.8090 | 0.7620 | 0.3317 |
| 5 | 2.0817 | 0.8890 | 0.4433 |
| **Average** | **1.932** | **0.8235** | **0.3597** |

Table 4.5: Comparison of Statistical Parameters for Transformed Wind Speed Data

To assess what type of time series model can be applied to the data, the autocorrelation function (ACF) and the partial autocorrelation function (PACF) were calculated for each year of transformed wind speed data. The annual ACFs are shown in Figure 4.17, and demonstrate a gradual decay towards a coefficient of 0. This decay is more obvious if the ACF is examined over a shorter time scale, for example 30 days. The majority of the autocorrelation coefficients, r(k), are also within confidence limits of $\pm 2/\sqrt{N}$. This result indicates an autoregressive (AR) process can be used on the data [20]. These coefficients, r(k), are then used to calculate the PACF, as shown in Figure 4.18. The PACF has only one significant peak at the start of the plot, and the remaining values are within similar confidence limits to those of the ACF. Based on these results, it is concluded that daily wind speed data is a first order autoregressive (AR(1))

process. The lag-one autocorrelation coefficients, for all years of data, range from 0.425 – 0.51, with an average value of 0.478. Again there is no pattern to the variation in this parameter.

For the generation of a typical wind speed data set, the following autoregressive (AR) model is suggested:

$$y_i = 0.478\, y_{i-1} + \varepsilon_i \tag{4.20}$$

Where $\varepsilon_i$ is white noise [11, 20] with a mean of zero and a standard deviation of 0.8235. To obtain a more representative output from the model process, it would be preferable to select the autoregressive coefficient randomly from a range of data values equal to those calculated from the actual wind speed data. This model is used to generate 365 data points that are used as the basis for the second stage of the daily wind speed model. This converts the generated data to a set of data with parameters similar to the transformed wind speed data, $W_N$, and is of the form:

$$W_{AR} = \sigma_A\, y_i + \mu_A \tag{4.21}$$

Where $\sigma_A$, and $\mu_A$, are the annual parameters selected at random from the range of standard deviations and mean values calculated from the original data.

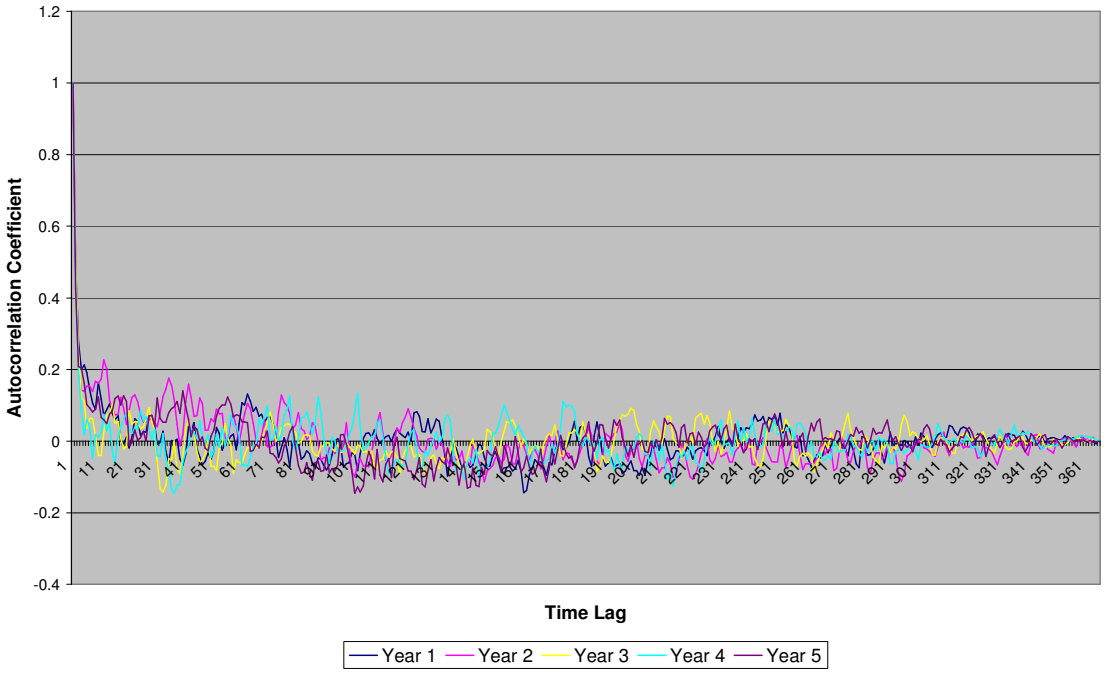


Figure 4.17: Comparison of Annual Autocorrelation Plot

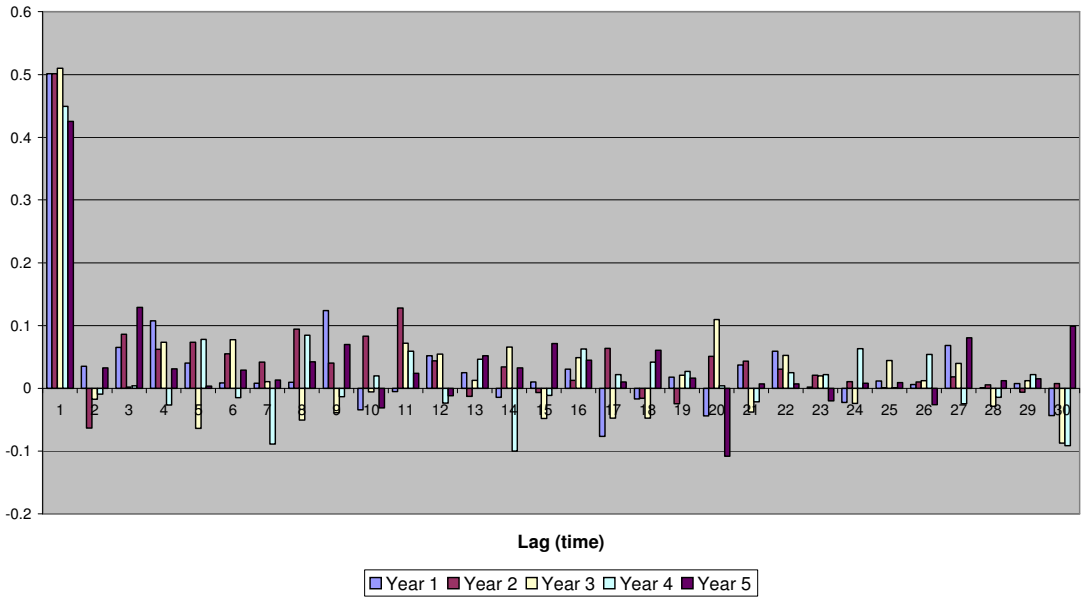


Figure 4.18: Comparison of Annual Partial Autocorrelation Function

Finally, the values of $W_{AR}$ have an inverse transformation from equation (4.18), applied using a power coefficient of 0.36. The average value of power coefficient was chosen to ensure that the data produced by the model procedure was more typical of the 5-year average. Again this power coefficient could be selected at random from the range 0.3 to 0.45 obtained from the original data.

A comparison between the wind speed data generated using the AR(1) model (in equations 4.20 and 4.21), and one year of actual daily data is shown in Figure 4.19. In general, the modelled data appears to follow the same annual variation that is present in the actual data. The minimum and maximum annual wind speeds values of the modelled data are within the ranges obtained from the actual five years of wind speed data. However, when using this modelling procedure repeatedly, the minimum value of the wind speed data has a tendency towards the lower end of the range of values obtained from the actual wind speed data.

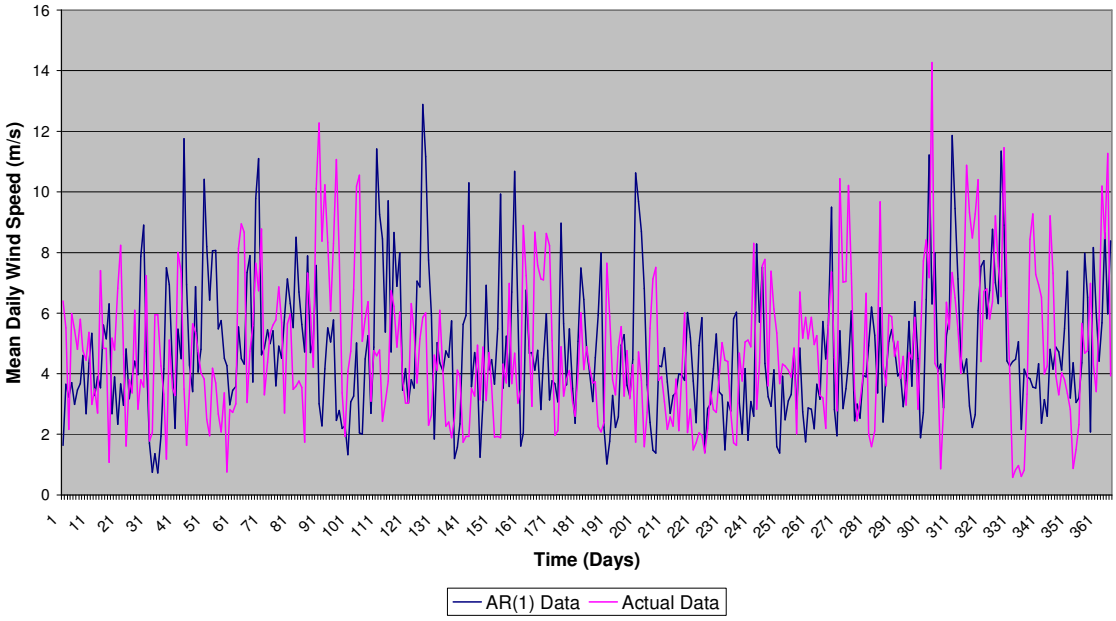


Figure 4.19: Comparison Between One Year of Actual Wind Speed Data and the Wind Model Output

The FFT of the modelled data is also compared with one year of actual data, and this comparison is shown in Figure 4.20. The majority of the frequencies present are similar in magnitude to those present in the actual data. However, due to the variation in the FFT content of the original data, as found from the annual analysis, it was expected that there would not be a great deal of similarity between the modelled data and any year of actual data.

The distribution function of the modelled wind speed data was also calculated, and a comparison between this and the Weibull distribution using the 5-year average values is shown in Figure 4.21. Both distribution functions are very similar, except that the modelled data increases the probability of higher wind speeds, and decreases the probability of low wind speeds. The Weibull parameters obtained from the modelled data are shown in Table 4.6, along with a comparison of the other key statistical parameters. In general most of the modelled data's statistical parameters are very similar to those of the actual data. The exception to this is the skew parameter, which on average is consistently lower for the actual data than the modelled data. This could relate to the distribution function illustrating that the model underestimates the probability of wind speeds within 6-8m/s. However, using the Weibull distribution function on a daily time basis, the function has a tendency, on average, for Aberdeen, to overestimate the probability of wind speed within 5-7m/s. This data is shown in Appendix A2.

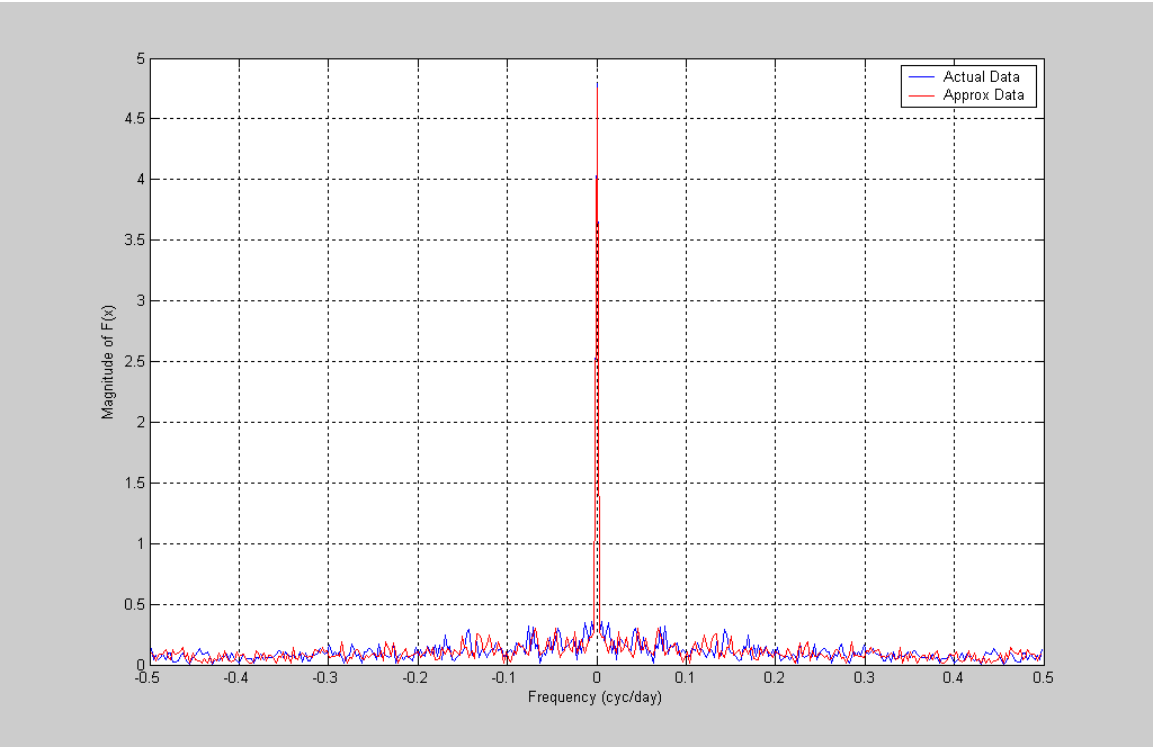


Figure 4.20: Frequency Spectrum Comparison

| Parameter | AR(1) Modelled Data | Year 1 | Year 2 | Year 3 | Year 4 | Year 5 |
|---|---|---|---|---|---|---|
| Mean | 4.752 | 5.122 | 4.292 | 4.794 | 4.435 | 4.629 |
| Minimum | 0.720 | 0.987 | 0.836 | 0.579 | 0.850 | 0.773 |
| Maximum | 12.880 | 14.500 | 12.100 | 14.269 | 10.900 | 10.870 |
| Skew | 0.988 | 0.745 | 0.975 | 0.791 | 0.627 | 0.471 |
| Standard Deviation | 2.239 | 2.340 | 2.090 | 2.338 | 2.027 | 2.042 |
| k | 2.673 | 2.754 | 2.407 | 2.159 | 2.966 | 3.388 |
| c | 5.692 | 6.273 | 5.226 | 5.585 | 5.283 | 5.000 |

Table 4.6: Comparison of Annual Statistical Parameters

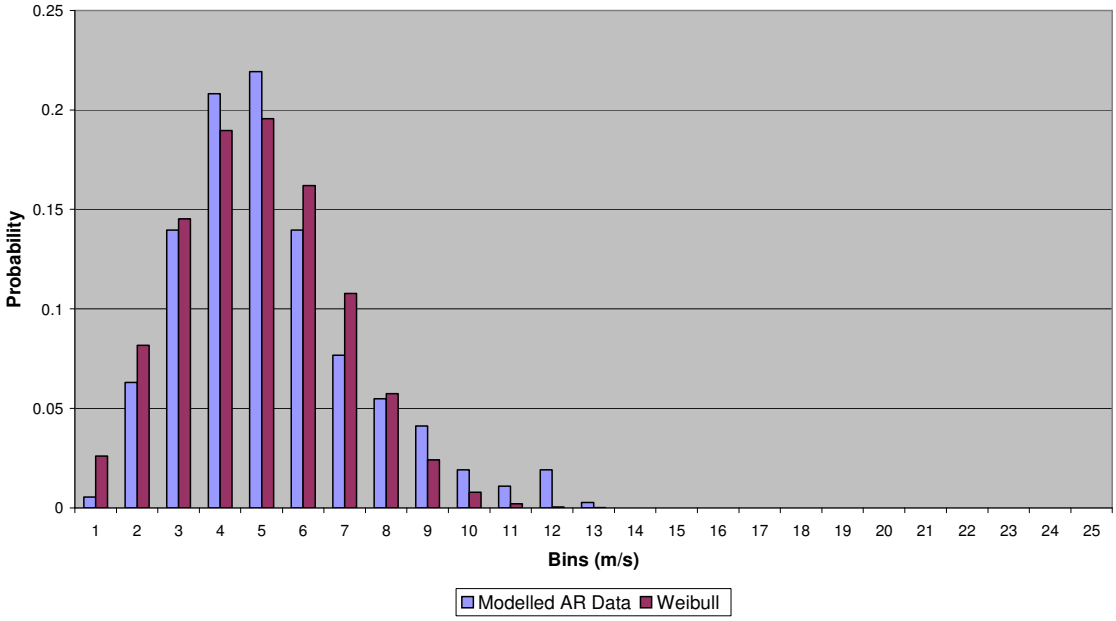


Figure 4.21: PDF Comparison Between One Year of Actual Wind Speed Data and the Modelled Wind Speed Data

### 4.5.2 Proposed Wind Model (2)

As stated earlier in Chapter 2, wavelet analysis is becoming a popular technique for modelling data series [21,22]. Most techniques involve the Discrete Wavelet Transform (DWT), which breaks down a set of data into high frequency and low frequency components. The process is similar to that of Fourier analysis in that it obtains a number of functions called 'Details' and 'Approximations' that represent different frequency ranges. An alternative way of describing the DWT is as a process that subdivides the known frequency range of a data series, and produces a set of sample functions representing each of these frequency bands. For full wavelet decomposition, the subdividing of data is carried out repeatedly until there is a single data sample left. This remaining value represents the long-term mean value of the data. However full wavelet decomposition can only be carried out on data sets that are equal in length to $2^N$, where N is an integer. The wavelet decomposition can be carried out for a number of levels on data that is not the length of $2^N$, but the approximation value obtained would represent a series of average values taken over a number of different time ranges, not the long-term average.

This section of work is an application of the DWT and the use of wavelet decomposition. A more comprehensive discussion of the DWT can be found in a number of texts including 'Ripples in Mathematics The Discrete Wavelet Transform [23,24,25]. There are a number of

different wavelet families that can be used in the DWT, however, for simplicity the Haar wavelet will be considered here. When using the Haar wavelet, the approximation functions are equivalent to taking the averages of the input data, and the detail functions are equivalent to the differences between the original data and the approximations. This process is summarised in Figure 4.22, showing a 5 level wavelet decomposition. This process illustrates that for full reconstruction of the data, six sub-functions are required.

**Decomposition**

- Approximation Function

  A1 = averages from original data

  A2 = averages from A1

  A3 = averages from A2

  A4 = averages from A3

  A5 = averages from A4

- Detail Function

  D1 = original signal – A1

  D2 = A1 – A2 (A1 = A2+D2)

  D3 = A2 – A3 (A2 = A3+D3)

  D4 = A3 – A4 (A3 = A4+D4)

  D5 = A4 – A5 (A4 = A5+D5)

**Reconstruction**

Original Data = A1 + D1

= A2 + D1 + D2

= A3 + D1 + D2 + D3

= A4 + D1 + D2 + D3 + D4

= A5 + D1 + D2 +D3 + D4 + D5

Figure 4.22: Summary of a 5 level Wavelet Analysis

From the frequency analysis of the daily wind speed data, it can be seen that the majority of the important cycles are contained within a frequency band of about 0 cycles/year to 6 cycles/year. Based on this, the use of wavelet decomposition for daily wind speed data seems a logical progression from the frequency analysis. The full frequency range contained within the daily wind speed data is from 0 cycles/year to 183 cycles/year. Using wavelet decomposition, detail

D1 would cover the frequency range from 93-183 cycles/year; detail D2 would cover 46-92 cycles/year and so on until the data has been completely decomposed to the required level. Assuming that the above frequency band of 0 – 5.7 cycles/year contains all the strongly structured wind speed data, it is proposed that a 5 level decomposition be used to obtain this underlying trend from the remaining high frequency components. The frequency bands of the detail and approximation functions are given in Table 4.7.

| Function | Mean | Standard Deviation | Frequency Band (cycles/year) | No. of Coefficients |
|---|---|---|---|---|
| Detail D1 | 0.0009 | 0.5982 | 93 - 183 | 183 |
| Detail D2 | 0.0148 | 0.5104 | 47 - 92 | 92 |
| Detail D3 | 0.0336 | 0.9991 | 24 - 46 | 46 |
| Detail D4 | 0.2207 | 1.1958 | 11.6 - 23 | 23 |
| Detail D5 | 0.1147 | 0.9870 | 5.8 – 11.5 | 12 |
| Approx A5 | -0.4640 | 1.5424 | 0 – 5.7 | 12 |

Table 4.7: Model Parameters Required for Detail and Approximation Estimation

As a detailed frequency analysis of the daily wind speed data has already been carried out, it is proposed that this information be used to model the underlying structure as a Fourier series approximation. The Fourier series approximation includes the 5-yearly average values for frequency components at 0.8, 1, 1.6, 2, and 4 cycles/year (as shown in Table 4.8), and a comparison of this trend component and one year of actual wind speed data is shown in Figure 4.23. This underlying trend function could also be normalised using the annual mean wind speed value, allowing for the function to be updated for more recent wind speed values. Using the information from the frequency spectrum (Figure 4.15), it can be assumed that if this trend is subtracted from one year of original data, the remaining data should contain only high frequency, random fluctuations.

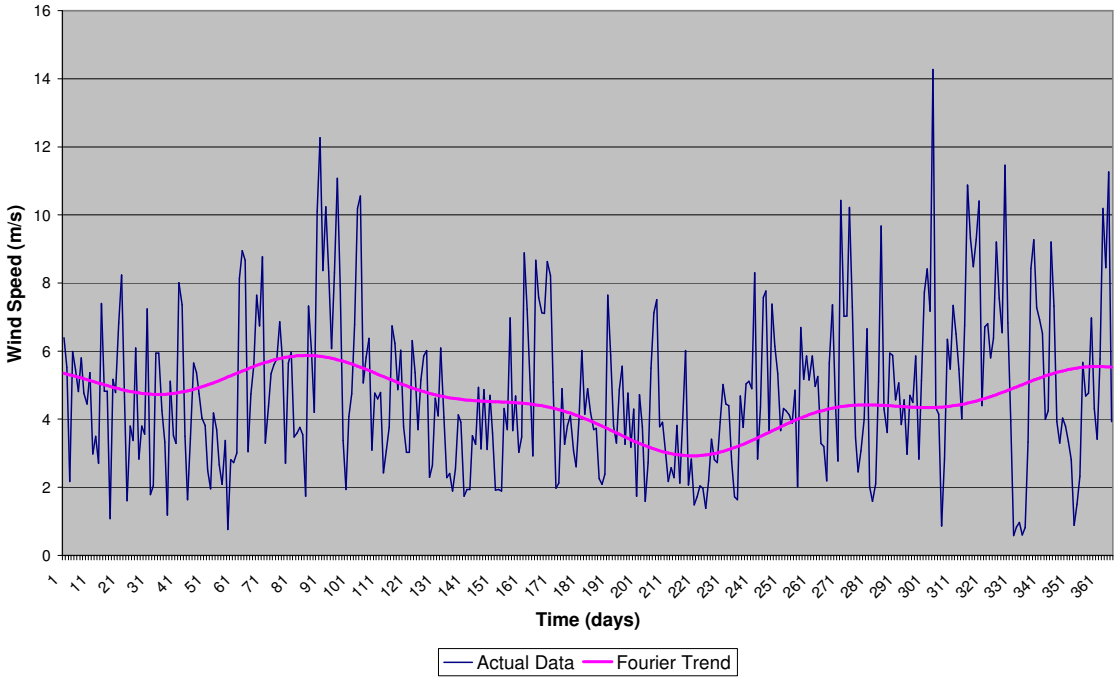


Figure 4.23: Comparison between the Average Fourier Trend and One Year's Actual Wind Speed Data

This remaining random data set is then used as the input to a 5 level Haar discrete wavelet decomposition. The approximation and detail functions are shown in Figures 4.24 and 4.25. These figure shows that the detail and approximation functions are represented as sets/groups of the same number, representing a step wave shape. The higher the level of detail function, the longer the set of data values used representing the lower frequency content. The detail functions required for this decomposition each contain the same number of data points as the original wind speed data series. Therefore to reconstruct the random fluctuations 5 sets of 365 data points would be required. The approximation function is also the same length as the original data series. The key advantage of wavelet decomposition is that it compresses the information contained within these functions into a single data set. The values used to calculate each detail and approximation function decreases as the level number increases. For example, for a data set of 365 points, detail 1 requires 183 values whereas detail 2 requires 92 values, and so on. These values are concatenated together to form a set of wavelet coefficients as shown in equation (4.22):

$$C = (a_5,\ d_5,\ d_4,\ d_3,\ d_2,\ d_1) \tag{4.22}$$

where $\mathbf{a}_5$ are the level 5 approximation coefficients and $\mathbf{d}_5$, …, $\mathbf{d}_1$ are the coefficients required for the five detail functions. These values, for the Haar wavelet, can then be multiplied by a set of scaling and wavelet functions to obtain the approximation and detail functions shown in Figures 4.24 and 4.25.

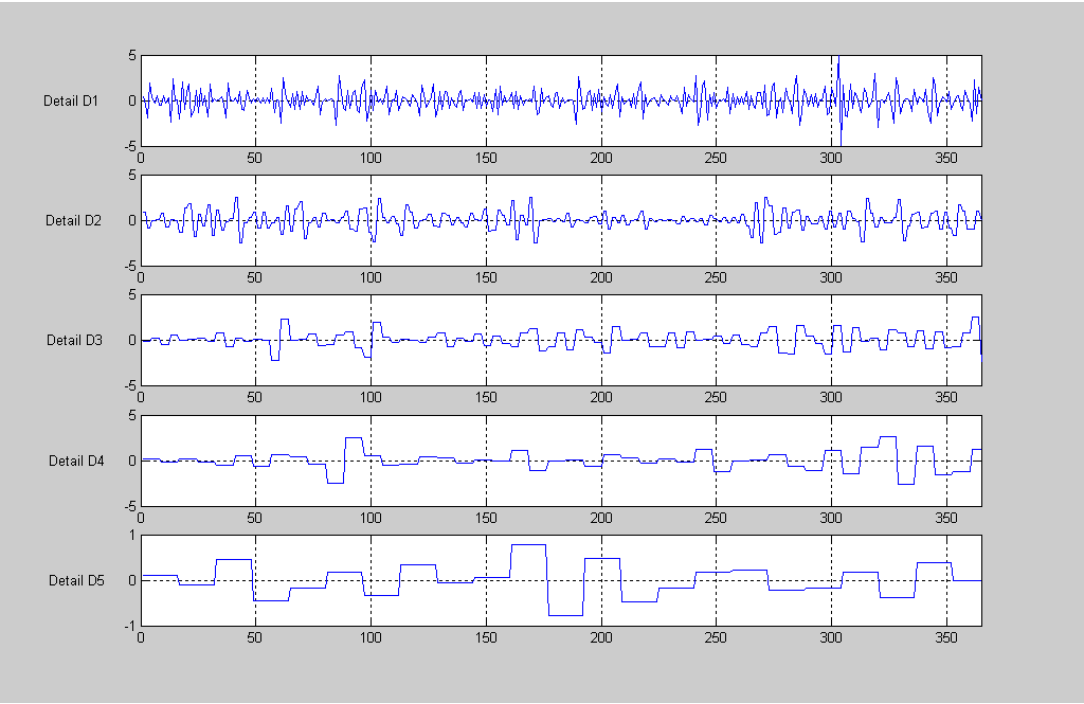


Figure 4.24: Detail Functions for Actual High Frequency Wind Speed Data

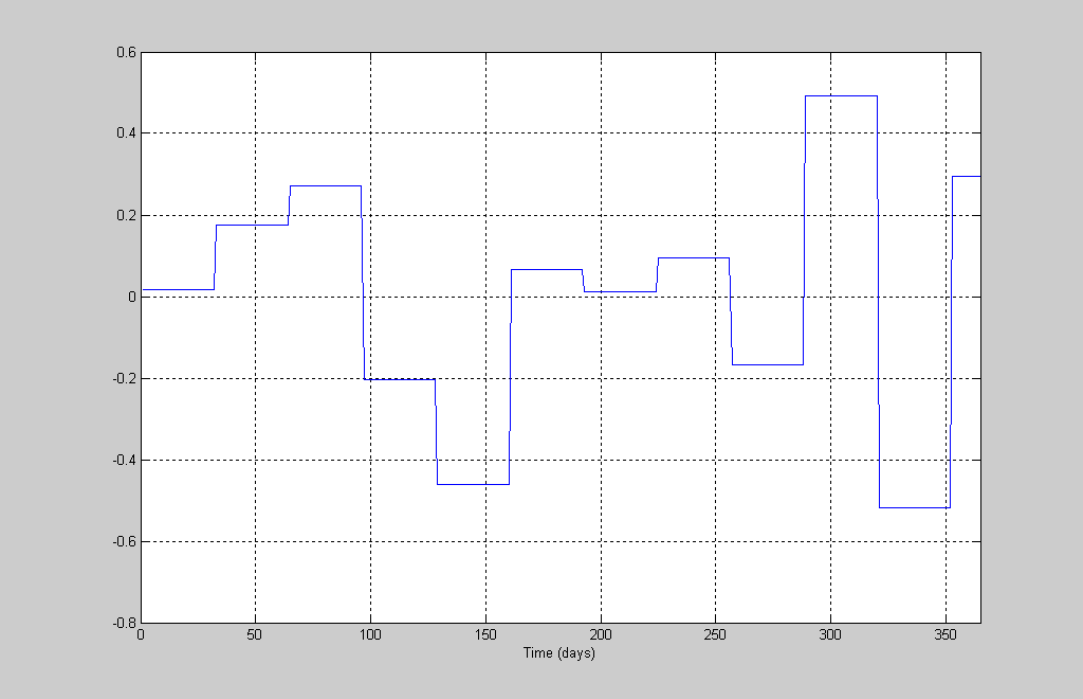


Figure 4.25: Approximation Function for Actual High Frequency Wind Speed Data

Further analysis of these detail functions shows that they all have a normal distribution, with mean values that increase, and standard deviation values that decrease as the level of detail increases. A comparison of the distributions for these 5 detail functions is shown in Figure 4.26. As these detail functions can be summarised by a set of coefficients, it is assumed that these coefficients are also normally distributed. As the inclusion of these detail functions is vital to the accurate estimation of the daily wind speed values, a procedure for generating the wavelet coefficients, and hence each detail function, is required.

Analysis of the approximation function illustrates that it follows a uniform distribution instead of a normal distribution. The wavelet coefficients were selected for modelling instead of the five individual detail functions, as there is a long lag correlation in the time series of the detail functions, requiring the use of high order autoregressive models. This long lag is due to the time frame for each constant value increasing as the level of decomposition increases. Modelling the detail functions individually would increase the number of parameters required to develop a model, reducing the simplicity and generality of the model procedure.

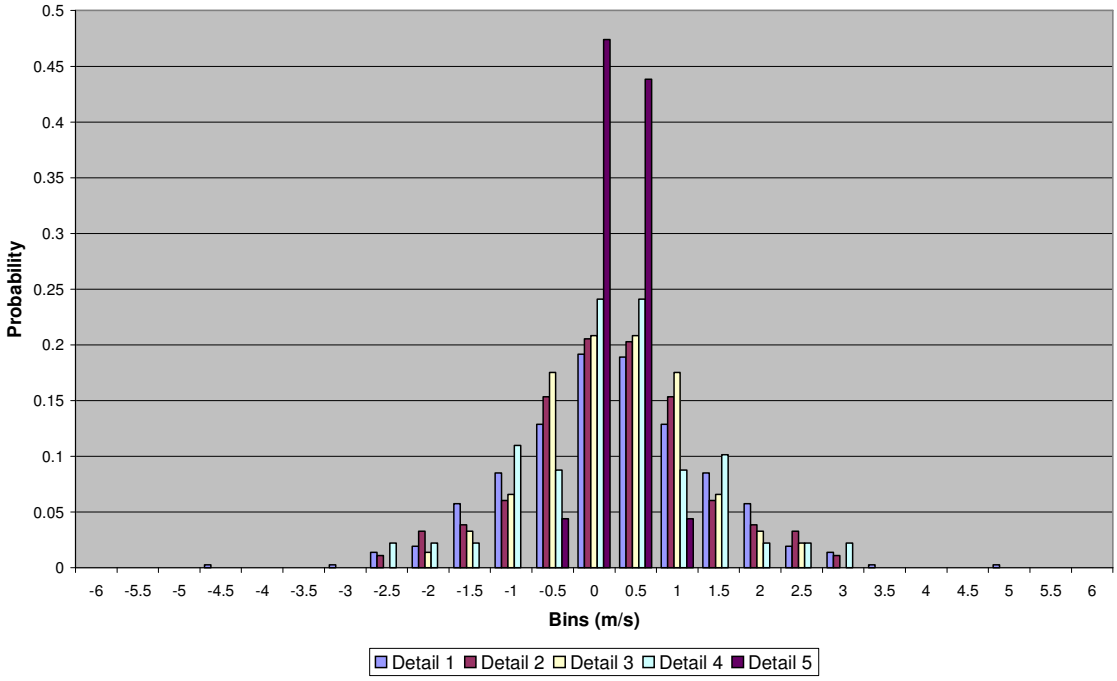


Figure 4.26: PDF Comparison of Detail Functions for One Year of Data

However, in order to maintain the shape of the distribution of the wind speed data it is important that the original input data also have a normal distribution. This condition is often a key requirement for the full DWT to be applied [25]. The underlying trend estimated using a Fourier series has a normal distribution, resulting in the remaining stochastic/high frequency data still having a distribution function similar in shape to that of the original wind speed data. Although this distribution resembles a Weibull distribution, the input parameter ranges from –6 to +10m/s. This range complicates the process required to normalise the wind speed values, as a constant would have to be added before any transformation took place. Based on this, the actual daily wind speed data should be normalised using the power transformation coefficients in Table 4.5, and equation (4.18) before any other process is applied. These transformations do not significantly alter the structure of the daily wind speed data. The same cycles identified previously are still present in the transformed data, but their magnitudes are significantly reduced.

Based on this a new corrected Fourier series covering the same key cycles is proposed to model the common underlying trends in the wind speed data. Table 4.8 shows the coefficients required for this new Fourier series. The differences between the transformed wind speed data and the long-term trend function are calculated for each year. These data sets are then decomposed using a 5 level Haar DWT, and the analysis of these functions demonstrates that again the detail

functions have a normal distribution. The new detail and approximation functions, obtained from the residual of the transformed wind speed data for one year, are shown in Figures 4.27 and 4.28.

The original Fourier trend component, based on the results from Table 4.4, was transformed using the 5-year average power coefficient (from Table 4.5). A comparison between this modified function, and the Fourier trend obtained using the coefficients in Table 4.8 was carried out to assess how similar these two functions were.

The correlation coefficient was calculated and was found to be 0.995. This demonstrates that the two functions are almost identical. Based on this, it may be possible to estimate the underlying trend in the daily wind speed data using the results of the FFT before the power transformation was carried out. The trend obtained (as shown in Figure 4.23) could then have its magnitudes modified to match the ranges of the transformed data. This modification could be applied using a simple linear relationship. The applicability of this would depend on the value of coefficient chosen for the data. As this value varies significantly over the 5 years used in this analysis, more data would be required to obtain an average coefficient value more representative of the transformation required. The advantage of using the average value, and the original Fourier trend is that there is no need to have a large data set that would require normalising before calculating the FFT. The original Fourier trend could also be used without knowing the properties of a number of individual years of daily wind speed data.

| Frequency (cycles/year) | $A_n$ coefficient | $B_n$ coefficient |
|---|---|---|
| 0.8 | 0.1250 | 0.0377 |
| 1.0 | 0.2156 | 0.0919 |
| 1.6 | -0.1024 | -0.1060 |
| 2.0 | -0.1328 | -0.0560 |
| 4.0 | 0.1152 | -0.0820 |
| 5.0 | -0.0308 | 0.0732 |

Table 4.8: Harmonic Components of Transformed Wind Speed Data

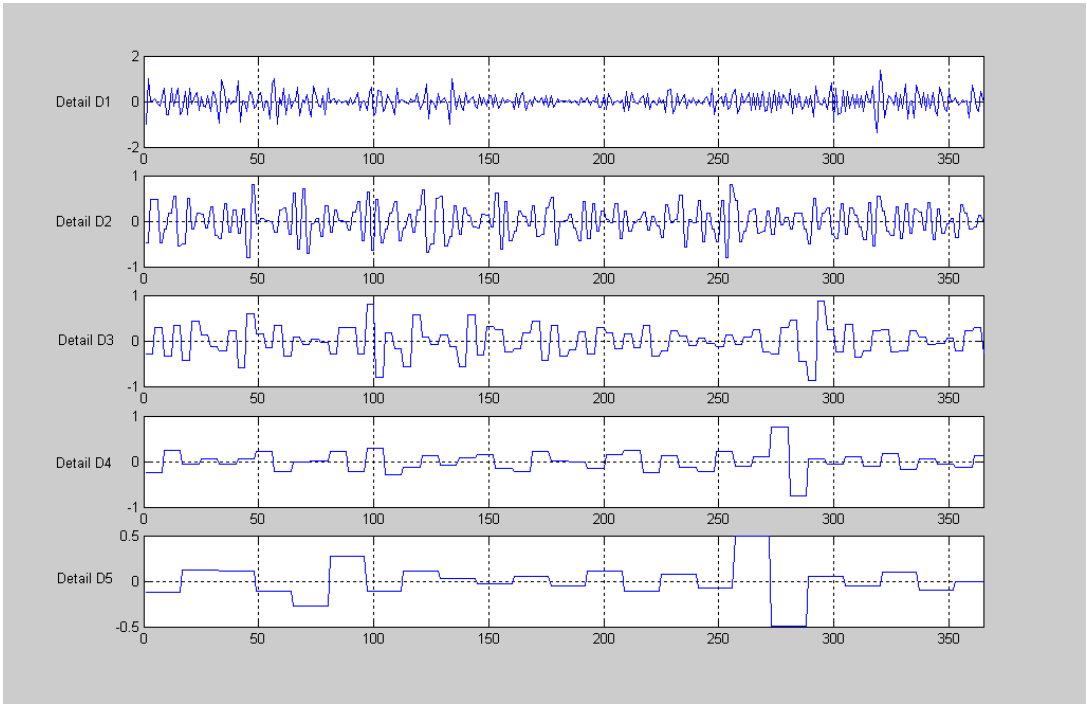


Figure 4.27: Detail Functions For Transformed High Frequency Wind Speed Data

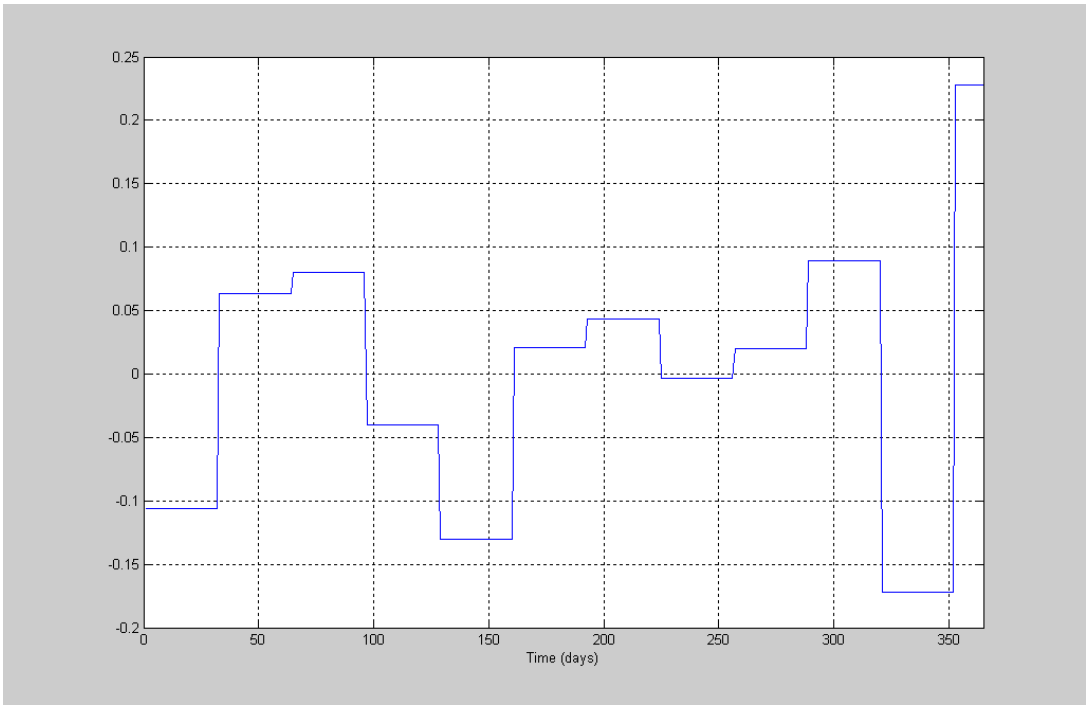


Figure 4.28: Approximation Function for Transformed High Frequency Wind Speed Data

In this modelling procedure it is proposed to generate 5 sets of random white noise of varying length. Each of these data sets can then be non-normalised using the known mean and standard deviation values of the detail coefficients, as shown in Table 4.7. These random data sets represent the coefficients that can then be used to estimate the detail functions. They also have statistical parameters similar to those obtained from the actual wind speed data. Analysis of the wavelet coefficient values for the actual data illustrate that there is no apparent autocorrelation between the coefficient values. The number of data points in each set reduces from detail D1 to D5. For the wind speed data in question, the required number of coefficients for each detail function is shown in Table 4.7. These values result from the fact that the wind speed data is not of length $2^N$. The approximation function coefficients are generated at random using a uniform distribution function. Table 4.7 also shows the 5 year averaged mean and standard deviation values associated with each set of coefficients. Once these coefficients have been generated, they are multiplied by the standard Haar scaling/wavelet functions to form new estimations to the detail functions. These new detail functions are shown in Figure 4.29.

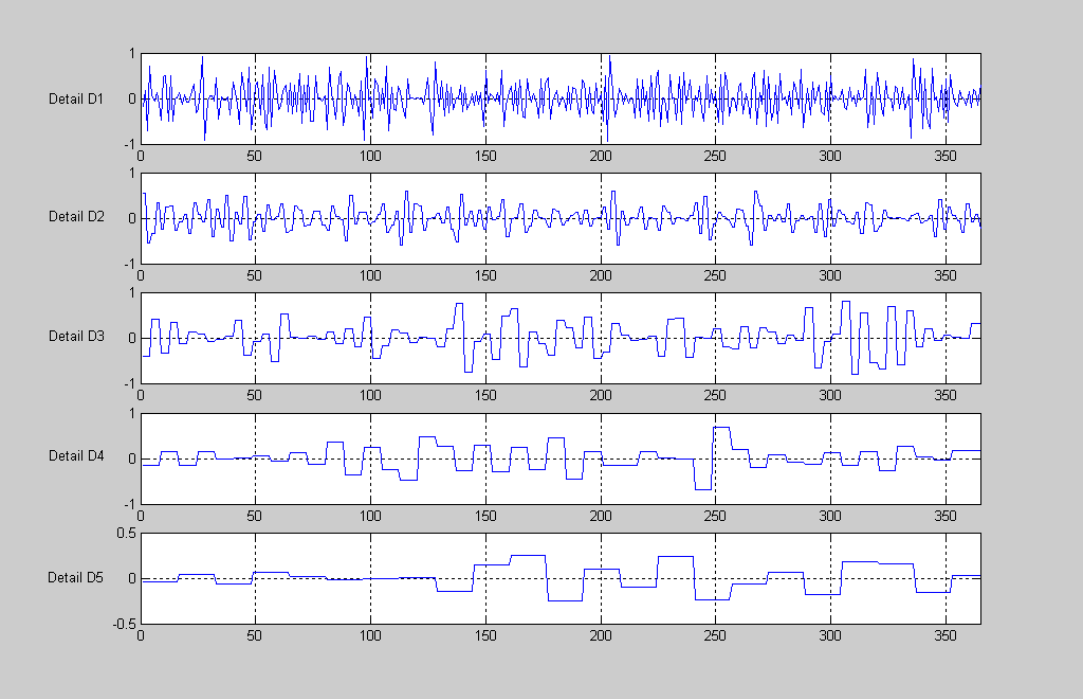


Figure 4.29: New Detail Functions Obtained from Modelling Procedure

These five detail functions and the approximation function, A5, are summed together on a daily basis to obtain a new approximation to the high frequency components of the daily wind speed

data. This output is then added to the long-term trend function obtained from the Fourier series approximation. This new wind speed data series will have a normal distribution due to the modelling procedure, therefore this data needs to be non-normalised with an inverse power transformation, using an average value of 0.36 (as shown in Table 4.5). A comparison between the output of wind speed model, and one year's actual data is shown in Figure 4.30. This shows that the model output is very similar to a year of actual data, and that the magnitudes of both sets of data are very comparable.

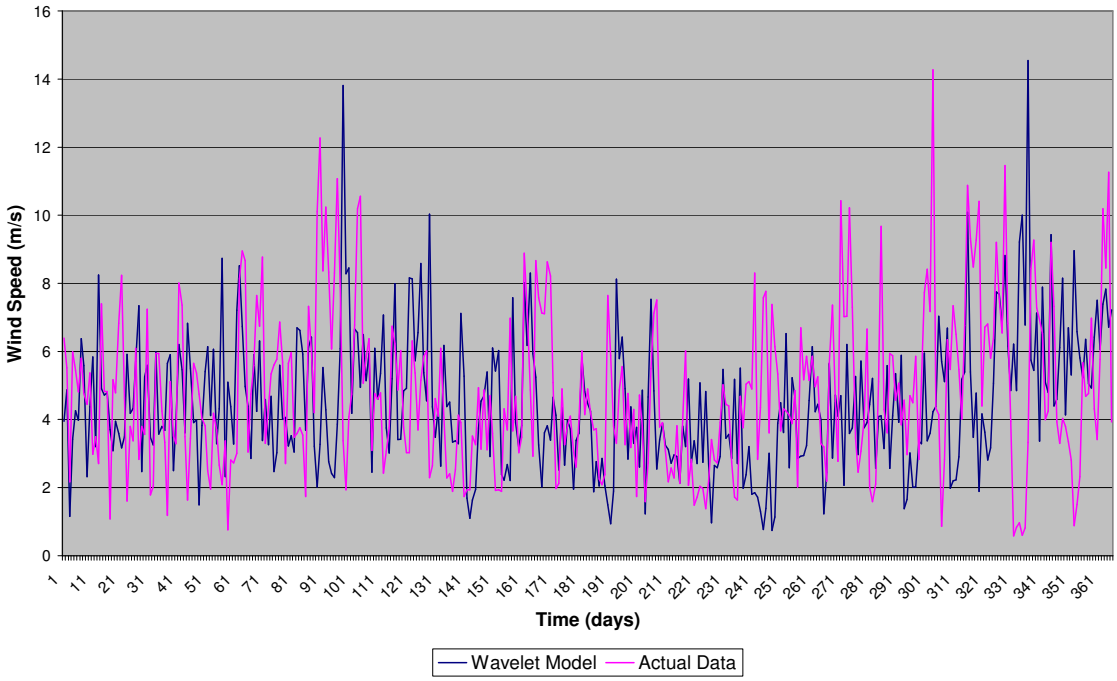


Figure 4.30: Comparison Between One Year of Actual Wind Speed Data and the Wavelet Model Output

The statistical parameters of the Fourier-Wavelet modelled data and those of the actual wind speed data are shown in Table 4.9. The majority of the parameters obtained are comparable with those of the actual data. However, the standard deviation for the modelled data seems lower than the values for each individual year. This could be due to a number of reasons. Firstly the averaging process implemented to obtain the modelling parameters (Table 4.7) used for estimating the detail functions may have affected the range of possible wind speed values from the mean. Secondly the choice of value for $\lambda$ used to non-normalise the results may have affected the spread. An average value from the 5 actual annual parameters was chosen, but this may be too low in comparison to the annual mean of the modelled data. The results in Table 4.9

also show that the modelled data's value of skew is significantly greater than those of the actual data. Again this is probably a result of the choice of the transformation coefficient, λ.

The distribution function of the modelled wind speed data was also calculated, and a comparison between this and the Weibull distribution using the long-term parameters for Aberdeen are shown in Figure 4.31. Although the shapes of the two distribution functions are similar, the modelled data tends to overestimate the occurrence of wind speeds in the range of 3-4m/s. Again this could be due to the averaging process used to obtain the model parameters given in Table 47.

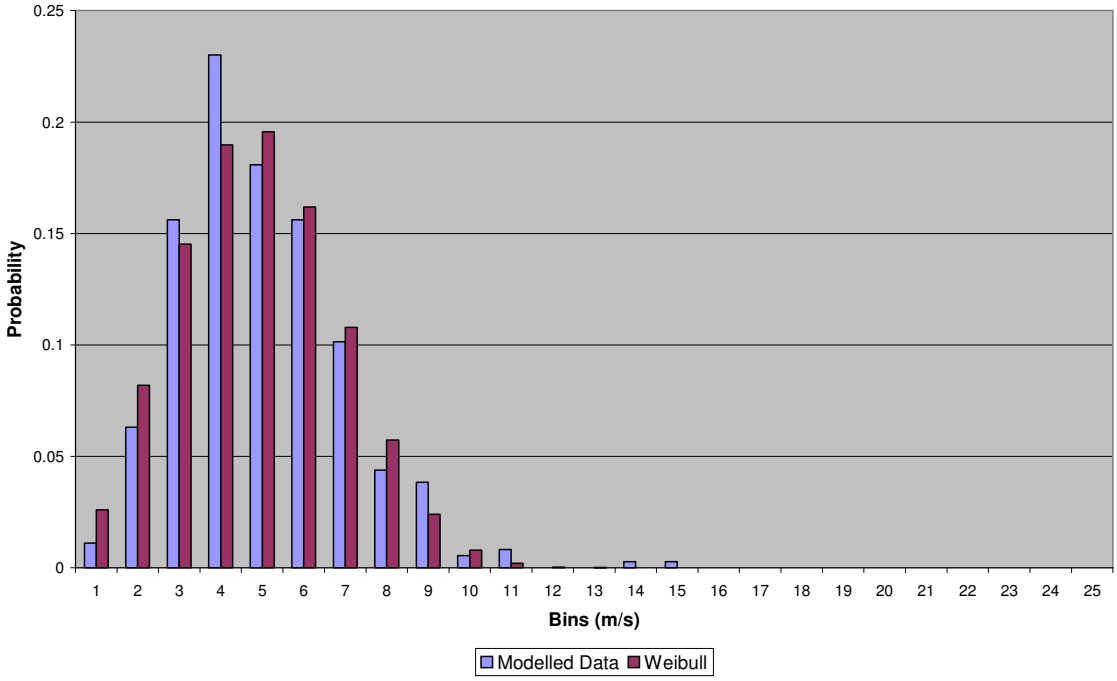


Figure 4.31: PDF Comparison Between the Modelled Wind Speed and the Typical Weibull Distribution

| Parameter | Wavelet Modelled Data | Year 1 | Year 2 | Year 3 | Year 4 | Year 5 |
|---|---|---|---|---|---|---|
| Mean | 4.494 | 5.122 | 4.292 | 4.794 | 4.435 | 4.629 |
| Minimum | 0.740 | 0.987 | 0.836 | 0.579 | 0.850 | 0.773 |
| Maximum | 14.547 | 14.500 | 12.100 | 14.269 | 10.900 | 10.870 |
| Skew | 0.999 | 0.745 | 0.975 | 0.791 | 0.627 | 0.471 |
| Standard Deviation | 1.989 | 2.340 | 2.090 | 2.338 | 2.027 | 2.042 |
| k | 2.393 | 2.754 | 2.407 | 2.159 | 2.966 | 3.388 |
| c | 5.524 | 6.273 | 5.226 | 5.585 | 5.283 | 5.000 |

Table 4.9: Comparison of Annual Statistical Parameters

The combined Fourier-Wavelet modelling process can be summarised using the following steps:

1. Using the coefficients given in Table 4.7, generate a Fourier series approximation, FS(t) to the underlying trend in the daily wind speed data.
2. Generate a new set of detail and approximation functions for the high frequency components using the statistical parameters given in Table 4.7.
3. Add the new approximation and detail functions to the Fourier approximation to obtain a new time series, such that:

$$W_{model} = FS(t) + A_{new} + \sum D_{new} \tag{4.23}$$

   where $A_{new}$ and $D_{new}$ are the approximation and detail functions estimated from the second part of the model procedure.
4. Using an average power coefficient of $\lambda = 0.36$ (as shown in Table 4.5) transform the time series $W_{model}$ into a set of wind speed values, $W_{new}$, with a Weibull distribution, such that:

$$W_{new} = [(W_{model}\,\lambda) + 1]^{\frac{1}{\lambda}} \tag{4.24}$$

Overall, both the proposed wind models generate synthetic sequences of daily data that are statistically comparable with historic data for the chosen location. As it is generally accepted that the distribution of wind speed data can be adequately described by a Weibull distribution function, it was important that the output from both these proposed models procedures also be representative of this distribution function. As can be seen from the model statistical parameters,

the Weibull variables are also within the ranges estimated from the actual data for the chosen location. Based on these comparisons, the model procedures would both be suitable for the use as an input for estimating the energy produced by a wind system.

However, the two procedures have differing levels of complexity. The first procedure is more straight forward, requiring only 5 parameters and 3 equations, whereas the number of parameters required for the second model procedure increases significantly to 25. Most of the discussion on time series models, in Chapter 1 has focused on the use of AR models for individual months. The method proposed here uses the same technique for a complete year, whilst reproducing the main structure expected in the data. The second model proposed, although more complex, has the advantage that it could be used with a different wavelet family. This could increase its accuracy in maintaining both the structure and the statistical properties of the actual data. However, to do this, a new set of model parameters would have to be estimated for each of the different wavelet families. In terms of model simplicity, the AR(1) model proposed would be the best choice and will be used in Chapter 6.

## 4.6 DISCUSSIONS AND CONCLUSIONS

The aim of this section was to provide a method for modelling synthetic data to represent the available daily solar and wind resources for Aberdeen. Two separate models were developed – the solar model was based on a Fourier series approach whereas the selected wind model was based on time series techniques.

The first part of the solar model is supported by a number of other studies [7,8,9] highlighting the ability of this section of the model to be used for any location. Also as the model equation can be normalised in terms of the annual mean, the typical annual time function can be modified to represent more up-to-date data based on other mean values. The stochastic component of the model is generated as white noise, and then adjusted using a set of monthly mean and standard deviation values. Unfortunately, these parameters are location specific and are unlikely to provide an accurate data set for anywhere else. To further develop the model in the future, the possibility of modelling these monthly parameters, potentially as a Fourier series, should be investigated. This would allow the model to be further generalised, with the potential for removing the location dependence.

The selected procedure for modelling the wind speed data also involves a number of stages. This is due to the assumed distribution function of the data not being directly suitable for time

series modelling. Unfortunately, although the use of time series techniques can be generalised for any location, the coefficients used to transform the data's distribution are likely to only apply to Aberdeen. The other key issue with these parameters is that there is no consistency in the magnitude of power coefficient required. This uncertainty may be eliminated if more years of wind speed data were available. The key advantage to this modelling procedure is its simplicity and use of a small number of model parameters. This allows the procedure to repeatedly generate an output quickly, providing a large set of wind speed data.

The Fourier – Wavelet procedure used to model the daily wind speed data could also be developed further. Firstly, a different Wavelet family could be used to decompose and reconstruct the data. The procedure discussed earlier illustrated the use of the Haar wavelet, however another family such as the Debauchies wavelet could better match the short-term fluctuations in the actual wind speed data. Using a different family of functions would affect the number of coefficients required for each detail and approximation function. Secondly, the potential for using just the DWT on the complete daily wind speed time series could be investigated. This would eliminate the use of the generalised Fourier series approximation to the underlying trend in the data, and could potentially reduce the number of parameters required for the modelling procedure.

Overall, both the solar and wind modelling procedures provide an accurate estimation of the original data. The key structures of the data are preserved, as were the main statistical parameters. The procedures could be used to generate large sets of data that can be used as inputs to estimate the energy production of various sizes of photovoltaic systems and wind turbines, ultimately assessing the potential production of such renewable systems without the need for long-term monitoring programs. It would also allow for a more accurate assessment of the energy production of small-scale systems, and what their potential contribution to the UK energy mix could be.

# CHAPTER 5

# ENERGY CONSUMPTION MODELLING

## 5.1 INTRODUCTION

The aim of this chapter is to develop a method for modelling the energy consumption within a domestic building. The model is built from the results of harmonic and autocorrelation analysis of actual consumption data, and is composed of three sections: (1) estimation of daily consumption data; (2) estimation of weekly and daily cycles, if applicable; and (3) the estimation of the random component. The summation of these three components will allow for the generation of a typical data set of energy consumption within a domestic building. This will allow a direct comparison to be made between energy consumption and available renewable energy.

## 5.2 DATA COLLECTION AND ANALYSIS

The main set of data to be analysed is domestic energy consumption. This data set comprises of daily total values of electricity and gas consumption for a semi-detached house in the city of Aberdeen [1]. The data was obtained from meter readings and covers a period of three years from the 1st January 2004 to 31st December 2006. Three years of data was collected to allow for a typical variation of electricity and gas consumption with time to be analysed. The house was constructed during the 1960's making it comparable with a significant proportion of the housing stock – UK housing figures show that 46% of houses are built between 1945 and 1984 [2]. Also semi-detached houses account for about 28% of the housing stock [3]. Obtaining detailed domestic energy consumption on a daily or hourly time scale is problematic and time consuming. However, monthly gas and electricity totals can be estimated from utility bills [4], which can then be used as inputs to the model being created.

The data was analysed in a number of ways including: identifying any patterns and trends through visual inspection; Fourier analysis; and the use of autocorrelation. The statistical parameters and probability distributions of the data were also considered. Some of the data will be analysed using specific energy analysis techniques widely used in energy audits and surveys.

### 5.2.1 Electricity Consumption Analysis

The electricity data was plotted against time for each year. This showed that the variation with time is similar for each year, but no obvious patterns or trends could be easily detected. However, if the three years of data are plotted concurrently, as shown in Figure 5.1, the annual variation is more apparent. This variation is more pronounced during the first year but can still be detected for the other years. It can also be seen that the daily electricity consumption is higher over the winter months. This could be due to a decrease in occupancy during the holiday periods over the summer months and the decrease in actual daylight hours in the winter.

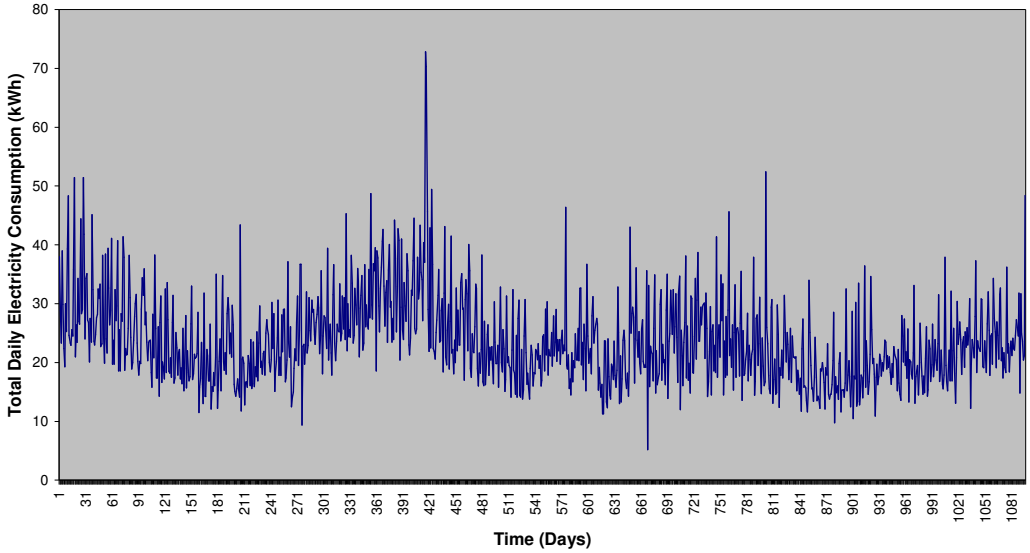


Figure 5.1: Three Years of Variation in Electricity Consumption

A comparison between the weekday electricity values and the weekend values was also made. The value of electricity consumption is slightly higher at weekends and could be attributed to a higher level of occupancy in households during that time period and more appliances being in use. This is supported by the 'Time of Use Survey' [5], which shows that on average less people are working over the weekend. This pattern of weekend consumption being higher persists throughout the whole year.

Comparisons have also been made between monthly electricity consumption and weather variables, in particular temperature [6,7]. These have indicated that there is a strong relationship between temperature and electricity usage, but as these studies were carried out in Spain and America, this relationship could be location dependent especially locations with warmer

climates. By comparing monthly total electricity consumption with the monthly average temperature for Aberdeen, there is a strong relationship between the two and that the temperature data can explain about 90% of the variation in the electricity data. Figure 5.2 shows the annual variation in daily electricity consumtion and daily temperature. It can be seen that the electricity consumption decreases slightly when the temperature increases but there does not appear to be any significant relationship between the two. Calculation of the correlation coefficient supports this as about only 20% of the variation in electricity consumption can be attributed to temperature. Therefore using temperature data to accurately model electricity consumption data will depend upon the required time scale of the data. To investigate the potential ability of renewable systems to provide consumption load matching, daily consumption data would be preferable to monthly data.

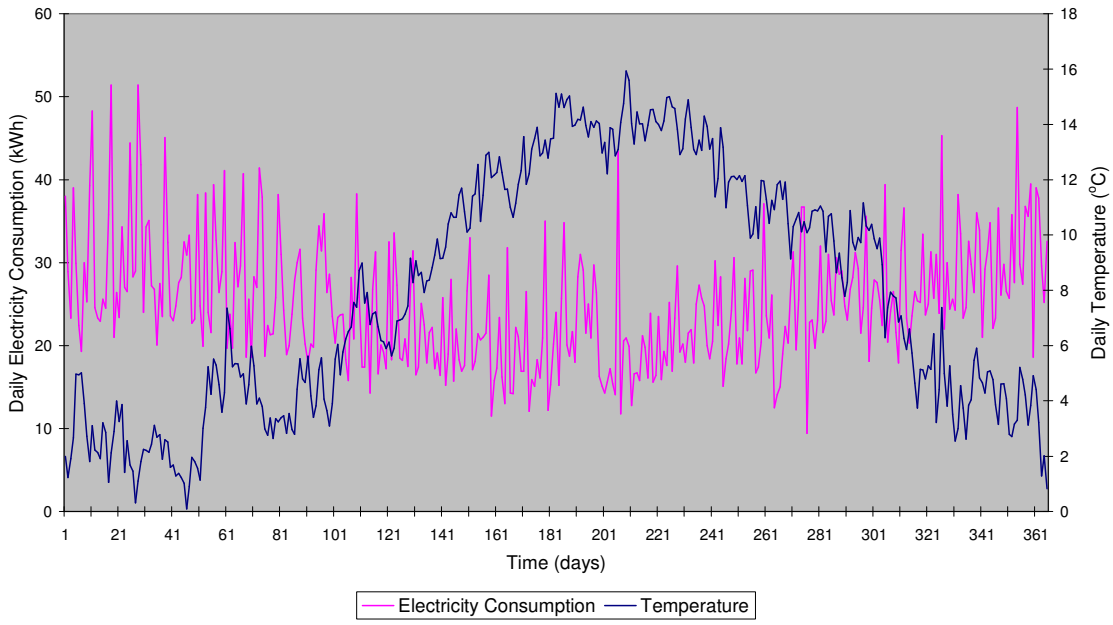


Figure 5.2: Annual Variation in Daily Electricity Consumption and Daily Temperature

Over the three years, the electricity consumption values vary from about 5kWh/day to 55kWh/day, with an average of 21kWh/day. The probability distribution function for each year was calculated and is shown in Figure 5.3. All the years have the same shape of distribution, which is right skewed. This shows that there are some extreme high values of consumption i.e. 75kWh/day, but that the majority of the data lies within the range of 18-35kWh/day. Year 3 shows an increase in the number of days with electricity consumption of 16-17kWh. This could indicate a year with a long, warm summer, or a decrease in occupancy over the year. Based on

the shape of the distribution, it is suggested that the daily electricity consumption could be modelled using a lognormal function.

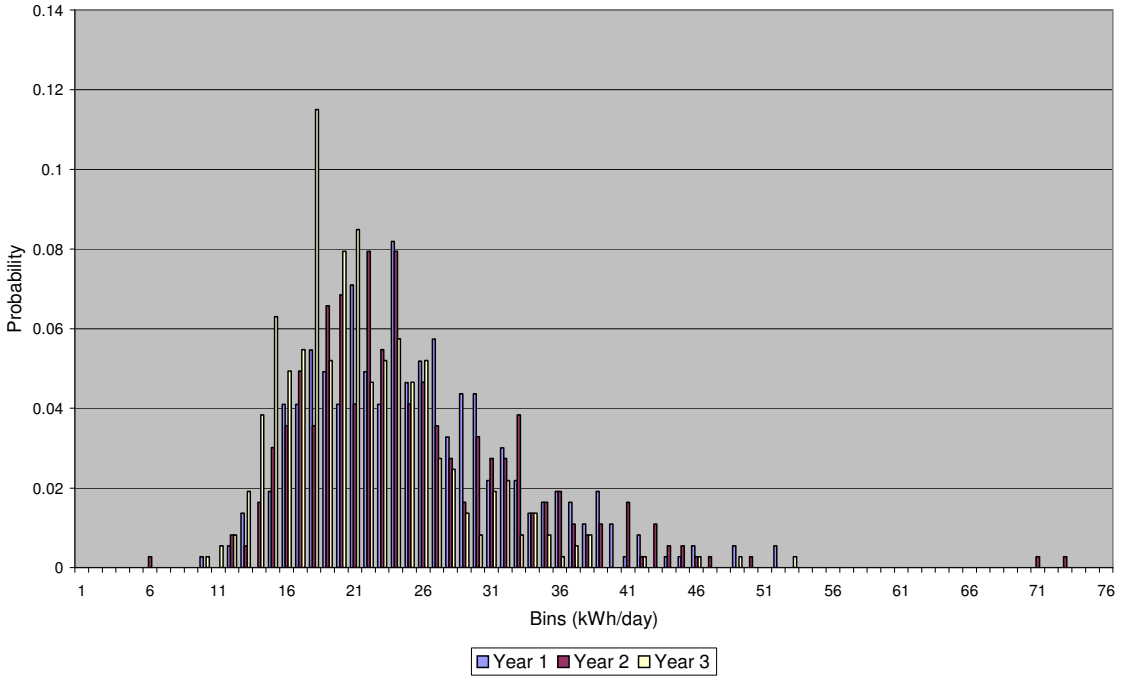


Figure 5.3: Electricity Consumption Probability Distribution Functions

Harmonic analysis was carried out on the electricity data using the Fast Fourier Transform (FFT) to identify the important features or cycles of the data series. The FFT was taken for each year individually and for a series of all three years combined. Each year has the same significant cycles. These are also present in the series of three years and are shown in Figure 5.4.

Apart from the average, or dc component, there are 4 significant peaks at specific frequencies. These frequencies correspond to a yearly cycle i.e. 1 cycle/yr, a cycle of 7 days – accounting for the weekly variation, and two cycles at 3.5 days and 2.33 days. This is supported by the work of Weron et al [8] who carried out frequency analysis of two years of daily electricity loads for residential and commercial customers in California. The periodogram of their data also showed well-defined peaks at cycles of 365 days, 7 days, 3.5 days and 2.33 days. The only difference between the two data sets is that Weron et al's most significant peaks were the annual and weekly cycle whereas the data for Aberdeen shows that the cycle at 3.5 days is more significant than the weekly cycle.

In general the frequency peaks shown in Table 5.1 can be assumed to be always present and always significant for daily data. The harmonic analysis of the daily data cannot provide any information about the daily variation in consumption over the day. This is due to the value of the sampling frequency of the data. For more information about the variation in electricity consumption, a higher level of measurement would be required i.e. hourly or minute-by-minute data. As well as visual inspection, the frequency peaks can also be shown to be significant by calculating their contribution to the overall variance of the data. Each cycle's variance contribution is also shown in Table 5.1 reinforcing the observations that the annual cycle and the 3.5-day cycle are the most important.

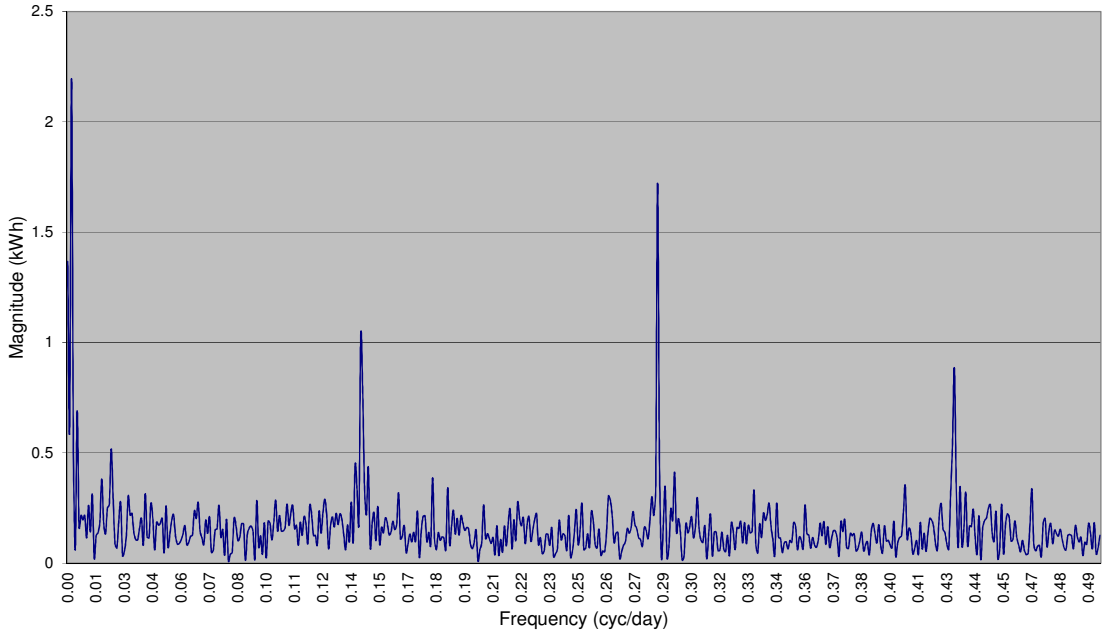


Figure 5.4: FFT of Three years of Electricity Data

| Frequency | Frequency Value (cycle/yr) | Time Value (days) | % Contribution To Variance |
|---|---|---|---|
| $f_1$ | 0.9999 | 365.33 | 17 % |
| $f_2$ | 51.9995 | 7 | 3.70 % |
| $f_3$ | 104.2380 | 3.50 | 10.50 % |
| $f_4$ | 156.5200 | 2.33 | 2.77 % |

Table 5.1: Three-Year Average Frequency Values

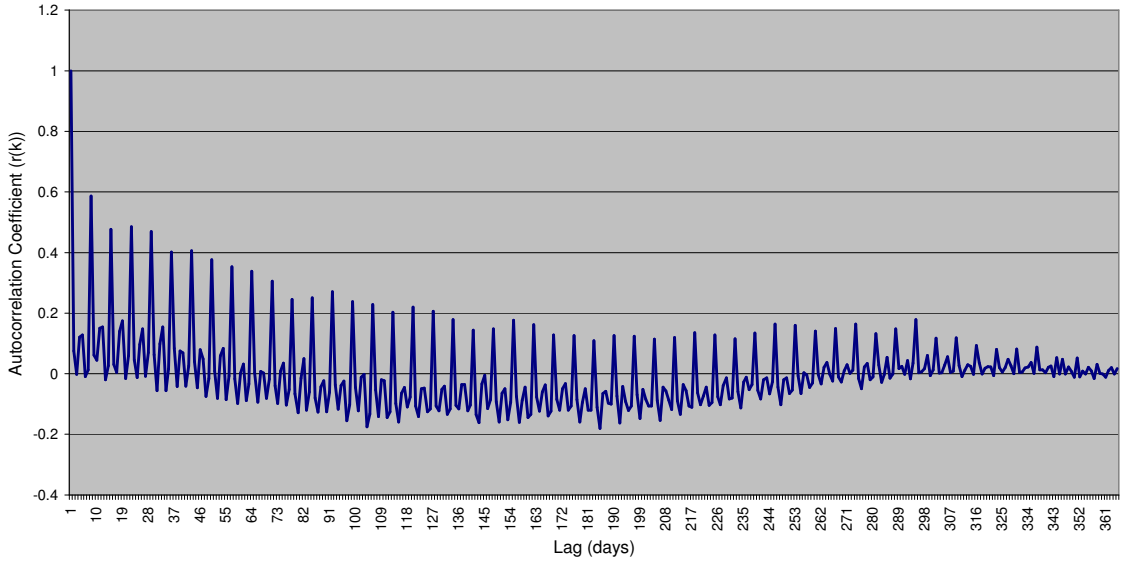


Figure 5.5: Autocorrelation Plot for One Year of Electricity Consumption Data

Looking at the autocorrelation of the daily electricity data also reinforces the importance of those cycles. The autocorrelation plot of the electricity is shown in Figure 5.5. The plot can be separated into two main components – the overall shape and the rapid fluctuations that decrease with time lag k. The overall shape of the autocorrelation plot represents the yearly variation in the data and the rapid fluctuations are caused by the daily variation, in particular cycles of 3.5 days and 7 days. The autocorrelation plot also contains some random fluctuations that may be associated with occupancy patterns, holiday periods and weather variables. The shape in the autocorrelation plot also decays, representing a decrease in the strength of the relationship between the sequential data points as the time lag increases.

### 5.2.2 Gas Consumption Analysis

The gas consumption data was plotted over the three year measurement period (Figure 5.6) and showed that there was an identifiable flat section or 'base load' over the summer months (July – September), and that there was a clear pattern due to the annual variation. This annual pattern indicates that the heating load is weather dependent, as would be expected, in that the consumption is greater in the colder months and vice versa. The pattern in consumption data is the same each year and the base load section lasts for the same period of time also. The base load has some small fluctuations to it but is relatively flat over the three-month period.

Therefore it can be assumed that the base load is not as strongly related to the weather as the rest of the heating consumption. The base load, for this dwelling, is caused only by the hot water heating load but for other dwellings it may also due a gas cooking load.

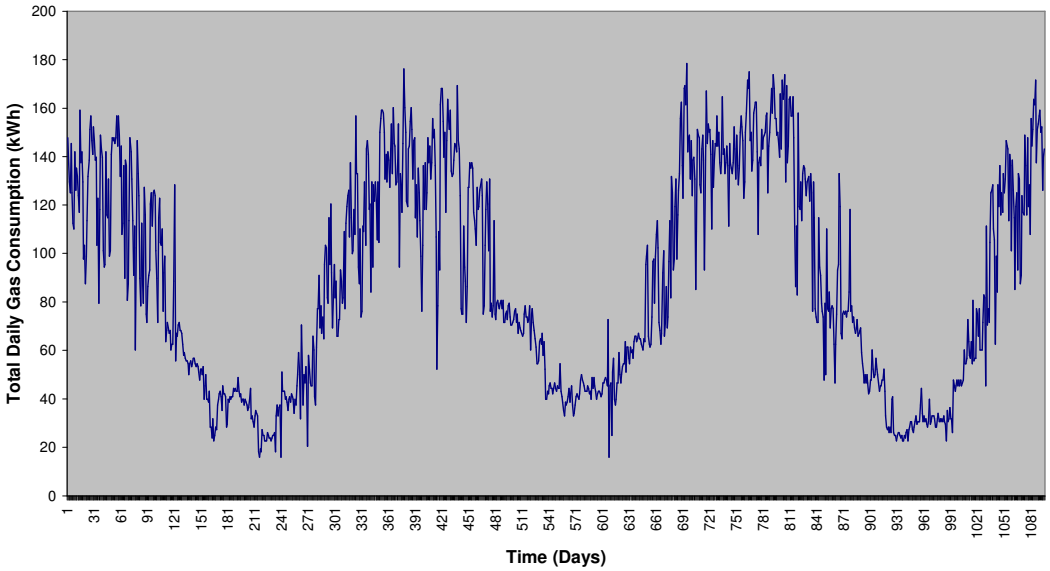


Figure 5.6: Three years Variation in Gas Consumption

Using standard energy analysis techniques, the magnitude of the average base load can be estimated from the 'Performance Line' of the dwelling (Figure 5.7). This is obtained from a scatter plot of monthly total gas consumption against degree-days. Degree-days are commonly used in energy analysis techniques [9] and are a measure of how cold the weather is and how long the cold weather lasts. They are calculated as the sum of the difference between the 'base' temperature of the building and the outside temperature over a specified period such as a day or a month. The base temperature is the minimum outdoor temperature at which no heating is required. Standard degree-day values for the UK are calculated using a base temperature of 15.5°C. The correlation coefficient value from this straight line helps to validate the accuracy of the relationship between the two variables [10] and shows that there is a strong relationship between degree-days and monthly total gas consumption. The base load is the y-axis intercept of the Performance line and is approximately 272kWh/month or about 8kWh/day. The actual hot water load can be calculated using a variety of methods [10,11] to provide a comparison with this figure.

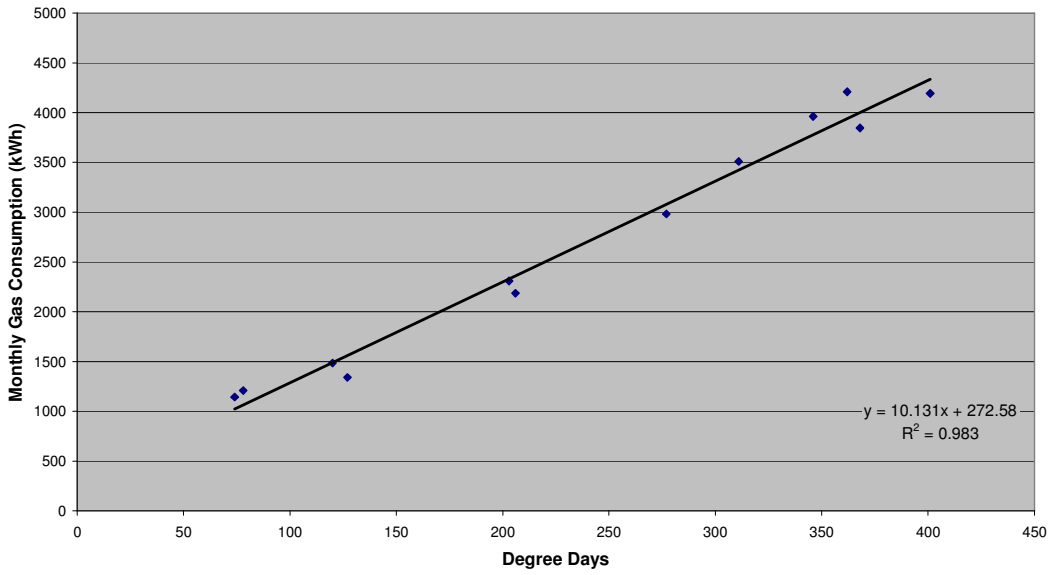


Figure 5.7: Average Performance Line

As the degree-days value is dependent upon the outdoor air temperature, the relationship between average daily consumption per month and average daily temperature was examined as shown in Figure 5.8. The best-fit straight line through these points is known as the 'Thermal Performance Line' of the dwelling, and the relationship between the two variables is expressed as:

$$y = -9.855\,x + 164.54 \qquad (5.1)$$

where y is the average daily total consumption (kWh) and x is the average daily temperature (°C). The thermal performance lines allows for an estimation of the building's base temperature. From equation (5.1) it can be seen that the base temperature of the dwelling is about 16.7°C.

If the three-year average daily consumption values were plotted against the average daily temperature for one year, the scatter about this 'Average Daily Thermal Performance Line' would be evenly distributed above and below the line. Between 0°C - 8°C the scatter is mainly above the line and from 8°C - 16°C the majority of the scatter is below the line. This will be illustrated later in Figure 5.21. This could represent some variation between the heating period and the non-heating period.

The average performance line, as shown in Figure 5.7, could be used to estimate the gas (heating) consumption load for other years as it gives an indication of how much extra fuel is required for an increase in degree days i.e. when it gets colder. This would allow for some estimation of monthly heating load if degree-day values were known for a number of years. However, it would be more useful to be able to estimate the daily total gas (heating) consumption.

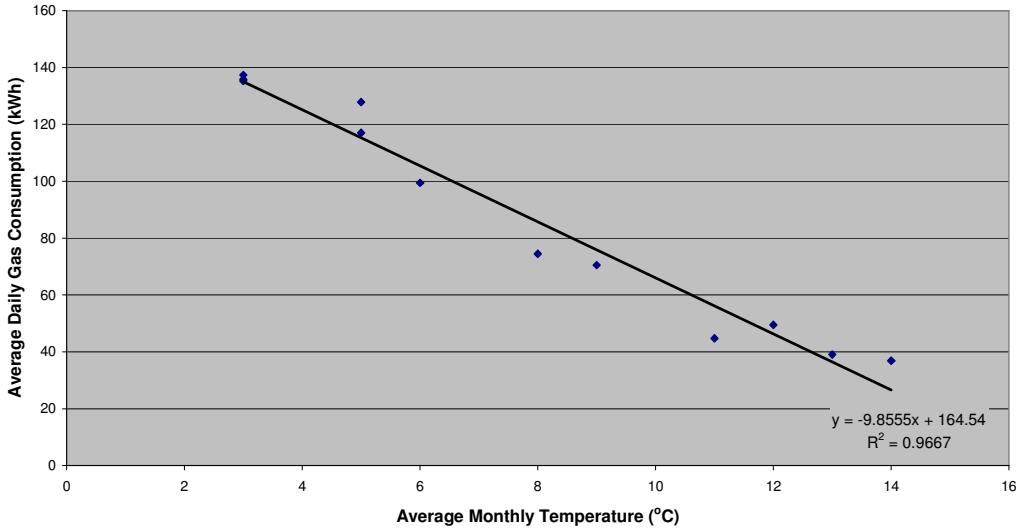


Figure 5.8: Average Thermal Performance Line

Over the three years the gas consumption ranges from 15kWh/day to 180kWh/day, with an overall average of 88.6kWh/day. The probability distribution function for each year is shown in Figure 5.9. This shows that all three years have the same pattern of variation and same shape of distribution. The distribution function is bimodal, with peaks at 40-50kWh/day and 140kWh/day. These represent the difference in consumption from summer to winter. Year 2 shows a lesser occurrence of consumption values within the range of 10-30kWh/day. Along with the information in Figure 5.8 this shows that there was a higher level of consumption over the summer months. This could be due to a number of factors such as the external temperature, or a change in occupancy levels resulting in an increase in hot water consumption for example.

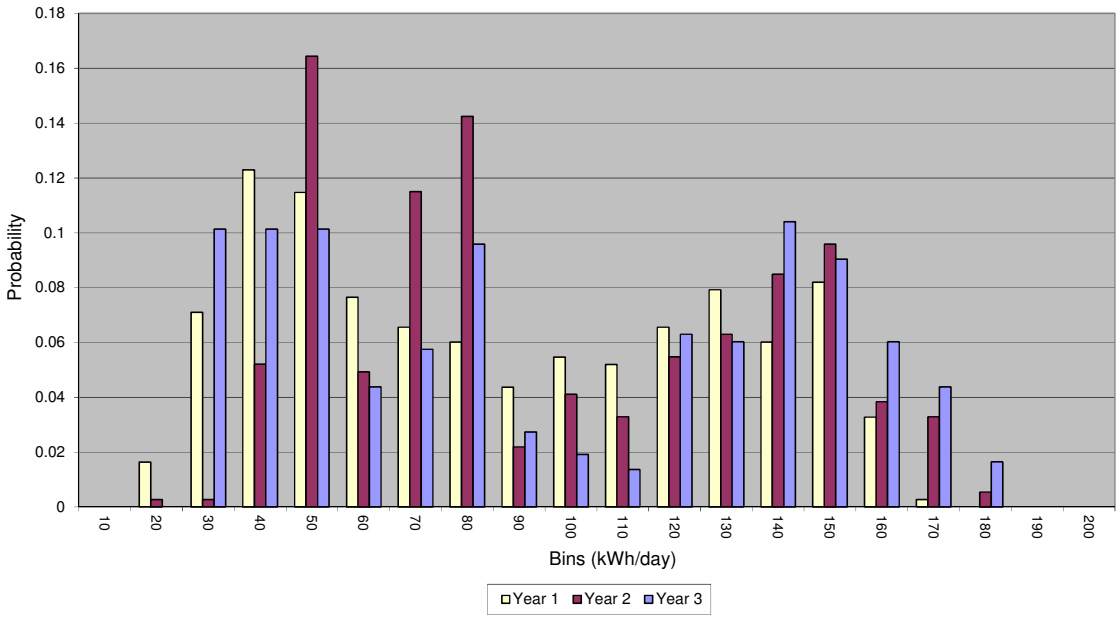


Figure 5.9: Gas Consumption Probability Distribution Functions

## 5.3 ENERGY MODELLING TECHNIQUES

### 5.3.1 Electricity Consumption Model

From the analysis of the electricity data it can be seen that the electricity consumption is composed of a trend or 'deterministic' part, associated with the cycles mentioned previously, and a random or 'stochastic' component. If the daily electricity consumption data, E, is indexed by day of the year, t = 1,2…365, where t = 1 is 1st January and t = 365 is 31st December, the decomposition of the data can be described as:

$$E(t) = ED(t) + ES(t) \tag{5.2}$$

where ED(t) represents the deterministic part and ES(t) the stochastic part of the data. Electricity consumption data can be modelled in two steps.

As discussed previously (CH4, p29), deterministic data can be modelled using the Fourier series. Daily data would be required to obtain the Fourier coefficients for the yearly and weekly cycles. However, as it is not always possible to obtain energy consumption data on that time scale a method for obtaining daily data from monthly averages will be investigated. As the data is periodic, there are a number of possible ways to approximate daily data including polynomial

fitting, interpolation, and splines. The Fourier series was shown to provide a better approximation to data than polynomials [12], therefore methods including polynomials and splines were discounted. In order to obtain daily data easily and quickly only two options were considered. The first is based on the work of Epstein [13] and involves using the harmonic content of the monthly data to estimate the daily values. This method has only been used on climate data, which is also periodic, and as an input requires the average daily climate variable for each month i.e. 12 values for one year. For electricity this would be the average daily consumption per month. The process is very straightforward and involves taking the FFT of the 12 values to find the coefficients for a Fourier series of the data. A new time vector is then created for daily values based on the monthly time scale and month number. More simply the 12-month time vector is divided into 365 equal sections. This new time vector and Fourier coefficients are recombined in a Fourier series of the form:

$$y(t) = a_0 + \sum \left[ a_n \cos\left(\frac{2\pi n t}{12}\right) + b_n \sin\left(\frac{2\pi n t}{12}\right) \right] \tag{5.3}$$

where $a_0$ is the monthly average daily value, t is the new time vector, and $a_n$ and $b_n$ are the coefficients obtained from the original data.

The second potential method was developed by Rymes and Myers [14] and is based on an interpolation algorithm. The algorithm repeats itself until the desired resolution of data is obtained. For example, if the inputs are the daily average values for each month, and 365 daily values are required, then the algorithm repeats 365 times. Based on the twelve average daily consumption values, a square waveform is created as the input to the algorithm. This waveform assumes that the input parameters are initially constant for each month. This waveform is then repeatedly averaged until a smooth approximation of the 365 daily consumption values is obtained. The algorithm is straightforward in that each data point it calculates is the average of that point and the two adjacent points. However, the beginning and end of the data i.e. the first and last days of the year are treated slightly differently. The first data point, representing the first day of the year, is the average of the last data point, the first data point and the second data point. A similar process is used for the last data point. Mathematically the algorithm would be represented as:

$$N(t) = \frac{O(t-1) + O(t) + O(t+1)}{3} \tag{5.4}$$

where N represents the new data approximation and O represents the original, or previous loop, data points. As well as this a 'difference term' is included in the algorithm. This difference term is used to calculate the difference between the original data and each iteration, with the aim of preserving the average over a specified time period e.g. each month.

Both methods were tested on the daily average electricity consumption for each month for one year. The total electricity consumption for each month was calculated from the measured data and the average daily total electricity consumption per month, $E_{ave,}$ was found by dividing the monthly total, $E_{tot}$, by the number of days in each month i.e.

$$E_{\text{ave}}(i) = \frac{E_{\text{tot}}(i)}{D(i)} \tag{5.5}$$

where i = month number i.e. 1 = January 2 = February, and D is the number of days in the relevant month. The results of both methods were compared with each other, and with the actual measured daily values (Figure 5.10). Both methods maintain the monthly average value, and Table 5.2 shows a comparison of the statistical parameters of the both sets of the approximated data. As can be seen from Figure 5.10, both approximation methods produce similar results and appear to estimate the annual variation present in the data. This can also be shown by the structure of both the approximations.

| Statistical Parameter | Fourier Data | Interpolated Data |
|---|---|---|
| Mean | 21.258 | 21.240 |
| Standard Deviation | 2.417 | 2.440 |
| Skew | -0.088 | -0.120 |
| Coefficient Of Variance | 0.114 | 0.155 |
| Minimum | 16.811 | 16.748 |

Table 5.2: Comparison of Statistical Parameters of Both Approximated Data Sets

Both these methods provide a simple way of estimating daily data from monthly values. However, based on the ease of use and reduced computational difficulty, the method based on the harmonic content [13] will be used in the remainder of the modelling process. This method

was also used due to the periodic content of the actual domestic electricity data and will be used to calculate part of the deterministic data.

The next step is to introduce the weekly harmonics. From the FFT (Figure 5.4) of the measured data, it was seen that the weekly cycle and associated harmonics is also present. These cycles will be estimated using a Fourier series approximation, as this is the simplest way of representing periodic data. The three-year average values of these cycles were shown in Table 5.1. All these frequency components are present each year but their magnitudes differ slightly, but the importance of each component remains the same.

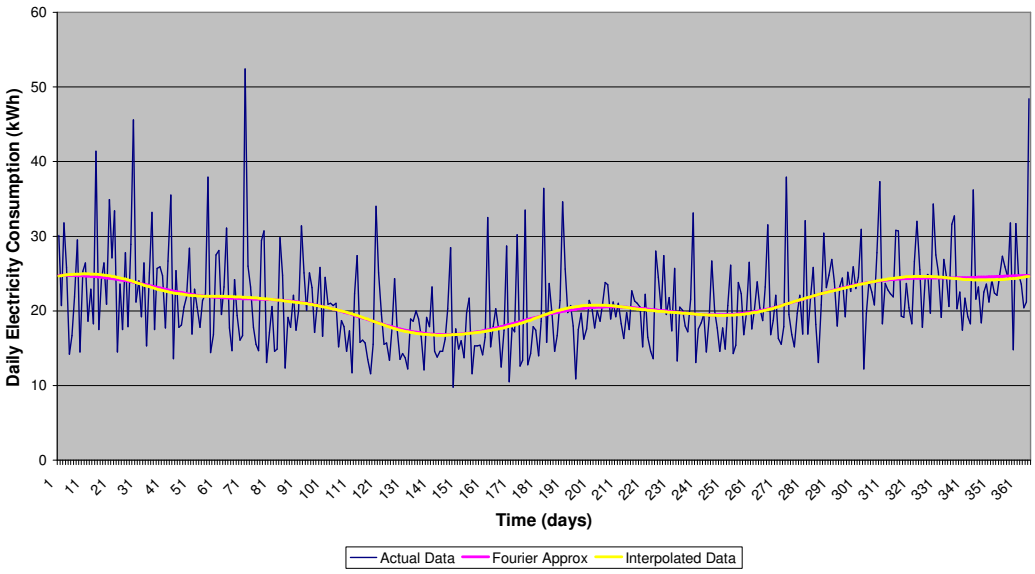


Figure 5.10: Comparison of Daily Estimation Methods For One Year

Applying the frequency values from Table 5.1, a Fourier series of these daily and weekly components is calculated using:

$$ew = 1.62\cos\left(\frac{103\,\pi\,t}{N}\right) + 1.25\sin\left(\frac{103\,\pi\,t}{N}\right) - 0.24\cos\left(\frac{208\,\pi\,t}{N}\right) - 3.44\sin\left(\frac{208\,\pi\,t}{N}\right) - 1.057\cos\left(\frac{313.33\,\pi\,t}{N}\right) + 1.417\sin\left(\frac{313.33\,\pi\,t}{N}\right) \quad (5.6)$$

for t = 0 to 365, and N = number of days within time period.

These values are added to those approximated from the monthly values to give the overall deterministic component of the electricity data. Therefore the deterministic model can be represented by:

$$E D(t) = e_{\text{app}}(t) + e w(t) \tag{5.7}$$

where $e_{app}(t)$ are approximated daily values, based on equation (5.3) and ew(t) are the weekly frequency components.

The overall trend component for one year is calculated and is shown with the actual data in Figure 5.11. As can be seen, only about 30-50% of the variation in the data is represented in the overall trend. If only 12 data points were known, the actual magnitude of the frequency contributions in Table 5.1 could not be calculated. To make the model applicable to dwellings of varying size, the coefficients from the Fourier series, equation (5.6), can be normalised in terms of the overall mean value, which could be calculated from the 12 monthly values. Each coefficient can be expressed as a proportion of the mean. A similar process was used by Riddell and Manson, [12], which also used the Fourier series to estimate the data. Therefore, these weekly/daily cycles can be adjusted for different years with different mean values, as can the annual data. The structure of this trend component is beginning to resemble the structure of the actual data since the overall shape comes from the monthly to daily data and some of the fluctuations come from the weekly cycles.

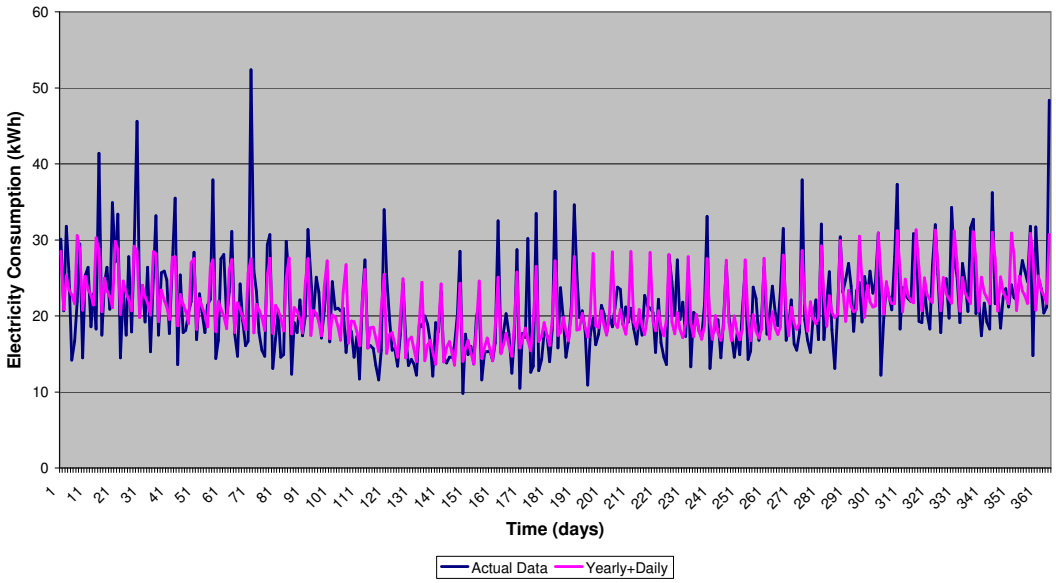


Figure 5.11: Deterministic Component of Electricity Model For One Year

However, there is still a random section of the data. This can be obtained by taking the difference between the actual electricity consumption data, E(t), and the estimated consumption, $\hat{E}(t)$. This will be referred to as the stochastic component, ES(t):

$$ES(t) = E(t) - \hat{E}(t) \tag{5.8}$$

The distribution of this error is approximately normal with a mean value of 0.0014 and a standard deviation of 4.569. The stochastic component or 'residual' should ideally be stationary, as the trend component has been removed using the deterministic model. To test for stationarity in the data, the autocorrelation function and partial autocorrelation function were calculated for each month. The values of these for each month lie within the values of the 90% confidence limits, calculated using $\pm 2/\sqrt{N}$ , where N is the number of data points, except for the r(0) value of the autocorrelation plots. This indicates that the covariance is 0 for all values except t = 0 (or k = 0) which shows that the data is stationary. The same process was carried out for the whole year of the stochastic component. Apart from some small residuals associated with the weekly cycles, the majority of the data lies within the confidence limits so it can be assumed that the data is stationary over the year.

The individual monthly mean values and monthly standard deviation values were also examined. The mean values ranged from –0.18 to +0.18, and the standard deviation varied from 3 to 6.5. There was no obvious pattern in the variation of these values over the year.

It is often assumed that this type of stochastic data can be modelled as white noise [15]. White noise is a series of random stationary variables with zero mean and standard deviation equal to the variance at t = 0, i.e. the standard deviation is approximately 1. These parameters are the same as those of a standard normal variable:

$$Err = \frac{ES(t) - \mu_{ES(t)}}{\sigma_{ES(t)}} \tag{5.9}$$

Where Err is the residual of the data series, $\mu_{ES(t)}$ is the global mean value of the residual, and $\sigma_{ES(t)}$ is the standard deviation of the residual These values have already been calculated as $\mu_{ES(t)}$ = 0.0014 and $\sigma_{ES(t)}$ = 4.569. The stochastic component was transformed, using equation (5.9), into a standard normal variable with mean of 0 and standard deviation of 1.

Assuming that the residual Err(t) ≅ ε(j) i.e. white noise, random data for the whole year can be calculated using a standardised normal variable. These values are then transformed using equation (5.9) in the form:

$$ES(t) = Err\,\sigma_{ES(t)} + \mu_{ES(t)} \tag{5.10}$$

where Err is the random variable generated or white noise, and the mean and standard deviation values are the same as those of the original data. Therefore the stochastic component of the electricity model is found from:

$$ES(t) = 4.569\,\varepsilon(t) + 0.0014 \tag{5.11}$$

This result can also be generalised using the mean and standard deviation values from all three years of electricity data. The values of the stochastic component are then added to the data based on the annual and weekly cycles. The results of this can be seen in Figure 5.12, showing a similar pattern in variation. This approximated data can be compared with the original data in a number of ways. Firstly, the FFT of both the original data and the approximated data were calculated and are shown in Figure 5.13. From this figure it can be seen that the two data sets are very similar – the mean values (dc component) are very similar and all the significant cycles are present in the approximated data (their magnitudes are also very similar).

The autocorrelation of the approximated electricity data was also compared with that of the actual data (Figure 5.14). The overall shape over the year is the same although there is some difference in the magnitudes of the peaks on the plot. This could be due to the beat frequencies, associated with the cycles at 7 days, 3.5 days and 2.33 days not being included in the model. However, these differences are within ±10% of the error of the actual data, which is an acceptable tolerance for this model.

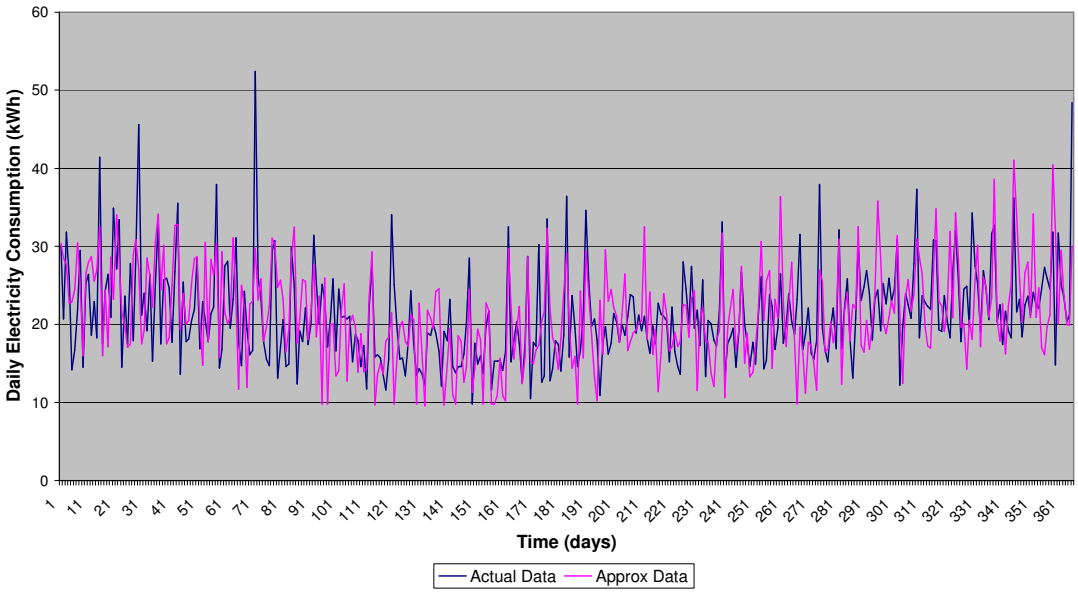


Figure 5.12: Comparison between Actual Data and Approximated Data

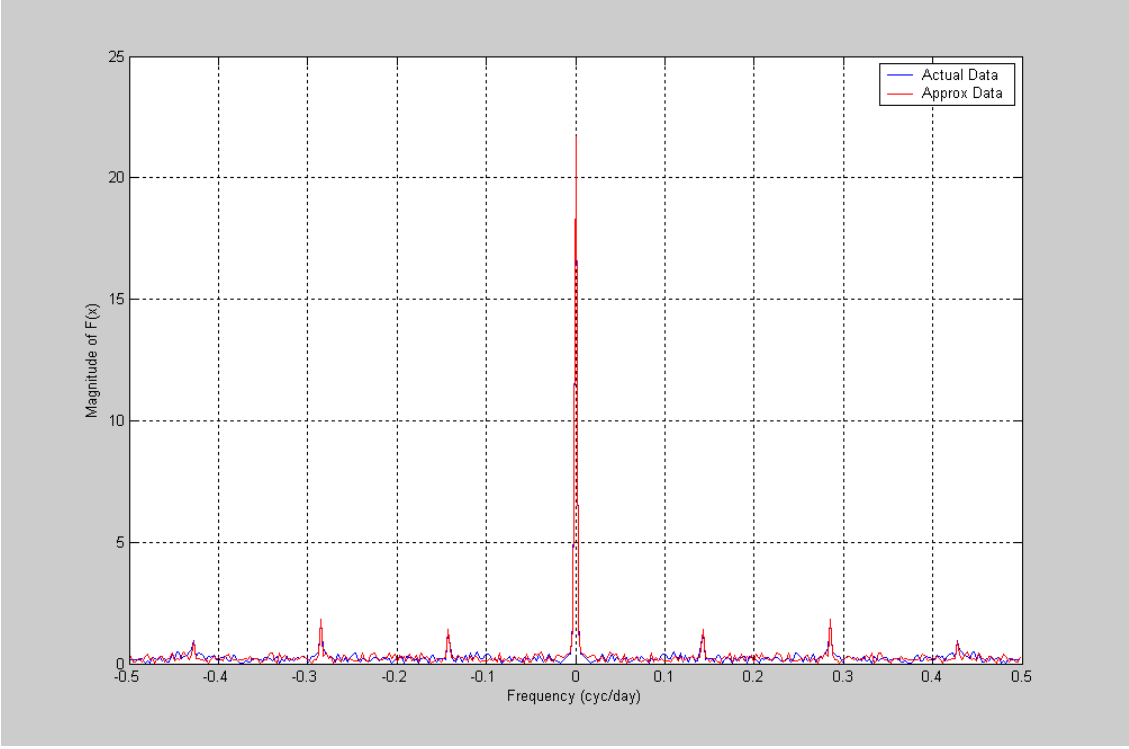


Figure 5.13: FFT Comparison between Actual Data and Approximated Data

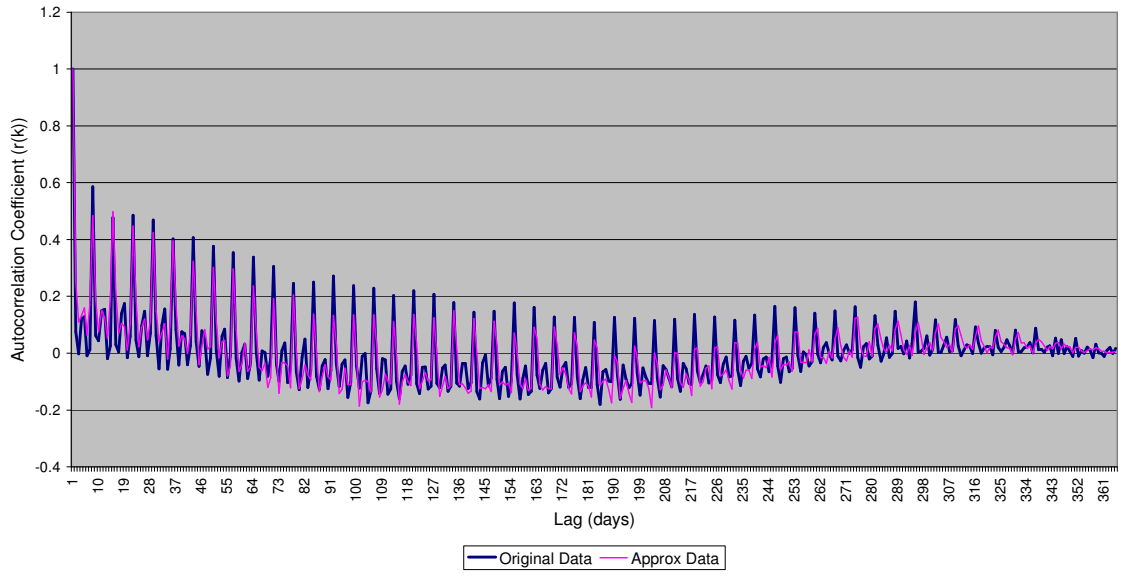


Figure 5.14: Autocorrelation Comparison Between Actual and Approximated Data

Finally the probability distribution function (PDF) and statistical parameters of both data sets are compared. The distribution function is shown in Figure 5.15 and the statistical parameters are shown in Table 5.3. The mean value, standard deviation and coefficient of variation vary by about ±10% of the actual electricity data. The distribution functions of the actual data and the approximated data are very well matched. Although there is a slight difference in the mean and standard deviation values the coefficient of variation values are very close, making the data sets very comparable. The skew of the modelled data is significantly smaller than that of the actual data. This shows that the modelled data is more symmetrical than the actual data in that the range of modelled data does not extend to the same high values as the actual consumption.

| Statistical Parameter | Actual Data | Modelled Data |
|---|---|---|
| Mean | 21.26 | 21.28 |
| Standard Deviation | 6.19 | 6.15 |
| Skew | 1.24 | 0.34 |
| Coefficient of Variation | 0.29 | 0.28 |
| Minimum | 9.80 | 9.55 |

Table 5.3: Comparison of Statistical Parameters

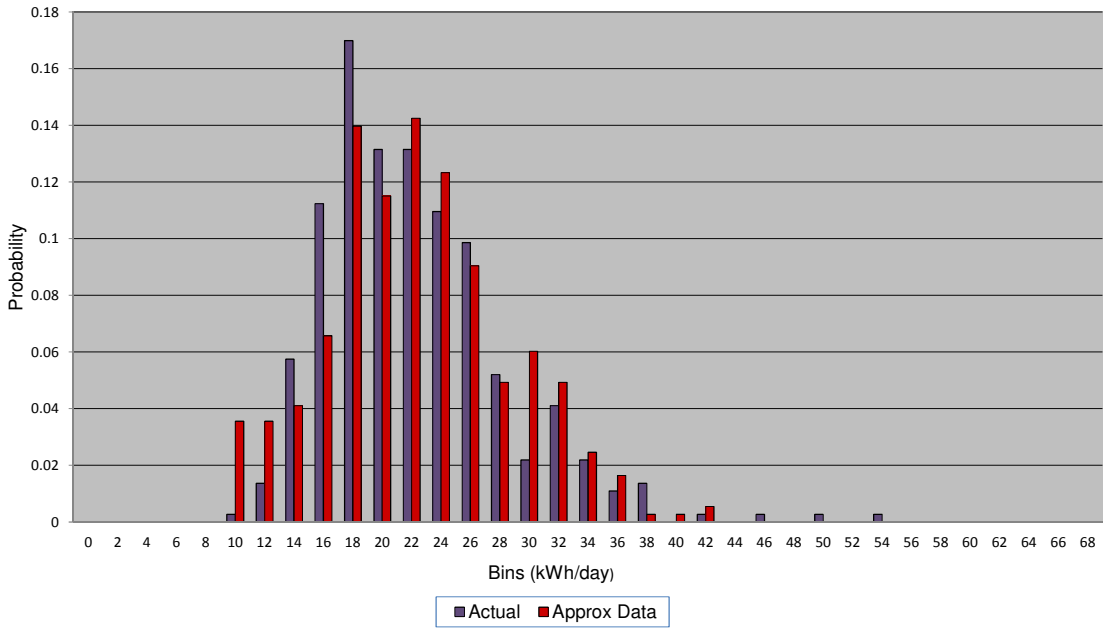


Figure 5.15: PDF Comparison between Actual Data and Approximated Data

Overall the proposed model for estimating daily electricity consumption provides a simple and relatively accurate method. It requires limited input values and can be used to generate any number of representative annual electricity profiles. Although the model is based on data obtained for a semi-detached house, the method could be further developed and generalised to use with different types of dwellings, as it contains no dependence on occupancy patterns, dwelling type or size.

The modelling process can be summarised using the following steps:

- Obtain the average daily electricity consumption for each month
- Take the FFT of these values and use the results to approximate the daily consumption values, $e_{app}$
- Add the weekly cycles, using the Fourier series in equation (5.6) to the approximated daily data
- Generate random white noise, $\varepsilon$, and transform it using equation (5.11)
- Add the components together to create a model of the electricity consumption data.

Therefore the generalised model for generating electricity data can be expressed as:

$$E(t) = e_{app}(t) + e\,w(t) + \left[4.569\,\varepsilon(t) + 0.0014\right] \tag{5.12}$$

where: $e_{app}(t)$ = approximated annual cycle

ew(t) = approximated weekly variations

ε(t) = white noise.

### 5.3.2 Gas Consumption Model

The analysis of the actual gas consumption data showed that the dwelling heating consumption is periodic. Therefore the gas consumption will be estimated using classical modelling techniques, involving a trend component and a random component, and will be represented by:

$$G(t) = G_d(t) + G_s(t) \tag{5.13}$$

where G(t) is the gas consumption (kWh), $G_d(t)$ the trend component, and $G_s(t)$ the random component. Based on the autocorrelation of the actual data, there is only an annual cycle present in the data. Therefore the trend component is comprised of daily values based on the annual cycle. The daily values could be estimated using the 'Average' Daily Thermal performance line for the dwelling as this shows that about 90% of the variation in heating consumption is represented by the variation in temperature data. If the heating consumption was to be predicted this way, all the data points would lie on the best-fit straight line and the consumption over time would not exhibit a period of low consumption values during the months of July to September. This is due to the fluctuations in the daily temperature over the summer months. Even with the addition of a random normal error the data would still not have the same pattern as the actual gas consumption, and the scatter about the Thermal Performance line would not exhibit the same pattern.

Therefore, a method similar to that used for modelling the electricity consumption will be used to model the daily gas (or heating) consumption. The average daily consumption values for each month were found from the measured data and the FFT of these was calculated to estimate the Fourier coefficients. Six pairs of coefficients were then used to create a Fourier series to accurately estimate the daily values of gas consumption.

Generally, the monthly consumption values can be obtained from utility bills. However, if the monthly values are not known for a building, they can be estimated by calculating the design heat loss of the building. The design heat loss, Q, is calculated using [10]

$$Q = \left(F_1 \sum U A + F_2\, 0.33\, N V\right)(t_c - t_{a\,o}) \tag{5.14}$$

where ∑UA represents the conduction losses of the building (i.e. the heat losses through the doors, windows and walls), 0.33NV represents the ventilation losses, with 1 air change rate per hour assumed for a typical dwelling, ($t_c$-$t_{ao}$) is the difference between the indoor and outdoor temperatures and $F_1$ and $F_2$ are temperature ratios relating to the amount of radiant and convective heat produced by the building's heating system [10]. This equation can be simplified if the building meets current standards in insulation and has low infiltration rates to estimate the 24hr average heat loss from a dwelling [11]:

$$Q = 24\left(\sum U A + 0.33\, N V\right)(\bar{t}_i - \bar{t}_o) \tag{5.15}$$

where $t_i$ is the mean 24-hour indoor temperature and $t_o$ is the mean 24-hour outdoor temperature. This equation can be interpreted as the design heat loss coefficient of the building, H, multiplied by the degree-day value, where:

$$H = \left(\sum U A + 0.33\, N V\right) \tag{5.16}$$

The heat loss coefficient depends greatly on the type and size of the dwelling, but for an average semi-detached house the values is H = 276W/°C [3]. Average values for other dwellings are given in Table 5.4. The calculation method for the average gas consumption values using degree-days is shown in Appendix A3.

| Dwelling Type | Average Design Heat Loss Coefficient (W/°C) |
|---|---|
| Detached | 365 |
| Semi-detached | 276 |
| Terraced | 243 |
| Bungalow | 229 |
| Flat | 182 |

Table 5.4: Average Design Heat Loss Values By Dwelling Type [3]

As stated earlier, standard degree-days are calculated using a base temperature of 15.5°C. This is only an average value, as the actual base temperature depends greatly on the amount of internal and solar heat gains to a building. From the analysis of the actual consumption data, the monthly base temperature was found to be about 16°C. If this is not known the base temperature can be calculated from [10]:

$$t_b = t_i - d \tag{5.17}$$

where $t_i$ is the average indoor temperature and d is the temperature rise due to internal heat gains.

The internal temperature of a residential dwelling depends upon the occupancy pattern of the building, the occupants desired comfort level, the activities of the occupants within the household (i.e. whether they are at rest or working) and the operating schedule of the heating system. The average temperature also varies from room to room within the dwelling and ranges from 18°C to 21°C. Winter average internal temperatures are about 19°C whereas summer temperatures can be as high as 25°C [16]. The internal heat gains are gains from people, appliances, hot water, etc. and provide a source of heat other than that of the heating system. Ultimately they cause a temperature rise in the building allowing for some reduction in the base temperature of the building. The amount of heat gains depends upon the type of dwelling. For a semi-detached or detached house, the total heat gains could be around 780W and for a smaller house or flat the gains are on average 615W [16]. Therefore the temperature increase due to internal gains is estimated from:

$$d = \frac{\text{Internal Heat Gains (W)}}{\text{Heat Loss Coefficient}} = \frac{Q_g}{(\sum U A + 0.33 N V)} \tag{5.18}$$

Using standard values for a semi-detached dwelling, the temperature rise due to internal gains would be:

$$d = \frac{780}{276} = 2.8°C \tag{5.19}$$

Additional heating can also be obtained from solar gains. These are additional heat gains through the windows and a reduction in the heat loss through the walls, and are therefore dependent upon the glazing area and the type and orientation of the glazing area. The amount of

solar gain also varies seasonally. Over the whole year, the greatest contribution to solar heat gain comes through south facing windows. The total solar gains can be found from [17]:

$$\bar{Q}_{s\,g} = \bar{S}\ \bar{I}\ A_g \tag{5.20}$$

where $\bar{S}$ is the mean solar gain factor, $\bar{I}$ is the mean total solar irradiance (W/m$^2$), and $A_g$ is the glazing area (m$^2$). 75% of all households have double glazing [3], therefore an approximated table of monthly daily mean solar gains per square metre of glazing area for Aberdeen is shown in Table 5.5. For the semi-detached house used for data collection, the total solar gains ranged from 910 - 1180W, depending upon the level of shading. Therefore the average internal temperature rise due to both solar and internal gains is 6°C.

| *Month/Face* | North | East/West | South | Average |
|---|---|---|---|---|
| January | 0 | 6.90 | 40.02 | 13.45 |
| February | 0 | 18.40 | 66.70 | 25.87 |
| March | 0 | 34.04 | 82.80 | 37.72 |
| April | 0 | 52.90 | 75.90 | 45.43 |
| May | 12.42 | 64.40 | 63.02 | 51.66 |
| June | 22.08 | 68.54 | 57.04 | 54.05 |
| July | 12.42 | 80.50 | 63.02 | 55.08 |
| August | 0 | 66.70 | 75.90 | 48.87 |
| September | 0 | 55.20 | 82.80 | 43.01 |
| October | 0 | 34.50 | 66.70 | 29.90 |
| November | 0 | 18.40 | 40.02 | 16.33 |
| December | 0 | 13.80 | 28.52 | 11.73 |

Table 5.5: Daily Mean Solar Gains per m$^2$ of Glazing Area for Aberdeen [17]

Based on this, the design heat loss becomes:

$$Q = \left(\sum U\,A + 0.33\,N\,V\right)(t_b - t_{a\,o}) \tag{5.21}$$

where $t_b$ is the adjusted base temperature (°C) and $t_{ao}$ is the outdoor air temperature (°C). This equation can either be used to find the total heat loss for the year or the average daily heat loss per month. The annual, or monthly, energy consumption depends upon the efficiency of the

boiler. This efficiency, η, depends upon the age and type of the boiler, whether it is continuously used or used intermittently, and ranges from 65% to 90% for newer systems [10,2]. From this the annual or monthly energy consumption can be found from:

$$\text{Energy Consumption} = \frac{\text{Energy Demand}}{\eta} \tag{5.22}$$

Values based on the calculation method outlined are shown in Appendix A3, along with the average daily gas consumption measured for the semi-detached dwelling.

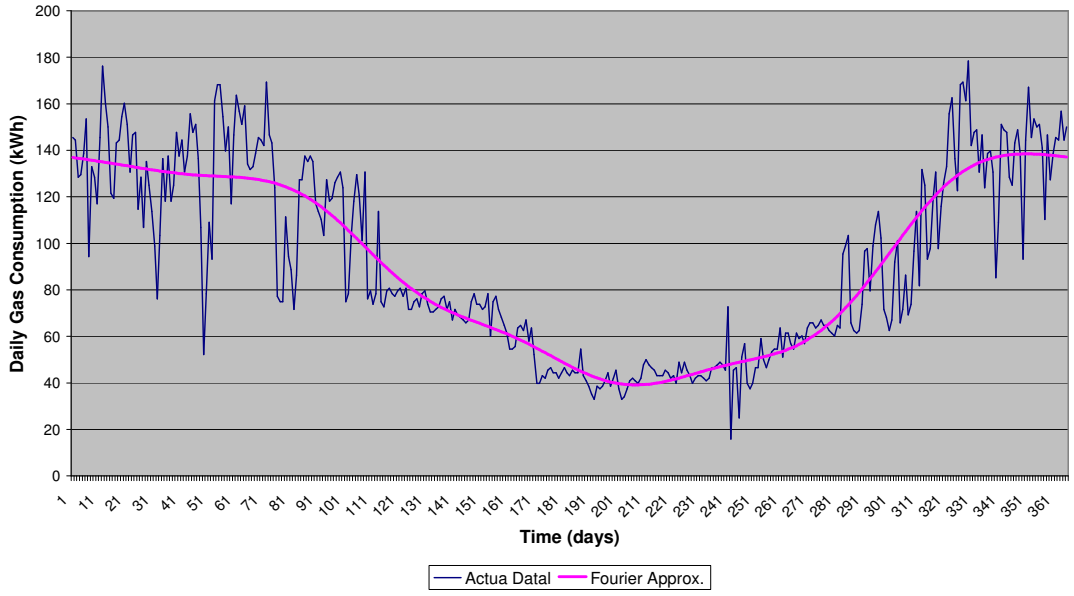


Figure 5.16: Comparison of Trend Component and Actual Gas Consumption for one Year

Figure 5.16 shows the estimated daily gas consumption values along with the actual consumption values for one year. As can be seen, the estimated daily values provide a smooth approximation to the annual variation, whilst maintaining the mean value for each month.

The random component from, equation (5.13), is the difference, or error, between the actual data and the trend component. These errors are approximately normally distributed, with an overall mean value of 0.05, and standard deviation of 14.6. The errors over the year appear to have no underlying structure, and the monthly error values also have a normal distribution and no structure. To maintain the base load, each month's mean and standard deviation of the error series need to be examined. Over the three years there is no obvious recurring pattern in the monthly mean values, and all the values are within ±3. The monthly mean values tend to have a

greater absolute magnitude over the summer months than the winter months. The standard deviation values have a strong sinusoidal pattern over each year, similar in shape to the overall annual cycle of the actual gas consumption. This variation is shown in Figure 5.17, and indicates that each month of errors should be normalised using their mean and standard deviation values. The three-year average values are shown in Table 5.6. Random white noise, ε, is then generated for each month and then the values are non-standardised using the monthly means and standard deviations, such that:

$$e_m(i) = \sigma_m \varepsilon(i) + \mu_m \tag{5.23}$$

where $e_m(i)$ are the error values for each month, $\varepsilon(i)$ is the white noise, $\mu_m$ the monthly mean, $\sigma_m$ the monthly standard deviation and m is the month number i.e. m = 1 is January, and i is the day index for each month. Twelve sets of error vectors/values were generated and joined together to form a 365-point long vector, $G_s$.

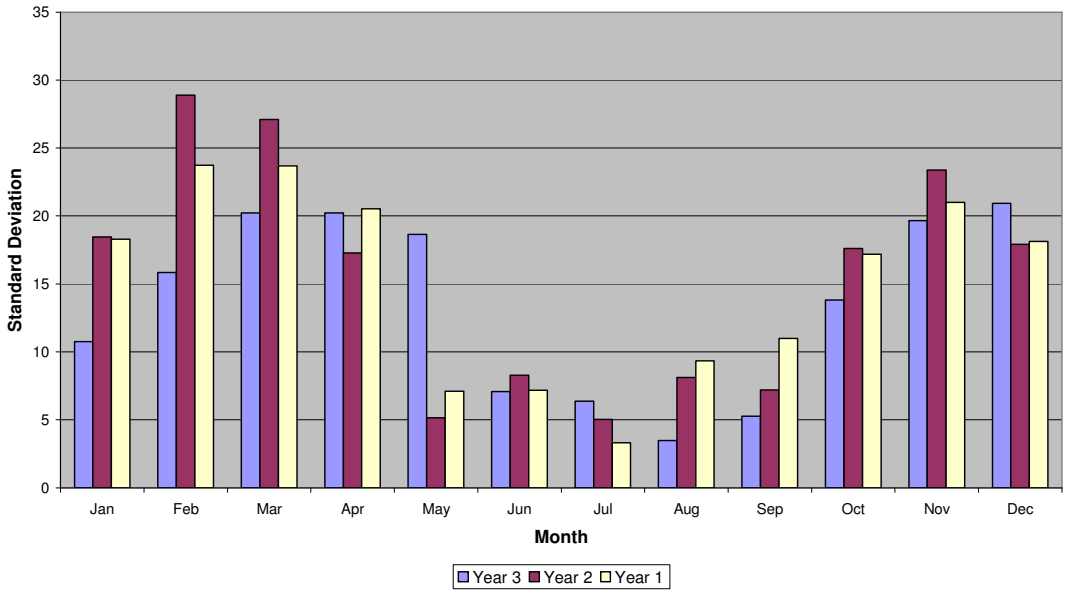


Figure 5.17: Annual Variation in Standard Deviation of Error Values

This new data set, $G_s$, is added to the deterministic model, $G_d$. A comparison between the actual consumption data for one year and the approximated consumption is shown in Figure 5.18. From this it can be seen that the overall pattern is the same and that the base load section has been maintained. The magnitudes of the fluctuations within this period are also of a similar size to those of the actual data. The autocorrelation structure of both sets of data is shown in Figure

5.19. It can be seen that there is only an annual cycle present, which is represented by $G_d$. The monthly random errors, $e_m$, adjusts the values to more accurately represent the gas (heating) consumption data. Therefore it can be said that the proposed model allows the structure of the data to be maintained.

| Month | Mean | Standard Deviation |
|---|---|---|
| January | 0.086 | 15.830 |
| February | 0.116 | 22.826 |
| March | 1.220 | 23.860 |
| April | -0.276 | 19.346 |
| May | -0.125 | 10.300 |
| June | -0.560 | 7.516 |
| July | -0.185 | 4.900 |
| August | -0.282 | 6.969 |
| September | -0.587 | 7.829 |
| October | -0.924 | 16.204 |
| November | 1.444 | 21.340 |
| December | 0.673 | 18.993 |

Table 5.6: Three-year Average Standard Deviation and Mean Values

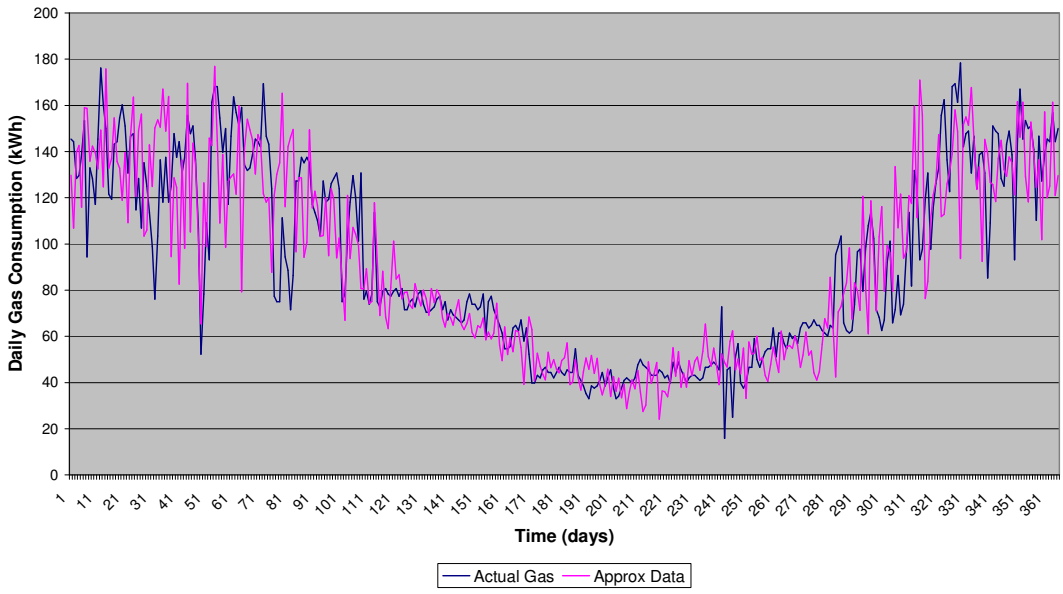


Figure 5.18: Comparison Between Actual Gas Consumption and Approximated Gas Consumption

Further comparison between the actual data and the modelled data can be made using the Thermal Performance Line and the Performance Line of the dwelling. These are both shown in Figures 5.20 and 5.21 for one year. The equations of both best-fit lines were compared and are shown in the figures. From the comparison in performance lines it can be seen that the best-fit straight lines are very similar, with slight spread at lower values of degree days. For the data set shown the actual base load was calculated as 26.776kWh/day, and the modelled data's base load was 26kWh/day, showing a difference of about 5% of the actual data. The comparisons in thermal performance lines are very similar, with a slight difference in base temperature values of $t_{act} \approx 19.22°C$ and $t_{app} \approx 19.33°C$. The spread of data around both straight lines also seems to match that of the actual data.

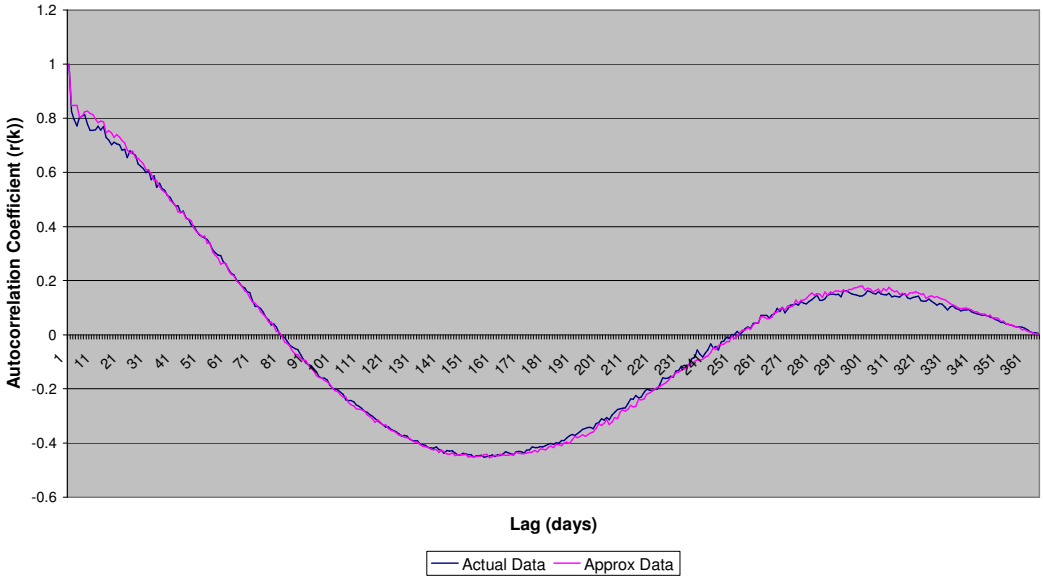


Figure 5.19: Autocorrelation Comparison Between Actual and Approximated Gas Consumption Data

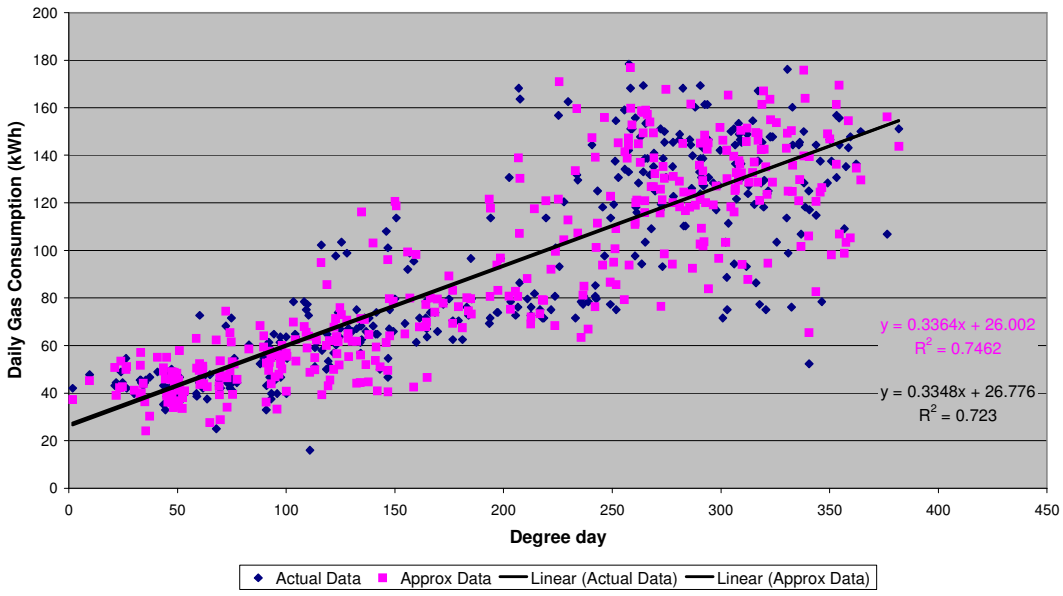


Figure 5.20: Comparison of Performance Line for One Year

Finally, the statistical parameters of both the actual gas consumption and the modelled gas consumption were compared. Table 5.7 shows the annual statistical values for one year of consumption. Most of the parameters are close in magnitude and vary by about ±10%. Figure 5.22 shows the probability functions for the same data sets. This shows that both data sets of daily total gas consumption have approximately the same shape of distribution, with peaks at 40-50kWh/day and at 140kWh/day. The modelled data's distribution has a similar pattern but there is a difference in the overall minimum. From the annual variation of the data it can be seen that the minimum value of around 15kWh/day only occurs on a couple of days in the year. If this minimum value were ignored, then the minimum values of both data sets would be closer in values at about 24kWh/day. From the distribution function it can be seen that the maximum value of the modelled data is in the same range as that of the actual consumption data. However, in the modelled data there is a higher occurrence of these maximum values but this difference is not very significant. It would be possible to set minimum and maximum limits when modelling the data without changing the structure of the data. However, without detailed analysis of actual consumption data it would not be possible to assess what these limits should be set to.

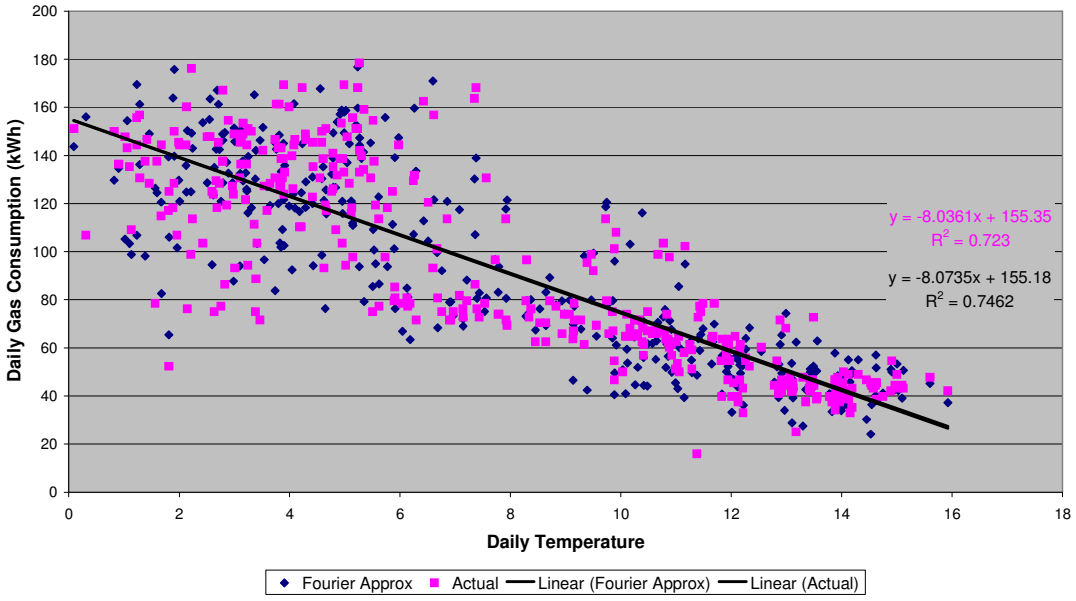


Figure 5.21: Comparison of Thermal Performance Line for One Year

| Statistical Parameter | Actual Data | Modelled Data |
|---|---|---|
| Mean | 91.510 | 91.040 |
| Standard Deviation | 40.810 | 40.360 |
| Skew | 0.291 | 0.266 |
| Coefficient of Variation | 0.446 | 0.443 |
| Minimum | 15.900 | 24.090 |

Table 5.7: Comparison of Statistical Parameters

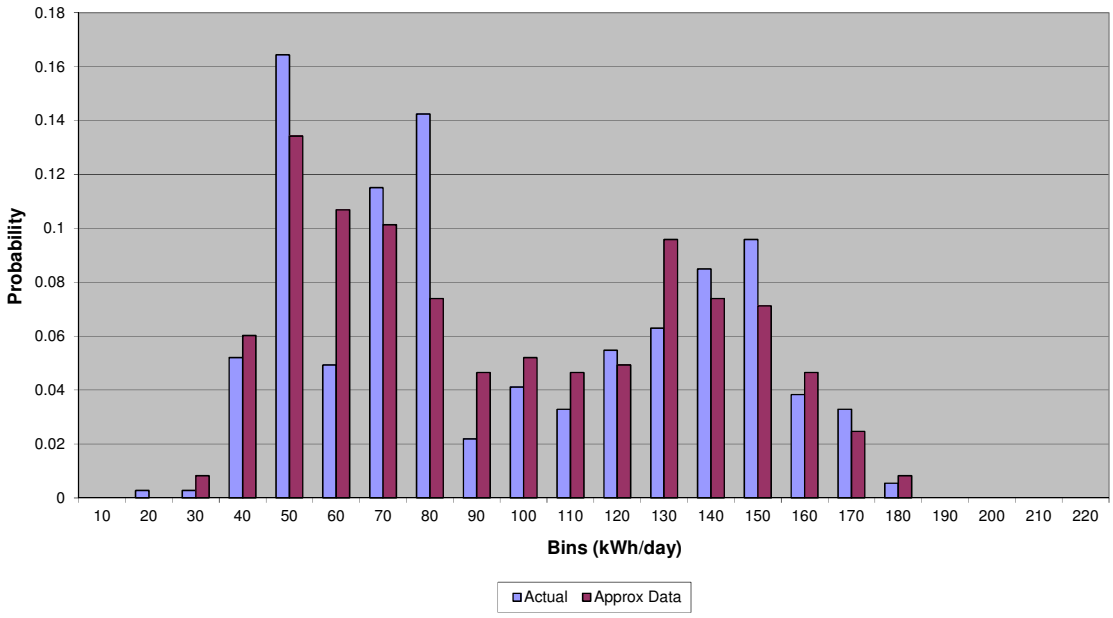


Figure 5.22: PDF Comparison Between Actual Data and Approximated Data

## 5.4 DISCUSSIONS AND CONCLUSIONS

The aim of this chapter was to provide a simple procedure for modelling both the electricity and gas consumption of a domestic building. Two separate models were developed for each consumption type, and the parameters of each model were based on a detailed analysis of actual energy consumption data for a semi-detached dwelling.

The first section of the chapter deals with the analysis of this consumption data. This involved examining the statistical properties of the data along with the structural content. This allowed for generalisations to be made about the distribution of both the daily electricity and gas consumption, and about the harmonic content of the data. The simplicity of the model should allow for the technique to be developed further to provide a simple modelling technique for energy consumption for a variety of types of buildings including offices, assuming prior knowledge of the weekly cycles.

As there is limited availability of energy consumption data, it was decided that the models should have as limited an input as possible. Therefore the basis for both models relies upon estimating daily data from monthly consumption figures, i.e. generating 365 data points from 12. This removes the need for a long term measuring programme to obtain actual consumption

data, as monthly data is usually readily available. The remaining detail in each model is based upon information obtained from the initial analysis of the actual consumption data.

For the electricity model, given more time, the possibility of generating the random component of the data using a different distribution function should be investigated. As it is suggested that the overall data is more likely to have a lognormal distribution, this would be the first choice of distribution for random data generation to be considered. This might help increase the skew coefficient obtained from the electricity modelling procedure, making the modelled data more similar to the actual data.

Both models provided an accurate way of generating daily electricity and gas consumption data. The structure of the original data was maintained well in both models along with the statistical parameters. The procedure allows for any number of representative annual load profiles to be generated, making the models ideal for the testing of the energy matching of domestic generation systems. The data could ideally be compared with that obtained from the resource models in Chapter 4, to assess the potential contribution of specific sizes of photovoltaic and wind systems.

## 5.5 FUTURE WORK

The next stage for these modelling procedures would be to obtain more daily data, and to assess if any of the random components modelled can be related to building size. This would allow for the procedure to be generalised further enabling data to be generated for a wider variety of size and style of households. The advantage of doing this would be to provide a wider range of demand profiles for comparison with the renewable resources, providing a more detailed estimation of the overall contribution of small-scale renewable systems. This approach could also be used on an individual household basis to assess the improvements due to energy efficiency measures, and to assess if it is worthwhile investing in an individual renewable system.

As the technique requires relatively limited information, it could be applicable for modelling the electricity demand in commercial or office buildings. An annual approximation to the daily data could already be obtained from the monthly mean values for any building used the procedure outlined earlier. However, detailed information would be required to assess if the significant cycles identified in the domestic data are present for other buildings, and if they contribute the

same importance to the data. If this data was available the generality of the modelling technique makes it appropriate for modelling the electricity consumption in other buildings.

# CHAPTER 6

# ENERGY SUPPLY AND DEMAND

## 6.1 INTRODUCTION

Based on the modelling procedures developed in the previous two chapters (CH4 and CH5), a comparison of domestic energy supply and demand can be carried out. To do this, the useable energy from the renewable sources needs to be estimated from the outputs of the solar radiation and wind speed models. These sources can be converted into energy's that when compared with the domestic demand will give an indication of the potential sizes of solar and wind electric systems required to match the domestic load, and what proportion of time and when the domestic load is matched. This analysis will give an estimate of the feasibility of small-scale renewable technologies for domestic generation. It will also give an indication of energy flows between domestic generators and the (national) grid system. Once the sizes of these renewable systems have been found, potential individual loads will be assessed for their suitability in matching this renewable energy.

## 6.2 ANALYSIS OF ENERGY SUPPLY AND DEMAND

To be able to estimate the actual energy supply from the solar and wind resources, the amount of solar radiation on a horizontal surface, and the daily wind speed values have to be converted into useable energy values. The following sections outline an example procedure for this conversion.

### 6.2.1 Solar Energy Supply

To utilise the energy from the solar resource most effectively, the energy production of building integrated, or building mounted photovoltaic systems will be estimated. These systems are generally mounted at an angle tilted from the horizontal, for example, they are often installed on the pitched roofs of houses. To estimate the available energy produced by such a photovoltaic system it is necessary to calculate the amount of solar radiation on a number of tilted surfaces. Using the results from the modelling procedure for daily total horizontal solar radiation (CH4), the total daily radiation on a tilted surface, $H_T$, can be found from:

$$H_T = (H - H_d)\,R_b + H_d\left(\frac{1+\cos\beta}{2}\right) + H\,\rho_g\left(\frac{1-\cos\beta}{2}\right) \tag{6.1}$$

Alternatively, this could be expressed as:

$$\frac{H_T}{H} = \left(1 - \frac{H_d}{H}\right)R_b + \frac{H_d}{H}\left(\frac{1+\cos\beta}{2}\right) + \rho_g\left(\frac{1-\cos\beta}{2}\right) \tag{6.1a}$$

Where H is the daily global radiation (kWh/m$^2$), $H_d$ the daily diffuse radiation on a horizontal surface, $R_b$ the ratio of the daily radiation on a tilted plane to that on a horizontal plane in the absence of the Earth's atmosphere [1, 2], $\rho_g$ the reflectance and $\beta$ the angle of the tilted surface. A constant value of 0.2 is used for the reflectance in urban environments [3]. This equation assumes that the diffuse, and reflected radiations are isotropic. As the chosen location for this study is in the Northern hemisphere, and assuming a south-facing surface, the ratio $R_b$ can be calculated from:

$$R_b = \frac{\cos(\phi-\beta)\cos\delta\sin\omega_s' + \left(\frac{\pi}{180}\right)\omega_s'\sin(\phi-\beta)\sin\delta}{\cos\phi\cos\delta\sin\omega_s + \left(\frac{\pi}{180}\right)\omega_s\sin\phi\sin\delta} \tag{6.2}$$

Where $\phi$ is the latitude angle for the chosen location, $\delta$ is the declination, $\omega_s$ is the sunset hour angle for the horizontal, and $\omega_s$' is the sunset hour angle for the tilted surface.

Equations (6.1) and (6.2) are based on an isotropic modelling process. This process was selected as it provides a conservative estimate of the solar radiation, ensuring that the energy produced by the solar systems is not overestimated. This calculation process is also relatively straightforward. Any additional energy produced by such a system could be used at the point of production (i.e. the dwelling) for any additional loads, stored for use at a later time, or fed back into the grid system to be used at another location. In order for the renewable systems to operate most efficiently, the systems will be grid-connected ensuring that there is always a load/demand to be met.

Most of the parameters in equations (6.1) and (6.2) can be calculated directly, apart from the ratio of the daily total diffuse radiation and a horizontal surface to the daily total radiation on a horizontal surface, $H_d/H$. It has been suggested that there is a relationship between this ratio and the daily clearness index, $K_T$ [2]. A number of expressions have been documented describing

this relationship [4,5,6], however, it is not the aim of this study to examine the accuracy of these relationships. The different expressions for the ratio $H_d/H$ do not seem to produce significant variation in results over the year [4,5]. Therefore, for simplicity, the following relationship (developed by Liu and Jordan, as cited by Duffie et al [2]) will be used to calculate the value of the ratio $H_d/H$ on a daily basis:

$$\frac{H_d}{H} = 1.0045 + 0.04349\,K_T - 3.5227\,K_T^{\,2} + 2.6313\,K_T^{\,3} \qquad (6.3)$$

The calculation process outlined is now used to calculate the available solar radiation on a number of tilt angles ranging from 10° to 70°. This range of angles was selected to allow for the energy estimation of systems installed on a variety of building types from flat-roofed to pitched-roofed. The average monthly daily total radiation on each tilted surface has been obtained for Aberdeen and is shown in Figure 6.1.

Regardless of the tilt of the photovoltaic array, the solar energy available is greater over the summer months, which coincides with the time of lowest domestic demand for electricity and heating. From Figure 6.1 it appears that the best availability of solar radiation over the whole year is produced for a tilt angle equal to the latitude of the location, 57° in the case of Aberdeen. This conclusion is backed up by a number of photovoltaic design recommendations [7]. Other design recommendations suggest that for photovoltaic systems, situated north of the equator, a tilt angle of the latitude ± 15° provides the optimum power production [8, 9]. For Aberdeen this would suggest an optimum tilt angle of 42° - 72°, but this would also have to be compared with the available roof pitch. However, as the solar trend is opposite to that of the energy demand, it may seem more appropriate to select a tilt angle that best maximises the energy production over the winter months while still producing a comparably high level of solar radiation over the summer months. Based on these criteria, a tilt angle of 70° may be more suitable. From a practical approach though, the photovoltaic (or PV) array tilt angle is likely to be limited by the pitch of each individual household's roof. Typically in the UK, the roof pitch angle is between 30° and 50°. This value will be used later as a practical comparison of the energy production.

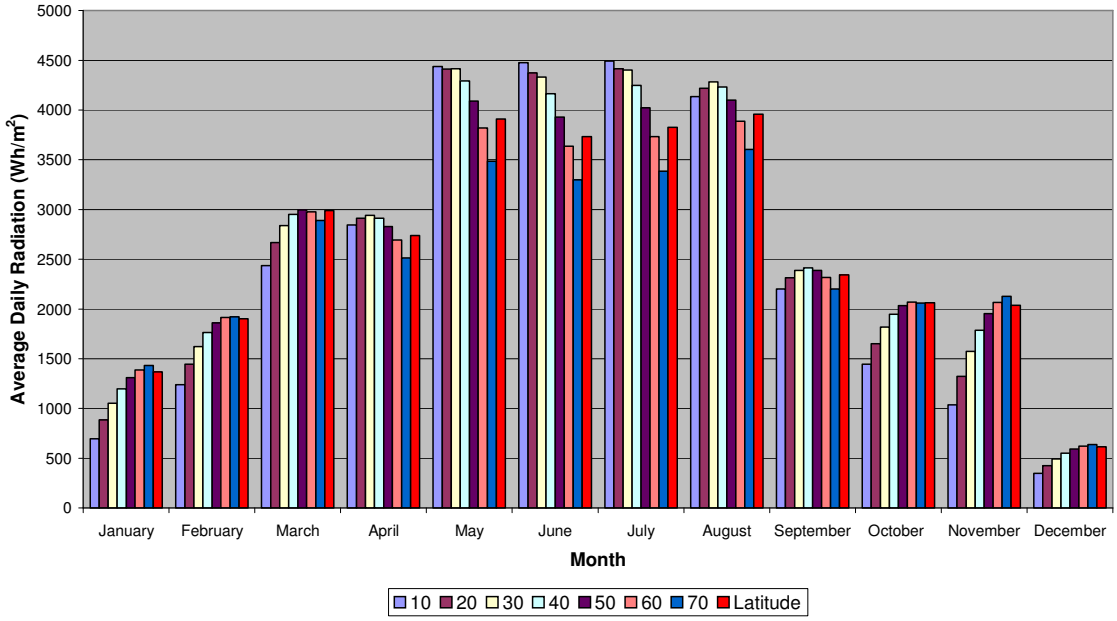


Figure 6.1: Average Daily Tilted Solar Radiation For Aberdeen

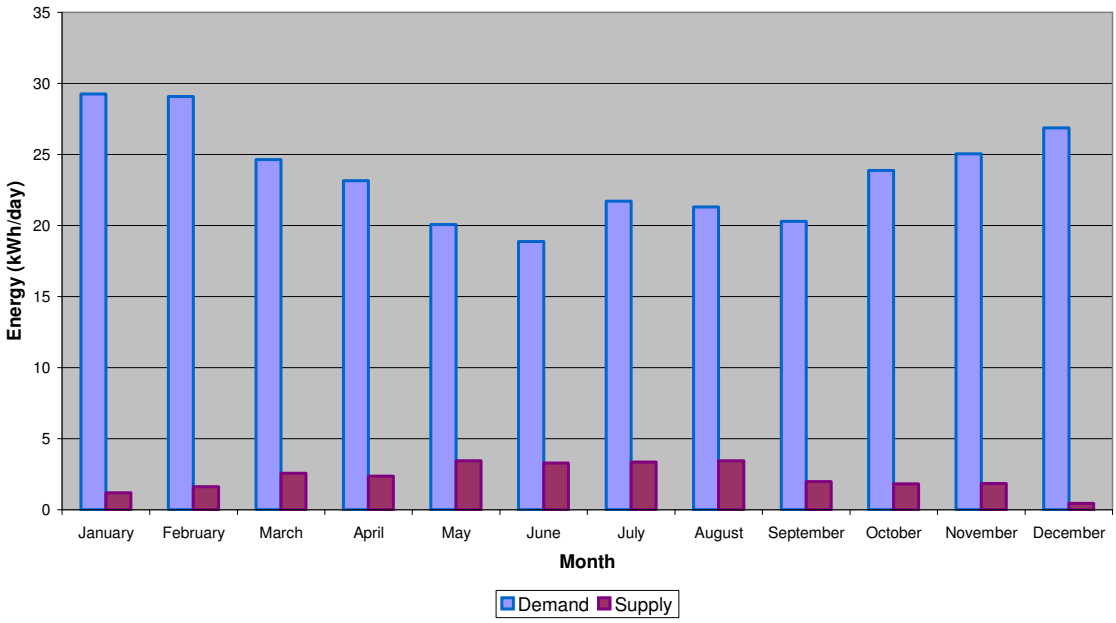


Figure 6.2: Comparison of Energy Supply and Domestic Demand

Based on the tilt angle of 70°, and neglecting the efficiencies of the components of the photovoltaic system, a comparison between the modelled electricity demand (kWh) and the solar energy supply density (kWh/m$^2$) is shown in Figure 6.2.

As the total domestic demand for any dwelling can be provided from a source of generated electricity, the only solar technology considered in this study is photovoltaics. Photovoltaic modules are comprised of a number of cells, each converting the solar radiation incident on the surface to DC electricity. A number of these modules can be connected together in either series or parallel to obtain the input voltage required for the building's demand load. To implement such a system on a domestic building an inverter would also have to be included to ensure that the voltage matches that required by the appliances, and to allow the system to feed any excess electricity back into the grid. For the analysis of matching energy supply and demand, a simplified approach is taken to estimate the energy produced by the photovoltaic system. The following expression will be used to calculate the anticipated daily energy produced by the system ignoring any shading effects, and the potential reduction in energy due to cloud cover and dirt accumulation etc.:

$$E_{\text{solar}} = \eta G A \tag{6.4}$$

Where $E_{solar}$ is the daily energy produced by the solar system (kWh), $\eta$ is the overall efficiency of the system, allowing for an inverter efficiency of 95% at full load, G is the total solar radiation on the tilted surface (kWh/m$^2$) and A is the photovoltaic array area (m$^2$).

Crystalline cells and amorphous silicon cells are the most efficient cells available commercially. However, the choice of which cell type to use will depend, to a certain degree on the application. For example, monocrystalline cells offer maximum power when space is limited but thin film cells are ideal for applications where the uniform appearance and aesthetics are important, and are suitable for environments with low light levels. For domestic applications it is generally anticipated that the installation area is limited, indicating that PV panels using crystalline technologies are more appropriate. Based on this technical assumption, typical conversion efficiencies of 15 or 16% are assumed for the PV system.

Assuming an efficiency of 16% for the photovoltaic modules, new sizes for the photovoltaic system can be estimated to match either the typical average daily winter or summer electrical loads. . These sizes range from 32m$^2$ (Array size 1) to 158m$^2$ (Array size 2) for a south facing array oriented at 70°. Both of these limits are impractical for the installation on a typical dwelling. An annual comparison between one year's electricity consumption, and the energy output from both a 32m$^2$ and 158m$^2$ photovoltaic array are shown in Figure 6.3. Due to the extremely large array sizes required for the electricity load, it is assumed that this technology would not make a significant contribution towards the domestic heating load.

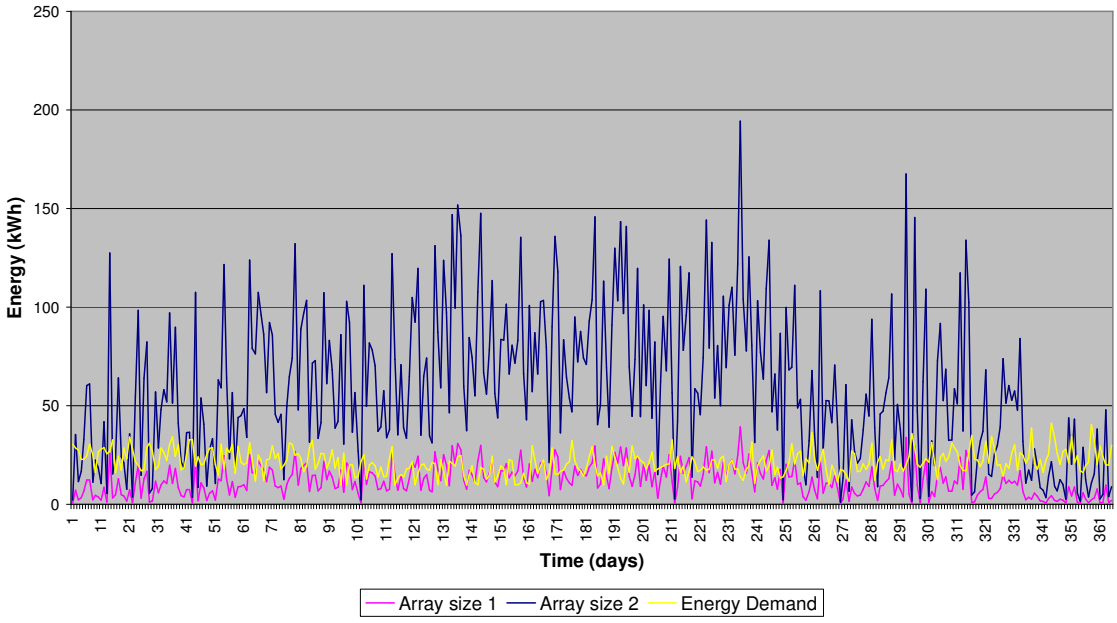


Figure 6.3: Annual Surplus/Deficit Comparison

From this comparison it can be seen that the smaller array size produces energy on a more similar scale to the demand required by the dwelling, and that it matches, or exceeds the expected demand for 20% (73 days) of the year, primarily over the period from May to August. The larger array size exceeds or matches the demand for 82% of the year.

Once the daily energy available for a chosen size of photovoltaic system has been calculated, it can then be compared with the daily energy demand of the dwelling (Model output from CH5). This will allow for the domestic energy surplus/deficit (S/D) curve to be calculated using the following expression:

$$S/D = \text{Energy Demand} - \text{Energy Available} \quad (6.5)$$

Using this expression two conditions arise. If the calculated difference is positive, the building requires additional energy from the grid system, i.e. a deficit condition has been created. If the calculated difference is negative, the building system has generated excess energy that could be stored or exported i.e. a surplus condition has been created. This surplus/deficit curve allows the estimation of the proportion of time the domestic load is met or exceeded and by how much.

A comparison of the monthly energy surplus/deficit for both the $32m^2$ and the $158m^2$ arrays are shown in Figure 6.4. This shows that the large array generates a large surplus of energy over the whole year, except December.

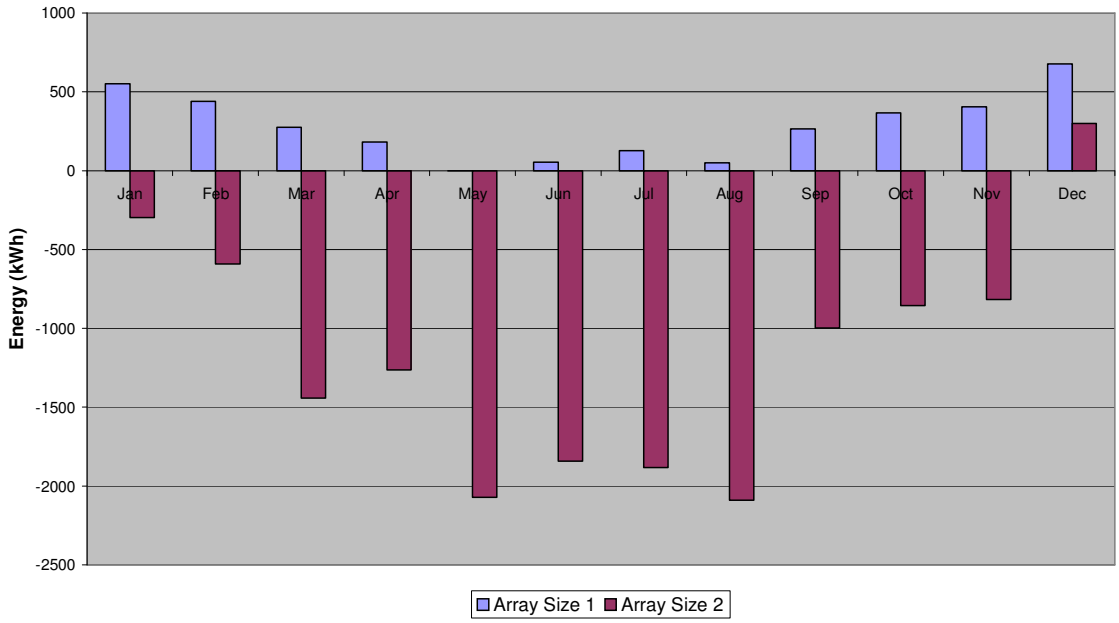


Figure 6.4: Monthly Surplus/Deficit Values for Large Array Sizes

### 6.2.2 Wind Energy Supply

The wind speed model output (CH4) can be used to calculate the power and energy available in the wind resource for a chosen site/location. The actual power extracted from the wind by a turbine is greatly dependent upon the wind speed at the location, and the size of turbine chosen, and is given by:

$$P = \frac{1}{2} C_p \rho A U^3 \tag{6.6}$$

Where ρ is the density of air, A is the swept area of the turbine ($m^2$), U is the wind speed (m/s) and $C_p$ is the power coefficient. The value of the power coefficient relates to the amount of energy that can be extracted from the free wind stream. Theoretically the maximum value of this power coefficient, known as the Betz limit [10], is 0.59, allowing 59% of the available energy to be converted into useful energy. In practice the value of $C_p$ varies with the turbine rotor tip speed, the number, shape and orientation of the turbine blades. Most commercial horizontal axis turbines have three blades and tend to have a maximum power coefficient of 0.4 [10]. Depending upon whether the wind turbine is a variable speed or fixed speed machine, the value of power coefficient can also be varied during the operation of the turbine.

However, as the focus of this study is to assess the applicability of small-scale renewable systems for load matching, the value of power coefficient will need to be adjusted to compensate for the difference in turbine size and performance. It has been stated that small wind turbines can extract no more than 20% of the energy available in the wind [11]. For simplicity in system sizing a value of 0.2 will be used for the power coefficient in equation (6.6). This value will be assumed to be constant over the year.

Most commercial small-scale turbines generate AC electricity which, for grid connected systems, is usually converted to DC and then converted back to AC to allow for synchronisation with the grid system. To account for this an inverter efficiency of 95% has been assumed for the power and energy calculations.

Although a simplified method for obtaining the typical diurnal wind speed profile for Aberdeen was summarised in equation (4.17), (CH4 p49), this result will not be used to estimate the range of wind system sizes. This is due to a number of reasons. Firstly equation (4.17) provides an average wind speed profile for a typical day, which may not always be accurately followed over the whole year due to changes in the monthly mean wind speed and the variation in wind speed values over a shorter time scale. Using this typical daily profile to assess the energy availability of the wind system per day may actually overestimate the energy production and the percentage of domestic demand that can be met due to the impact of the chosen turbine cut-in wind speed. Secondly, the typical diurnal profile may not be applicable for other locations, however using the modelling procedures described in Chapter 4, the annual availability of small renewable systems for other locations could be estimated.

Based on this information, and assuming that power can be extracted from the wind over a 24 – hour period, the power output obtained from equation (6.6) can be multiplied by 24 to obtain the daily energy produced. This value can then be used to estimate the area of turbine required. Using the typical diurnal wind profile for any month, and the known characteristics for a specific turbine, the total daily energy produced is generally always greater than that obtained by multiplying the average power (from equation 6.6) by 24. This result is demonstrated in Appendix A4 and shows that the energy available will typically be an underestimate of that actually achieved.

A comparison between this wind energy density, per $10m^2$, and the heating and electricity demand of a typical dwelling are shown in Figures 6.5 and 6.6. Both the domestic demand profiles exhibit the same annual variation, being lower over the summer. Based on the analysis of the wind speed data, and the estimation of the available energy, there is no clear trend as to the time of year when the wind supply is at a maximum. However, comparison of the average daily values of these three energy data sets demonstrates that the energy availability increases marginally, over the winter period, coinciding with an increase in the domestic demand.

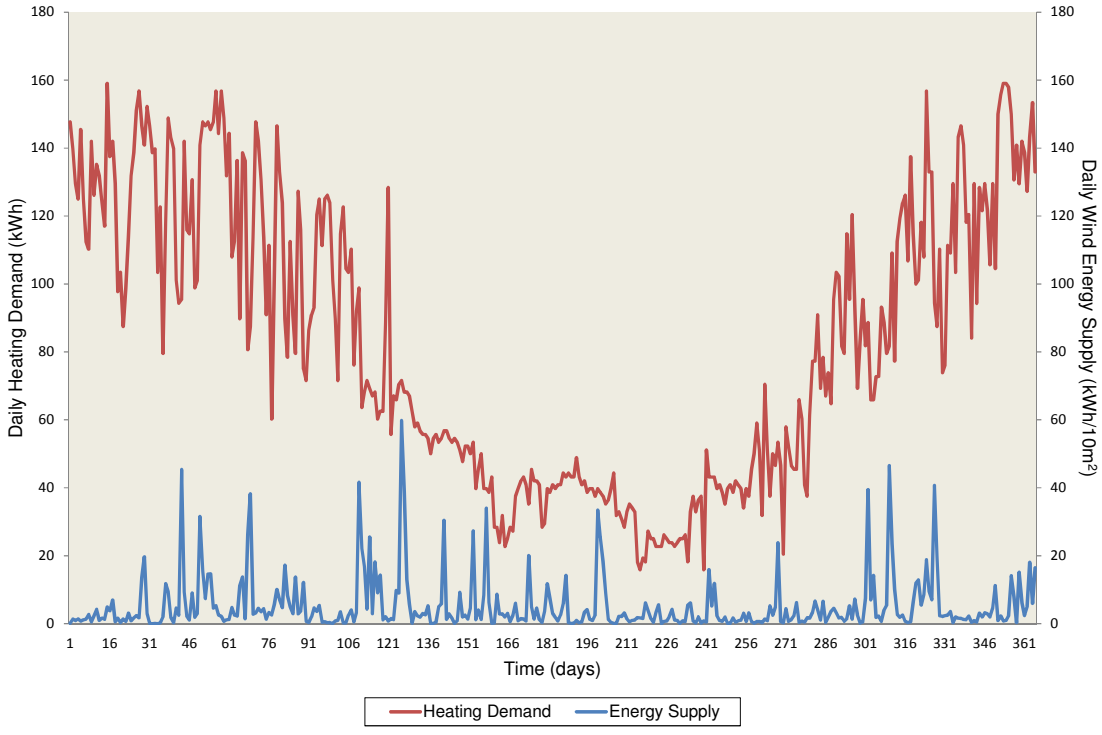


Figure 6.5: Comparison Between Domestic Heating Demand and Wind Energy Supply

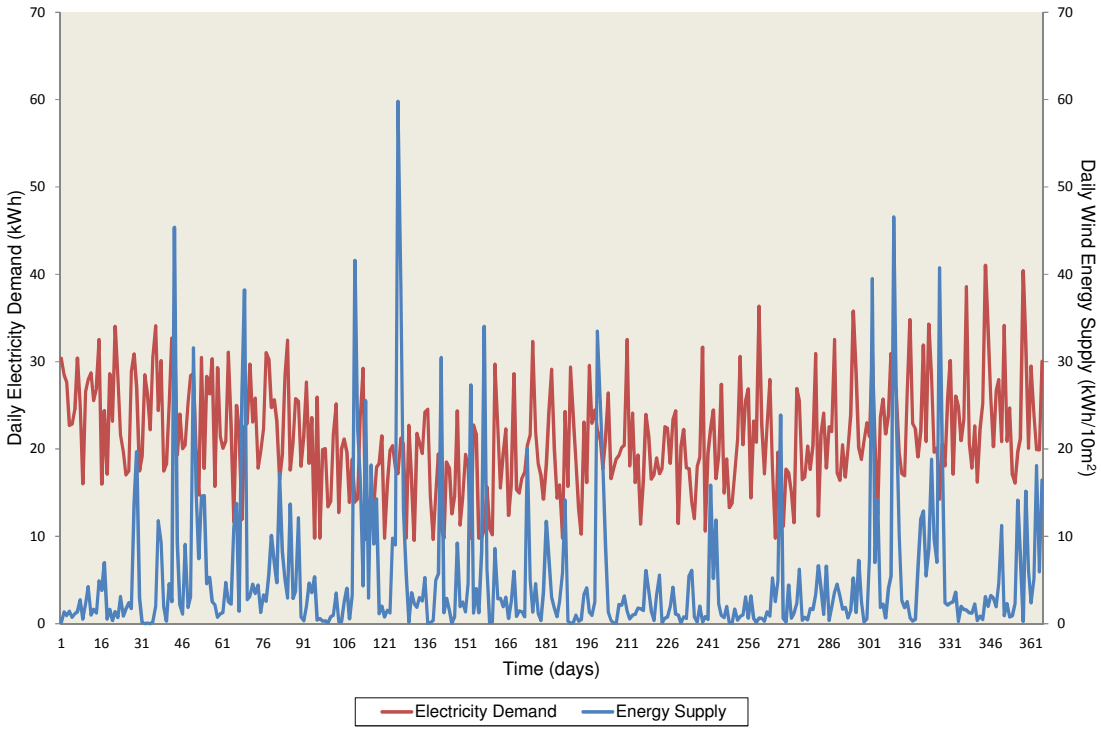


Figure 6.6: Comparison Between Domestic Electric Demand and Wind Supply

These average energy values can be used to estimate the approximate swept area of wind turbine required to match either the average daily heating or electric load required for both the maximum winter and minimum summer periods. For example, the minimum average daily electricity consumption occurs during June, which has a corresponding daily energy availability of 0.572kWh/m$^2$. To match this energy demand a turbine area of 34m$^2$ would be required. Table 6.1 shows the calculated 'wind' swept areas required to match the four key demand categories. However, turbine ratings are not directly related to swept area and small-scale wind turbines tend to be available with power ratings of 1-1.5kW, 5-6kW and 10kW and greater [12]. From a planning and economic perspective, this area of turbine required might be better met by more than one turbine. But from an individual dwelling perspective, it is simpler to assume that only one wind turbine is to be used. Using the calculated areas, and assuming a rated speed, $U_R$, of 12m/s, the turbine power rating, $P_R$, can be estimated from:

$$P_R = \frac{1}{2} C_p \rho A U_R^3 \tag{6.7}$$

Using the calculated areas (shown in Table 6.1), and based on the assumption that most turbines achieve rated power at a speed of 12m/s, a range of power ratings can be estimated for both the

domestic heating and electricity demands. These turbine ratings are also shown in Table 6.1, and range from 7kW to 50 kW. However, these results could not be used directly as the height of the turbine increases with swept area. The typical height of a free standing turbine tower required for a 7kW turbine would be 10 – 20m, whereas a 50kW turbine is more likely to require a tower of height 20 – 40m. As the height increases, the wind speed increases resulting in a significant increase in the available wind power. Therefore, a smaller turbine mounted at a greater height may provide a significant proportion of the domestic demand. Unfortunately the installation of turbine towers is limited by the proximity to surrounding buildings, which is also limited by the available area. [11]. Based on the above, this study will only consider the application of turbines with a rated power of less than 10kW, as these can be more realistically installed in built-up locations.

| Energy Demand Period | Magnitude of Energy Demand (kWh) | Wind Area ($m^2$) | Turbine Rating (kW) |
|---|---|---|---|
| Minimum electricity demand | 19.12 | 33.45 | 7.00 |
| Maximum electricity demand | 31.08 | 110.19 | 23.30 |
| Minimum heating demand | 27.86 | 99.48 | 21.00 |
| Maximum heating demand | 132.94 | 209.32 | 44.30 |

Table 6.1: Wind Energy System Sizes

Once the power rating of the wind turbine has been selected, the actual energy output from this turbine needs to be estimated using the input wind speed data. The simplest way to assess this energy supply is to use an idealised power curve for each turbine as shown in Figure 6.7. The power curve can be divided into three regions of operation. Firstly there is an exponential rise in power output between the cut-in wind speed, $U_{ci}$, and the rated speed of the turbine, $U_R$. Secondly, there is a period of constant output at rated power between the rated speed and the cut-out speed, $U_{co}$, and lastly there is the region after the cut-out speed when the turbine is not producing an output.

As stated earlier, the rated speed of most commercial turbines is about 12m/s. However, the cut-in speed and the cut-out speed typically vary depending on the swept area of the turbine. The power will also vary between the cut-in and rated speed depending on the turbine rating. To allow for a generalised approach in estimating the power output without selecting a specific turbine from a manufacturer, the power curve will be estimated mathematically based on the

three regions of operation. The power output can be described by the following conditions [13,14]

$$\begin{array}{lll} \text{(i)} & P = 0 & \text{for } U_i < U_{ci} \text{ and } U_i > U_{co} \\ \text{(ii)} & P = P_R & \text{for } U_R \le U_i < U_{co} \\ \text{(iii)} & P = aU_i^3 - bP_R & \text{for } U_{ci} \le U_i < U_R \end{array} \qquad (6.8)$$

Where P is the output power of the turbine, $U_i$ is the daily average wind speed (m/s) and a and b are constants calculated from:

$$a = \frac{P_R}{U_R{}^3 - U_{ci}{}^3} \qquad (6.9a)$$

$$b = \frac{U_{ci}{}^3}{U_R{}^3 - U_{ci}{}^3} \qquad (6.9b)$$

As the wind speed input values are the daily averages, the power values obtained from equation (6.8) must be multiplied by 24 hours to obtain the total daily energy supply from the wind. It is estimated that this will underestimate the daily energy produced compared with that obtained using typical diurnal wind speed profiles.

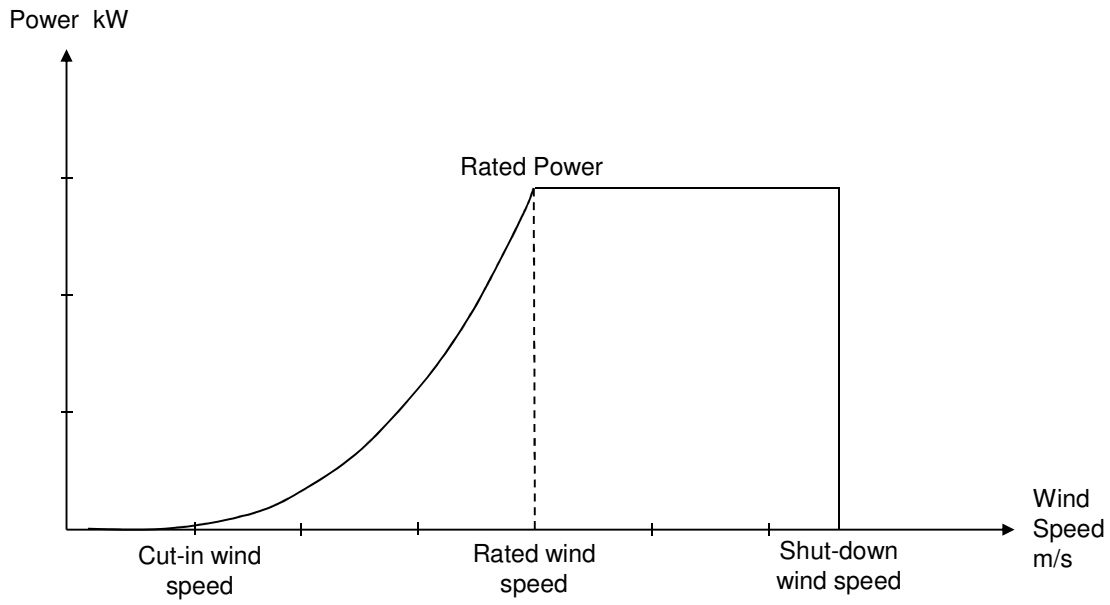


Figure 6.7: Typical Wind Turbine Power Curve

Based on a comparison of small-scale turbines [15], it appears that the cut-in speed is typically 3m/s. and although there is often no specified cut-out speed a value of 20m/s is generally used. Most wind turbines power production is affected by the local terrain, in that the rougher the land surface, the more turbulent the wind stream. If this is the case, the power output of the wind turbine may be reduced. Taking this into consideration, the idealised power curve may tend to underestimate the turbine production at rated power.

### 6.2.3 Total Renewable Energy Supply

As neither the solar resource or wind resource are suitable for matching the total domestic demand individually, the combined energy available from both these sources should be compared with the domestic electricity demand and the heating demand. This could allow for a reduction in either the size of photovoltaic array or the rating of the wind turbine required. The total renewable energy supply was obtained be summing the results of equations (6.4) and (6.8) on a daily basis. The wind and solar resource availabilities complement each other, with the solar resource being higher in the summer and the wind resource typically higher in the winter, providing a more constant level of energy over the year. A comparison of the total renewable supply and the domestic demands are shown in Figures 6.8 and 6.9. Using this combined energy supply, the total area of the PV and wind system required for matching the electricity demand has reduced to $19m^2 – 32m^2$, and that required for the heating demand has now become $35m^2$ to $270m^2$. The electricity demand could therefore be met by either a 7kW turbine or a combined $10m^2$ PV array and a 4.6kW turbine. The minimum heating demand could be met by a turbine 7kW, but the maximum heating demand would require a much larger wind turbine. The large variation in the area required to match the heating demand is due to the large annual variation in the heating consumption.

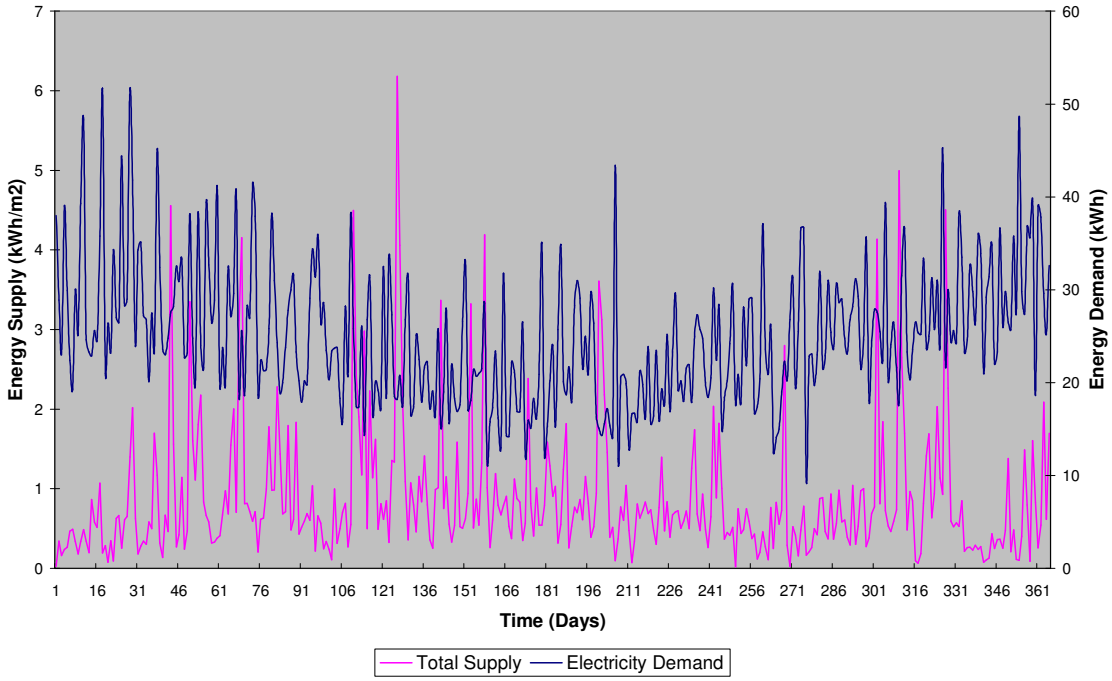


Figure 6.8: Comparison of Domestic Electric Demand and Total Renewable Energy Supply

By restricting the assumption to those sizes of systems that can be practically be installed for a domestic building, an estimation of the proportion of time that the domestic demand is met can be made. Firstly, considering the electricity demand, the largest renewable system (32m$^2$) would match or exceed the demand 40% of the time, whereas the largest heating system (270m$^2$) would match or exceed the demand for 79% of the year. By combining the available solar and wind resources, the time of year during which the potential renewable systems provide the best energy matching has been shifted to the months of April to August. From the analysis of only the solar resource, it could be seen that the best energy availability appeared over the summer months. Therefore the shift in time, over the year, for maximum energy availability for the combined resources appears to be due to the variation in the wind energy potential. For both domestic demand sectors, the renewable supply is primarily limited during the winter months of December to February.

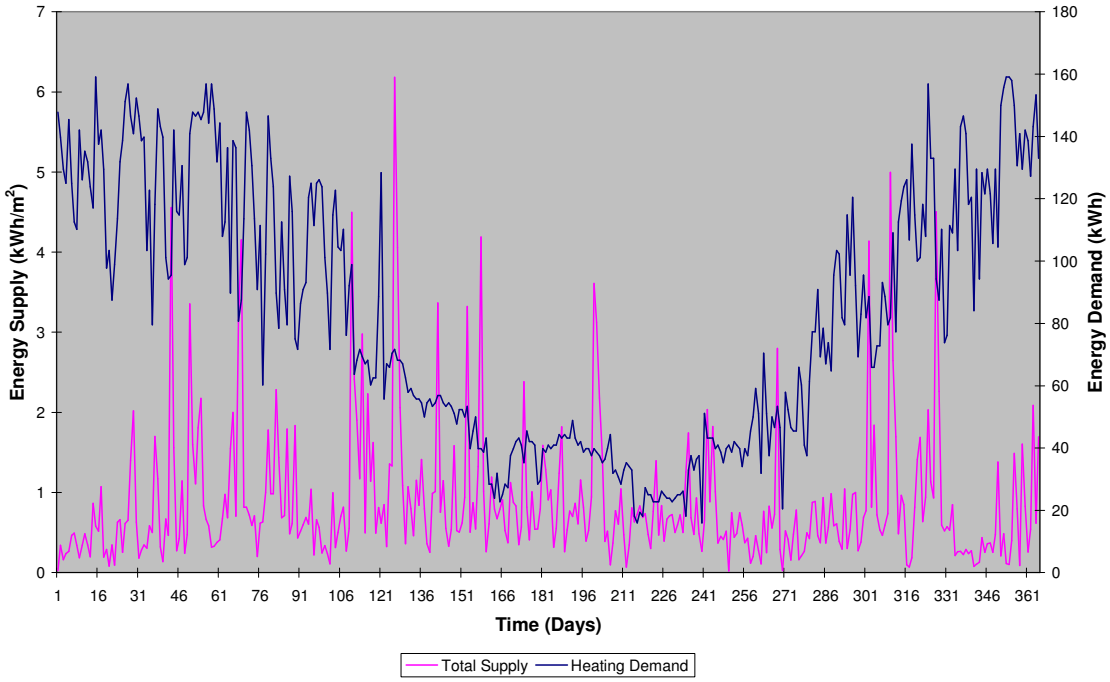


Figure 6.9: Comparison of Domestic Heating Demand and Total Renewable Energy Supply

## 6.3 RENEWABLE SYSTEM SIZING

Most of the system sizes estimated in section 6.2 are greatly in excess of those systems that can be practically installed on a typical domestic household. To assess the realistic match of domestic energy demand and renewable energy supply, the energy output of solar, wind and combined systems that can be realistically installed must be estimated. These outputs will provide a better estimate of the percentage of the domestic usage that can be supplied by such renewable energy systems. As it is anticipated that these suggested renewable sources are unlikely to match the full demand, an assessment of the most suitable domestic end-uses will be carried out to select the individual loads that can be met.

### 6.3.1 Domestic Load Analysis

Due to the large variation in the amount of energy required to match the domestic heating load, the practical renewable system sizes proposed will be primarily used to match the domestic electricity load. From a householder's perspective, and to effectively utilise the energy produced at the dwelling, an assessment of what the common household appliances are, their individual energy consumptions, and their annual and daily load profiles must be carried out. Information on the breakdown of domestic loads is limited for each individual household in the UK, but in

general the domestic load varies with occupancy pattern; the age and number of appliances; the income, age and 'energy' attitudes of the occupants. Due to these variations, and to provide a more generalised approach to domestic energy matching, average consumption values will be used for the most common appliances present in UK households.

Over the past 30 years, the sector covering brown goods has become the largest component in the UK domestic electricity breakdown, currently representing 21% of the overall demand [16]. This sector, and the miscellaneous category include appliances such as computers, televisions, other home entertainment appliances and consumer electronics. These appliances are probably most linked to the income and age of the household occupants, and their ownership and contribution to the overall electricity consumption is set to continue increasing over the next 10 years [16]. These sectors are also those most likely to contribute to standby loads. Out of these appliances, televisions are the largest single contributor to the demand, and are currently owned by 98% of households. The size of this consumption could be due to the number of households containing more than one television set [16,17], again affecting the magnitude of the standby load.

It is estimated that cooking accounts for 5% of the total domestic energy consumption for a typical dwelling [18]. This consumption value would cover either electric or gas cooking, or a combination of both, and is split between the energy required for the cooker hob and oven. UK appliance ownership figures [19] estimate that 54% of households have a gas hob, whilst 57% have an electric oven. Out of these two appliances, the oven has the highest usage pattern with an average rate of 5 hours per week. This is almost double the typical usage time for the cooking hob [17]. However, on average, regardless of fuel source, the typical consumption of the oven is significantly higher than the typical consumption of the hob [20]. Based on this, and the usage patterns, it is estimated that the largest contributor to the domestic cooking load is the oven. Assuming that a dwelling has both a gas hob and oven, the total average annual cooking consumption is 586.9kWh [20]. This value would depend on the operation pattern, size and age of appliance. There may be a mismatch in the time at which the energy is required and the energy which is available from the renewable system, however this factor applies equally to both gas and electric cooking loads. More fundamentally, it is unlikely that the energy consumption of a gas cooker could be met by a renewable energy system. This is due to the inability of a renewable energy system to produce an equivalent fuel for the cooking system, without it being replaced by another type of cooker.

Table 6.3 shows the average daily consumption of the most common domestic appliances, along with the percentage of households containing these appliances [17]. Although the average daily

consumption has been estimated by assuming that the total consumption is evenly distributed throughout the year, some consideration should be given to how often each appliance is used per day. The operation of certain appliances such as washing machines, tumble dryers, and dishwashers will greatly depend on decisions made by the occupants as to how often and when each appliance is used. To assess which of the individual appliance demands can best be met by the renewable system, it is important to consider how these appliances are used and how their consumption patterns may vary throughout a typical day or year. Figure 6.10 shows a typical weekday domestic load profile for a UK household [21]. The shape of the load profile is consistent over the four seasons throughout the year, with some variation in the magnitudes of the peak loads. This typical load profile shows two distinct peaks – the first occurs at about 8.30am, and probably represents the time of day when most people are getting up, and getting ready for the day's activities, e.g. work or school. The second peak begins at 5.30pm – 6.30pm coinciding with the occupants returning home, and the preparation of food and an increase in the use of appliances for entertainment. These assumptions are supported by the results of the 'Time Use Survey' [22] illustrating the activity patterns of people in the UK. The other key factor affecting the shape of the daily load profile is the operation pattern and consumption of the central heating pump [23]. This is responsible for circulating the heating fluid/water around the house and has an average power rating of 70W. The operation times of this end-use match the domestic heating profile, occurring between 7am – 9am, and 4pm – 11pm [24]. Figure 6.10 also shows the typical weekend load profile, showing that the same minimum load is present throughout the whole week.

| Appliance | Average Daily Electricity (kWh) | Percent ownership |
|---|---|---|
| Freezer/FF | 1.918 | 64% |
| Cooking | 2.038 | |
| Dishwasher | 1.562 | 25% |
| Lighting | 1.205 | |
| Refrigeration | 0.822 | 43% |
| Tumble Dryer | 0.712 | 40% |
| Kettle | 0.685 | 97% |
| Television | 0.822 | 98% |
| Washing Machine | 0.726 | 79% |
| Iron | 0.274 | |
| Vacuum | 0.137 | |

Table 6.2: Typical Daily Appliance Consumption Values [17]

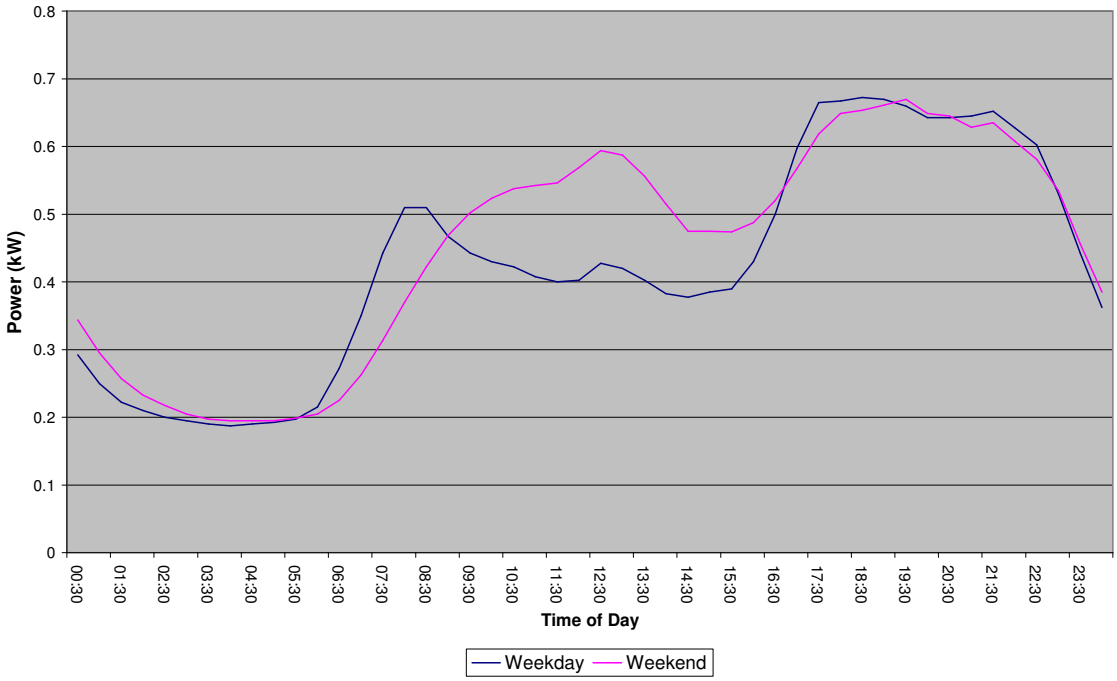


Figure 6.10: Typical Domestic Load Profiles [21]

The load profile also indicates a base load of about 0.2kW present throughout the whole day. This load corresponds to the power consumption of appliances that require continuous operation. From Table 6.2, this is likely to represent the use of refrigerators, freezers or fridge-freezers, and small miscellaneous loads such as LED displays and clocks on appliances, as well as some consumer electronics standby loads. As these loads are fixed and relatively predictable, it would be simpler to assess what proportion of these loads could be matched by a renewable energy system than those loads that are more dependent on the dwelling occupancy patterns.

In the UK most households have 1-2 cold appliances depending on whether they have a combined appliance or separate 'fridges and freezers, and currently cold appliances are the third largest contributor to the overall domestic electricity demand. The annual consumption of these appliances typically has a strong seasonal variation [25,26], however this trend is more noticeable in the consumption pattern of freezers, where the daily summer consumption is up to twice that of the winter consumption. The magnitude of this variation is greater in warmer countries, so is unlikely to be as significant in the UK. The consumption of both fridge-freezers and freezers also decreases over the winter indicating a response to changes in the ambient temperature of the room in which the appliance is located. These variations make cold appliances, in general, ideal for matching with the UK's solar resource. The annual consumption

pattern of these appliances also varies with age and type. The hourly load profile of cold appliances also exhibits a small fluctuation, however, this is unlikely to affect the size of renewable system required. Therefore, assuming that the consumption of these appliances is constant over the day, the average daily consumption ranges from 1.90 – 2.79kWh/day [17,26]. These appliances are also ideal for using the power generated from renewable systems, as any inconsistencies or loss of power will not seriously affect their operation.

If any of the renewable systems generate more than enough energy to match the domestic base load, the specific use of that energy will be assessed for each renewable resource based on the time that the excess energy is generated. If the excess energy cannot be used at the point of production due to changes in occupancy patterns and demand, it is recommended that it be fed back to the grid system. This would offset the total energy required by the dwelling and potentially reduce the total energy costs for the dwelling. The energy costs could be further reduced if the renewable system was eligible for either a net metering scheme or a feed-in tariff [27, 28]. In a net metering scheme, the electricity produced at the point of production would reduce the amount of grid supplied electricity that the dwelling would need to purchase, and reduce the energy bills. Any excess electricity would then be purchased by the dwelling's energy supplier at a rate typically lower than the consumer pays for units supplied from the grid. The rate paid to the customer depends on the utility's renewable tariff, and the technology installed. A more recent alternative to these schemes would be the application of feed-in tariffs where the energy supplier provides payments to the dwelling for all the electricity that their renewable system produces. The total payment is divided into two types – the rate paid for all the electricity produced, and the rate for the excess electricity generated. The other factors affecting the size of the tariff are the type of renewable technology implemented, the size of the system and whether the system is building incorporated or retrofitted. Based on these tariff schemes, the potential financial contribution of the practically installed renewable system sizes will also be considered in the following sections.

### 6.3.2 Practical Solar Energy Matching

For the typical semi-detached dwelling described in Chapter 5, it can be estimated that the available roof area ranges from $20m^2$ to $40m^2$ [29] depending on the pitch angle. This area does not take into consideration any loss of space due to roof dormers, and does not account for roof area that is not suitable for energy production due to shading from neighbouring buildings. Based upon this, and assuming that the typical dwelling has a south-facing portion of roof space, the energy production of both a $5m^2$ and $10m^2$ practical photovoltaic array are estimated on a daily basis using equation (6.4), for a tilt angle of 70°. These array sizes would be the

equivalent to rated systems of 0.6kWp to 1.25kWp. Due to the uniform nature of the available PV panels, the array sizes will be analysed in terms of available area. The daily surplus/deficit values were also calculated using equation (6.5), and the monthly totals for each system are shown in Figure 6.11. Neither of these system sizes generates enough energy to meet the minimum total electricity load experienced over the summer months. However, both these systems can match a set proportion of the domestic load, which can be used to offset the energy required from the grid, and can be used to power certain domestic appliances. The smallest array of $5m^2$ matches, on average, 10% of the domestic electricity load, generally over the months from March to August. Over the remainder of the year the system is likely to match between 2%-6% of the electricity demand. As expected, doubling the size of the photovoltaic array doubles the percentage of the domestic load that can be met on average. However, over the year the proportion of load met ranges from about 5% over winter to more than 25% over the whole summer period.

Over the year, the energy production from the range of these two array sizes is calculated as 684kWh and 1368kWh. Assuming that either of these two sizes are retrofitted to an existing dwelling, a feed- in tariff of 41.3p would be paid for every unit of electricity generated, and any excess electricity would be bought for at an additional 3p/kWh. The energy generated by these array sizes would be worth at least either £284 or £567, and assuming that all this energy is used in the dwelling this would result in a saving of £79 or £159 on the energy bill. If the photovoltaic system were installed at 50°, to match a more typical roof pitch angle, the energy produced over the year would range from 740kWh to 1480kWh. This increase in energy is due to the increase in solar energy over the summer months. If the roof pitch angle were 30°, the annual production would increase again. The problem with these tilt angles is that the solar energy supply would reduce significantly over the winter months and is unlikely to make much of a contribution to the domestic base load during the winter months.

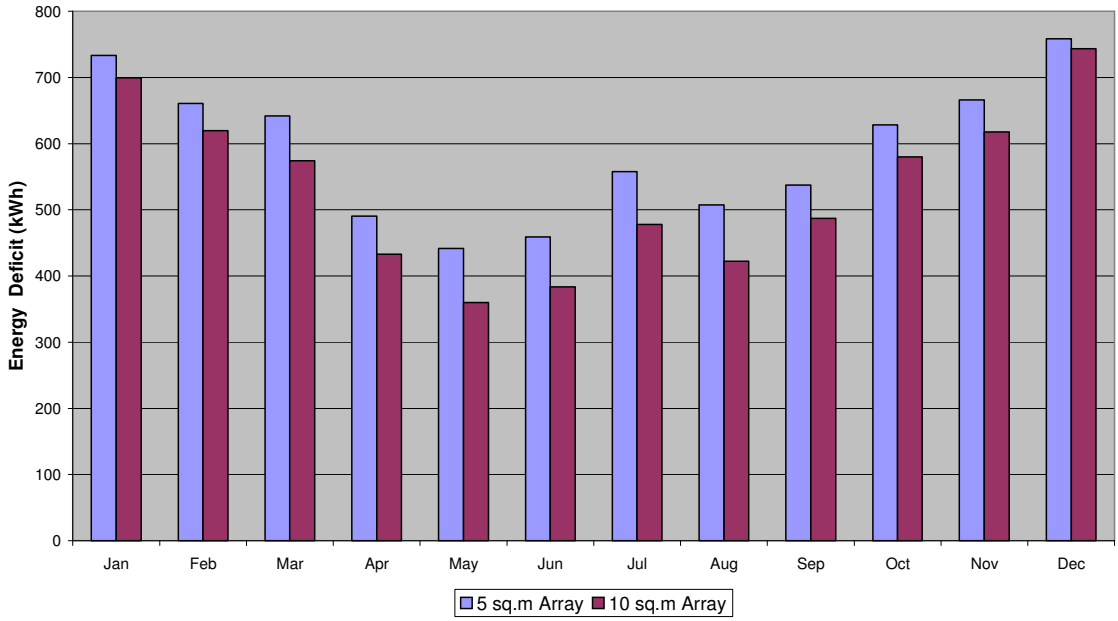


Figure 6.11: Monthly Total Energy Deficit for Practical PV systems

For both these practical limits, of $5m^2$ – $10m^2$, the energy required from the grid, per day, varies from 1.53kWh to 40.40kWh, with an average value of 18.40kWh. The probability distribution functions of both these energy surplus/deficit values are also plotted, and are shown in Figure 6.12. These distribution functions both look approximately normal, and the spread of energy values increases as the array size increases, representing an increase in load matching. The key statistical parameters of the two array limits are shown in Table 6.3.

| Statistical Parameter | $5m^2$ Array | $10m^2$ Array |
|---|---|---|
| Mean | 19.405 | 17.531 |
| Standard Deviation | 6.498 | 7.040 |
| Skew | 0.338 | 0.289 |
| Minimum | 6.217 | 1.530 |
| Maximum | 40.350 | 39.725 |

Table 6.3: Comparison of Statistical Parameters for PV System Energy Deficits

From the statistical parameters of the energy curves it can be seen that the mean value of the data is just the difference between the mean domestic electricity demand and the mean energy available for the photovoltaic system. The mean energy supply/availability can be calculated

from equation (6.4), for any size of system provided the average daily solar radiation on the required tilt angle is known. It is proposed that a normal distribution function be used to estimate the values shown in Figure 6.12. Based on this, it is possible to quantify the proportion of time a domestic photovoltaic system can meet or exceed the domestic electricity demand. The function, when multiplied by time allows for an estimation of the amount of time that any value of extra energy is required from the grid.

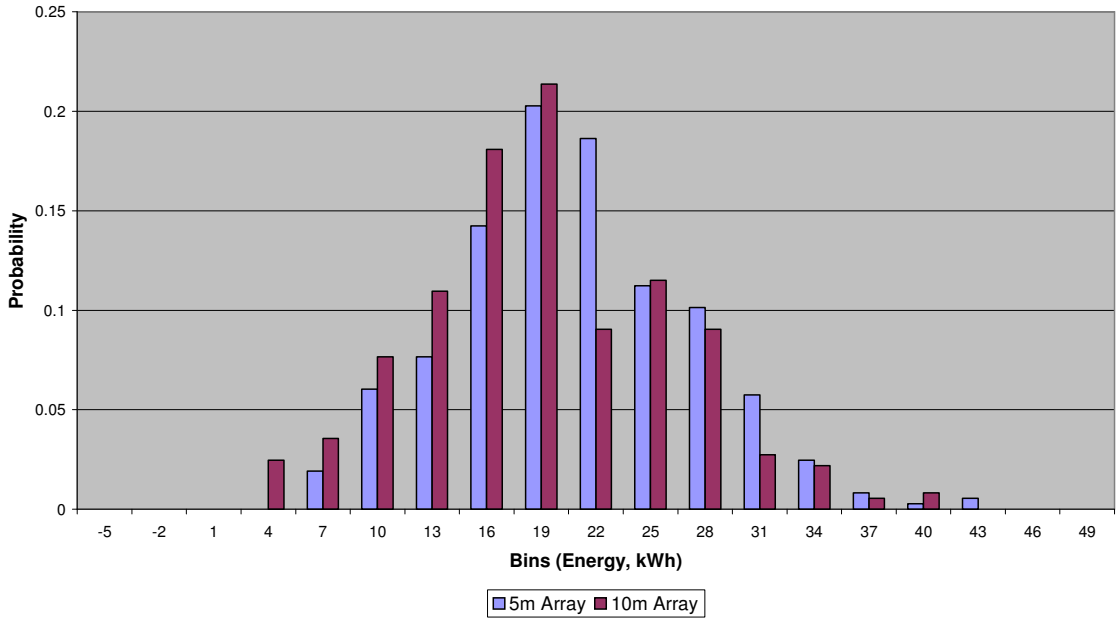


Figure 6.12: Probability Distribution of Solar Surplus/Deficit Energy

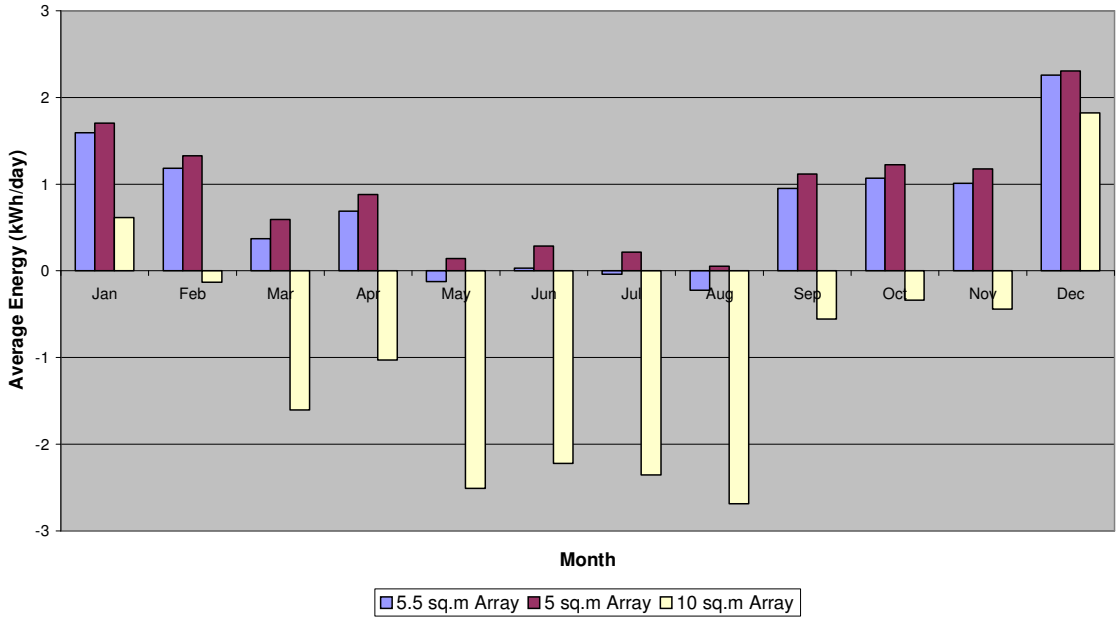


Figure 6.13: Average Daily Surplus/Deficit Energy for Cold Appliances

Based on the available solar energy, at an array tilt angle of 70°, an area of 5.5m$^2$ would ideally be required to match the maximum consumption for cold appliances of 2.79kWh/day over the summer. Using a photovoltaic array of this size it is estimated that this demand is matched for about four months of the year. The energy deficit in June is a result of the outputs from the resource and energy models described in the previous two chapters, in particular an over-estimation of the energy load. Repeated analysis, on a yearly basis, of the level of supply and demand matching would give a better level of confidence in the number of months that the refrigeration demand is met. During the remaining months, the demand for cold appliances is partially met requiring on average an additional 40% of energy from the grid per day. Over the year, a system of this size would typically meet or exceed the demand for 30% of the year. The estimated daily surplus/deficit values for cold appliance for the 5m$^2$, 10m$^2$ and the 5.5m$^2$ array are shown in Figure 6.13. This shows that the largest limit of the solar area typically exceeds the required demand for cold appliances over ten months, generating a typical excess of energy of 1.4kWh on a daily basis. If this 10m$^2$ array surplus/deficit is considered on a daily basis, the refrigeration demand is met and exceeded for 63% of the year.

However, some problems arise when comparing the continuous load of these appliances on an hourly basis to the available solar energy. On a typical day the solar energy is available from 7am to 8pm with the maximum energy available at 12noon. On average there would be a 13-hour deficit of energy where the continuous power of the refrigeration devices was not met. Therefore on a daily basis only 45% of the total cold appliance energy consumption is met. However, the photovoltaic system would produce in excess of the continuous refrigeration demand for between 7 to 8 hours over a typical day. This excess power produced could be used for some small power loads in the household, but due to the occupancy patterns it could better be utilised by being fed back into the grid system, offsetting the total domestic load required. This would only be beneficial to a consumer using a smart meter and assuming a reasonable tariff for the electricity they have generated, to make the investment in the system worthwhile. A better analysis of the hourly demand matching would be achieved with more detailed information on the diurnal variation of the solar resource. However this is out with the results of the solar resource model outlined previously in Chapter 4.

### 6.3.3 Practical Wind Energy Matching

As discussed previously, the contribution from small-scale wind systems has been limited to systems smaller than 10kW due to the practical constraints of installing these wind turbines in urban areas. Based on this, the daily energy production of three turbine sizes, 1.5kW, 6kW and 10kW, was estimated using equation (6.8), and compared against the domestic electricity

demand. The values of 1.5kW and 6kW were chosen to represent the potential minimum and maximum energy production limits from commercially available turbine sizes. The 10kW turbine analysis is used for an estimation of the energy production for dwellings in a more suburban, or rural location. From this comparison it was seen that the smallest turbine size does match, and exceed the domestic electricity consumption on days that correspond to higher than average wind speeds. On the days when the wind speed is much lower, the 1.5kW turbine does not match the minimum electricity demand. The monthly energy surplus/deficit totals were calculated for each turbine size, and are shown in Figure 6.14. On average, the 1.5kW turbine meets 18% of the domestic load, generally over the period of February to June. Similar conclusions can be made for the other two turbine sizes. However, as expected on a daily basis they do meet a higher percentage of the demand. The proportion of the demand met by the 6kW turbine, ranges from 25% to 125%, again with the best production occurring between February and June. The 10kW turbine meets, or exceeds the domestic load for 27% of the year, on average supplying 119% of the domestic demand. These figures show that the when the larger two turbine sizes generate excess energy, they generate at least 50% of the typical domestic load as extra energy. However, the total annual energy production for the three chosen turbine sizes ranges from 1234kWh to 8220kWh, the larger value representing about 105% of the total domestic electricity load for this example dwelling. For these practical turbine sizes, the amount of energy required from the grid per day ranges from 1-2kWh to 40.4kWh. Again, using a feed-in tariff of 26.7p for every unit of electricity generated, these turbine sizes would provide on average a minimum of £329 - £2194 of income to the householder.

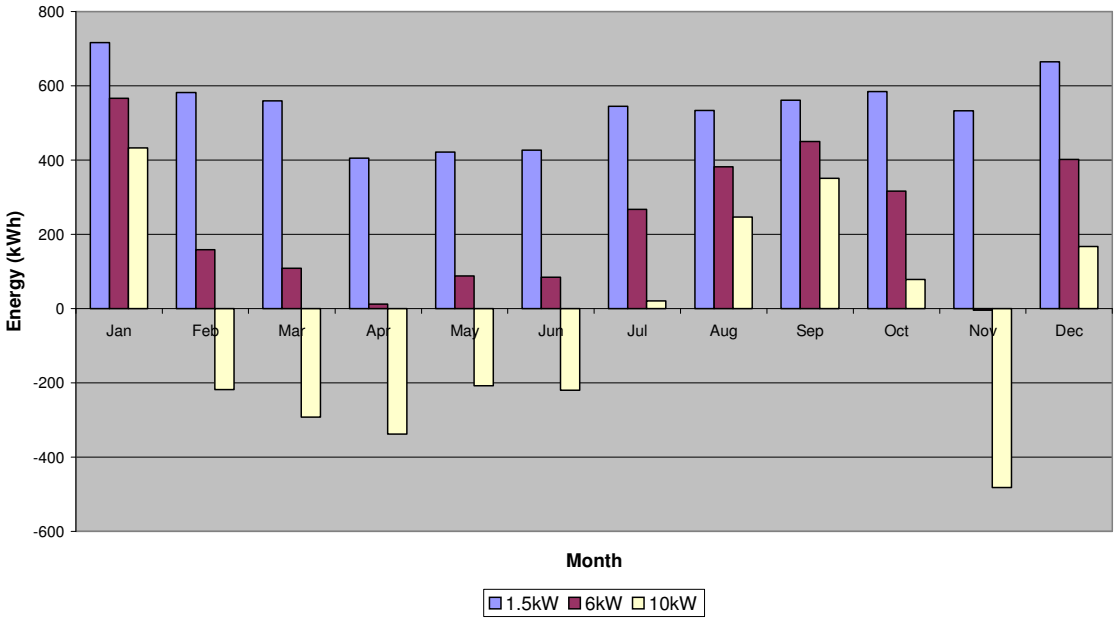


Figure 6.14: Monthly Total Energy Surplus/Deficits for Practical Wind Systems

The distribution functions for the daily energy surplus/deficit values for each turbine size were calculated and are shown in Figure 6.15. There is not the same similarity in pattern to the distribution as there is with the solar energy supply, but the function appears to have a left-hand skew. The tail of the distribution function also appears to increase as the turbine rating increases, representing an increase in the number of days when the domestic demand is exceeded. These energy values will also coincide with the days with the highest wind speed values over the year, the occurrence of which is quite variable over the years.

As the annual average diurnal variation in the wind energy follows a sinusoidal shape with a constant supply (as shown in Figure 4.14), and a peak at about 1 –2 pm, the most appropriate domestic loads to be matched first would again be the base loads. The smaller turbine of 1.5kW does not produce enough power to meet the continuous load of 120W for the cold appliances, so a comparison between the power produced on a typical weekday [21] for a 6kW turbine and the typical domestic load profile was carried out. This comparison is shown in Figure 6.16, and shows that the refrigeration base load can be met, on average, quite easily over the whole day. Based on this profile it can also be seen that the wind energy production exceeds the domestic demand for about 14% of the day. This excess percentage would vary depending upon the domestic profile, which varies seasonally, and from weekdays to weekends. The typical diurnal power variation for a 10kW turbine produces a minimum constant power of about 3kW, with the peak load at midday exceeding the domestic demand.

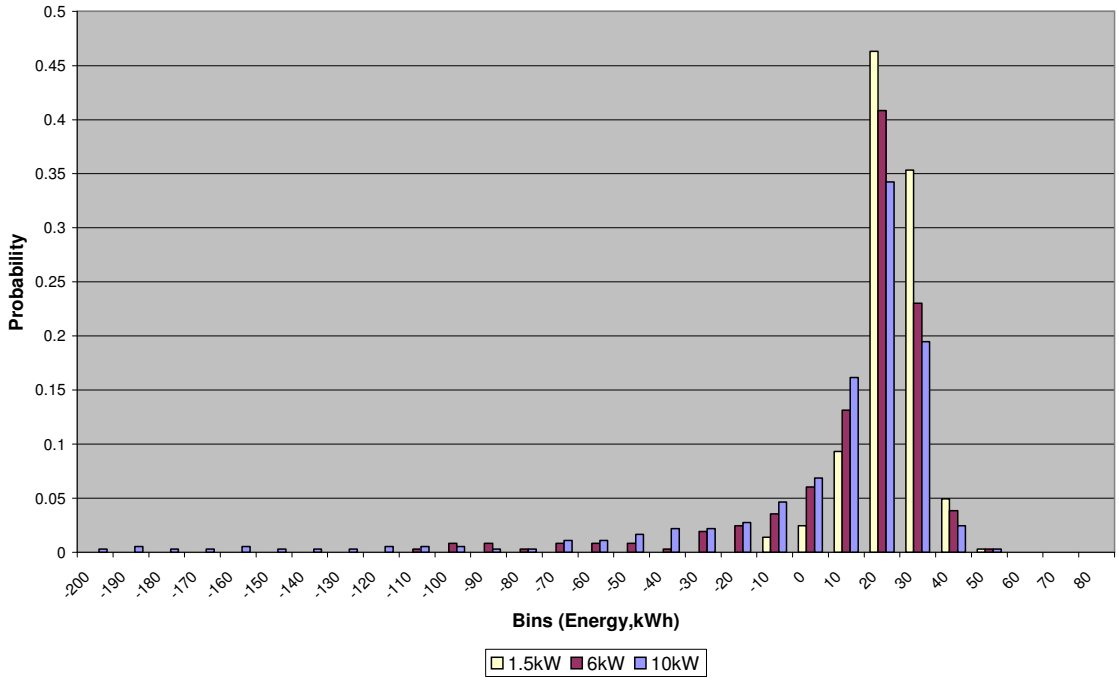


Figure 6.15: Probability Distribution of Wind Energy Surplus/Deficit

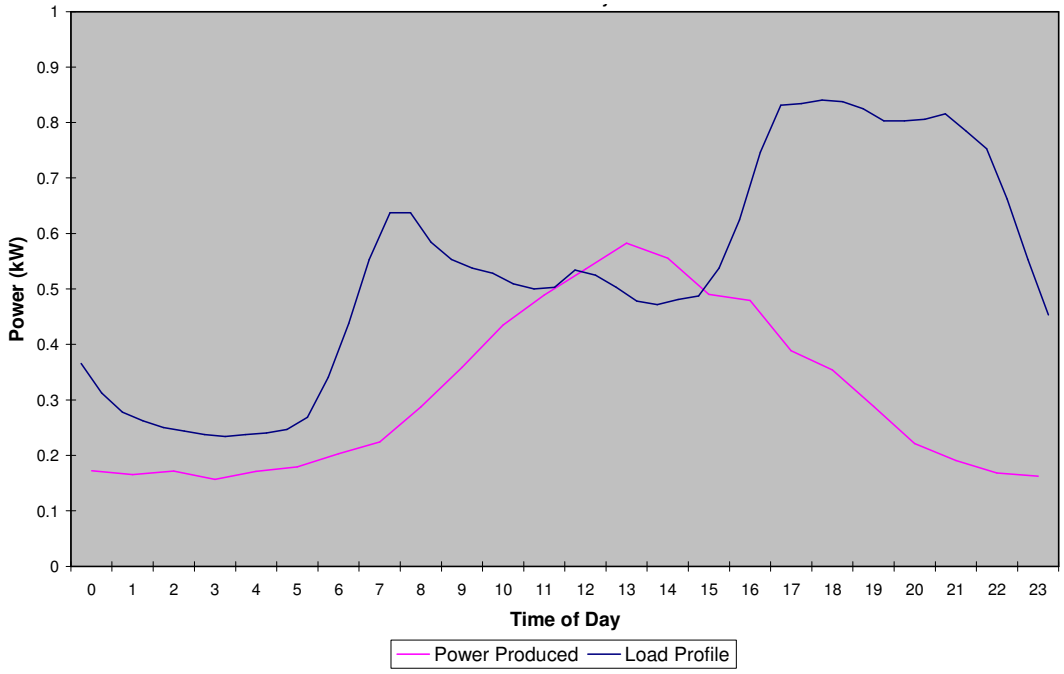


Figure 6.16: Comparison of Domestic Load and Wind Power Produced by a 6kW Turbine for a Typical Day

### 6.3.4 Total Practical Renewable Energy Matching

Based on the reduced potential of the individual renewable systems meeting the domestic electricity demand, four practical combined systems are considered. These four systems consist of a photovoltaic array and two different sizes of wind turbines, and are summarised as:

(1) $5m^2$ array and a 1.5kW turbine
(2) $5m^2$ array and a 6kW turbine
(3) $10m^2$ array and a 1.5kW turbine
(4) $10m^2$ array and a 6kW turbine.

These system sizes were selected to give an indication of the minimum and maximum energy produced by commercially available renewable systems. If the typical wind and solar energy surplus/deficit probability distributions could be quantified, then the energy production of system sizes within these limits could be easily assessed.

The total energy produced by each of these system combinations is estimated on a daily basis, and then compared to one year's domestic electricity demand. This information is then used to estimate the average percent of the domestic load that is met by each system, and the proportion of the time that these systems match, or exceed, the domestic demand. This information is summarised in Table 6.4, and shows that increasing the array size increases the percent of the daily load that is met on average, whereas increasing the turbine size increases the proportion of time that the load is met over the year. The results show that combined system 4, of a $10m^2$ array and a 6kW turbine appears to provide the best annual match to the domestic electricity demand.

| Combined System Number | Average % of Demand Met | Number of days that total demand is met or exceeded |
|---|---|---|
| 1 | 21.7% | 15 |
| 2 | 29.7% | 64 |
| 3 | 63% | 18 |
| 4 | 71% | 73 |

Table 6.4: Analysis of Combined Renewable System Performance

The energy produced by each of these systems is then used to calculate the monthly total energy surplus/deficit values. A comparison of the daily averages of these values is shown in Figure 6.17. This shows that on average the largest amount of energy required from the grid occurs over the winter months, of October to February, for the two $5m^2$ combined systems. For systems 3 and 4 using a $10m^2$ array there is still a substantial energy deficit over January. The energy surplus value produced in again in June is most likely the result of the outcomes of the resource and energy models. This could be due to issues with the wind speed model, reducing the energy availability over the summer. More repeated analysis of yearly values could improve the confidence level in the energy surplus/deficit results.

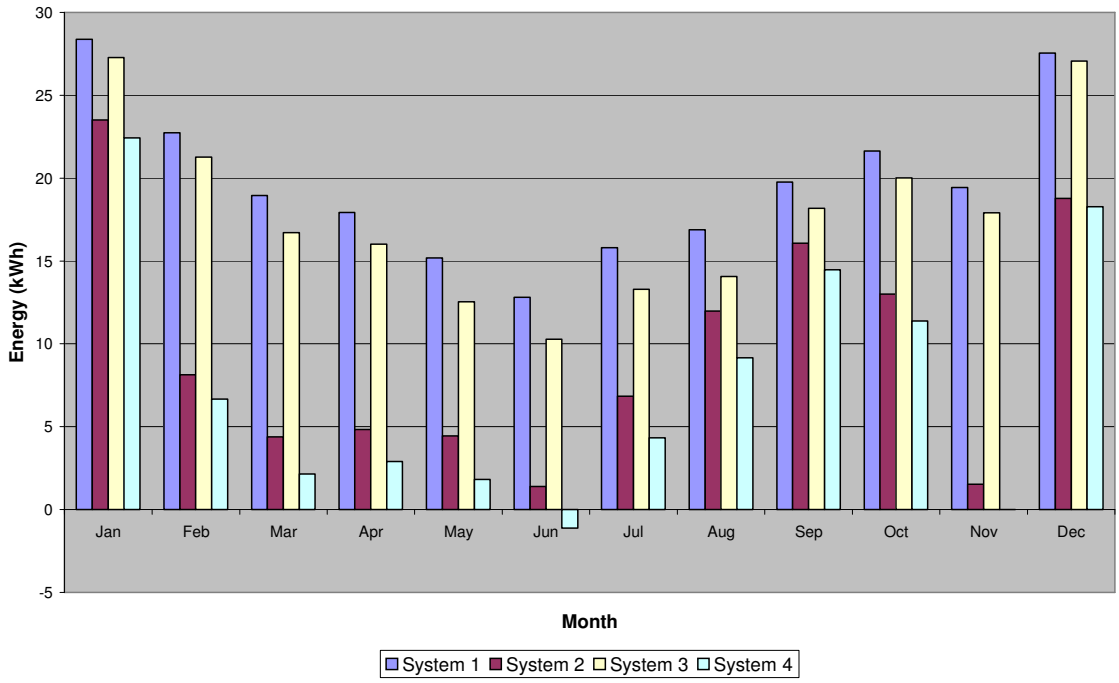


Figure 6.17: Average Daily Surplus/Deficit Energy for Combined Systems

Based on the percentage of domestic demand that is met on average, any of the four combined systems would adequately match the typical daily demand for cold appliances. The larger two systems would also be able to supply power to other small domestic power loads, or feed their excess generation into the grid, offsetting a larger proportion of the domestic user's energy requirements.

## 6.4 POTENTIAL CONTRIBUTION TO SCOTLAND'S ENERGY

According to the 'Scottish House Condition Survey' [30] there are approximately 1.36 million dwellings (excluding flats) in Scotland. Assuming that 94% of these dwellings have pitched roofs and that 50% of the pitched roof dwellings have a portion of their roof south facing, there are 640,000 dwellings suitable for the installation of photovoltaic systems. From the analysis of the practical solar systems, it is assumed that each of these dwellings is capable of supporting a $10m^2$ array, which is anticipated to produce between 15% - 25% of each dwelling's total electricity demand. Based on this, the total amount electricity generated by these solar arrays would be 848GWh per year, which is equivalent to around 1.5% of the total domestic energy consumption in Scotland.

This figure can be compared with regard to the potential energy contribution of small-scale wind systems. For simplicity, in relating available building space with turbine mounting area, it is assumed that each dwelling in Scotland is suitable for the installation of a 1.5kW turbine. This turbine size was again estimated to produce between 15% - 25% of a dwelling's total electricity demand. Based upon this, it is estimated that small wind turbines would generate 1.67TWh of electricity, equivalent to 3% of Scotland's total domestic energy demand.

These figures illustrate that small-scale domestic wind and solar systems do not make a significant contribution to the total Scottish domestic energy demand. However, if these systems were combined and compared with the proportion of electricity used to meet the Scottish domestic demand, then their overall contribution would raise significantly to 20%. This figure could be improved by considering the contribution of more rural dwellings with larger turbines.

## 6.5 DISCUSSIONS AND CONCLUSIONS

This chapter has aimed to use the modelled available renewable energy over the year to estimate the typical average sizes of generating systems required to match the domestic electricity and heating demands. This renewable supply was estimated for solar systems, wind systems and a combination of the two technologies.

The initial results demonstrated that excessively large sizes of both solar and wind systems were required to match the domestic heating demand. From this it was concluded that it was impractical to use these renewable technologies, on a small scale, to effectively match the heating load/demand. The system sizes required to match the domestic electricity demand were also quite large, but it was concluded that these systems could contribute a minimum of 10% to the domestic electricity demand, and could make a more significant contribution.

As either of the renewable systems could be grid connected, the energy production of both practical photovoltaic and wind systems were calculated to assess how much a typical dwelling could expect to generate, and offset consumption from the grid system. As expected the solar systems were unable to generate enough energy at the time of demand to fully supply the dwelling's electricity load. The typical daily profile of the solar resource is more ideally matched to the load profile of commercial and office buildings. Once the domestic base load has been met, it would be sensible to use the additional energy generated to match the demand of local offices. If detailed information on office electricity demand was available, a comparison between the solar energy supply could be carried out to assess how suitable these systems are

for other building types. If a large number of domestic buildings installed photovoltaic systems, sized between $5m^2$ and $10m^2$, they would be able to offset certain proportion of the demand of commercial buildings, reducing the amount of energy that the grid must provide for them.

The smaller wind systems also generated between 20-30% of the domestic demand. However, the typical diurnal wind power profile demonstrated that these devices could generate electricity for the majority of the day, making them ideal for matching constant base loads. The reduced level of wind energy matching obtained in the previous sections could be partly due to some issues with the modelled wind speed data. Although the wind speed data used for the energy supply input has the same structure and distribution function as actual wind speed data, the modelling procedure has a tendency to produce some wind speed values that are lower than expected, compared with the actual wind data. This would reduce the energy production over a number of days per month, without matching the lowest monthly averages. However, it could be argued that underestimating the energy production would provide better reliability in energy matching. If the energy production were overestimated, it would require the occupant to either purchase more energy/electricity from the grid, or require the building to have a backup energy source.

Combining the wind and solar systems, provides a better match on average for the domestic electricity demand, and could result in a reduction in the required system sizes. When combined, these systems may provide a more constant level of energy matching. This demonstrates that to match the domestic demand more evenly, using renewable sources, a combination of a number of technologies is required. It also demonstrates that although the use of solar energy for generating electricity is currently limited in the UK, it could be used quite effectively to offset 10-20% of the domestic demand. This analysis was based on data for Aberdeen, but it is anticipated that energy supply data generated for a more southerly location could provide a higher percentage of the load, primarily due to an increase in the available solar energy.

As with any self-generating technology, there are a number of issues facing every potential dwelling. Firstly, the main issue would be the available area for installing either photovoltaics or wind turbines. From a planning perspective, it might be simpler to install a solar generating system, as it is typically roof mounted. However, consideration should then be given to the level of shading at each individual site. Wind turbines generally require a distance of at least 20m from any building before being installed, making them more suitable for more rural locations. However, if a small scale turbine is to be installed in an urban environment, it should be placed

at a height greater than any nearby buildings and obstacles, or in a position that has a clear view of the prevailing wind direction [31].

Over the past 5-10 years there has been a renewed interest in the use of building mounted turbines. Due to current planning regulations limiting the size of their diameters, these turbines are generally no greater than 1kW in rating [32]. To estimate the energy production of such turbines, detailed knowledge of the wind speed profile in urban areas is required. The urban wind energy availability would greatly depend on the density of the buildings within a chosen location, and on their interaction with the wind flow. To assess the energy availability, wind speeds at a height of 7m to 10m are typically used for these building mounted turbines [32, 33]. This is comparable with the height used for the development of the wind speed model, as illustrated for Aberdeen in Chapter 4. At this height, and within an urban location, the wind speed values would be reduced, resulting in a lower energy production. Due to the shapes of some buildings, it may be possible to increase the available wind speed and energy production through the careful selection of the turbine locations [32]. To optimise the contribution from small building mounted turbines, more detailed analysis of the wind flow around buildings is required, along with site specific consideration of the mounting possibilities.

The second factor affecting the energy production relates to the power curves of the individual turbines suitable for building mounting. These curves are typically based on information from each manufacturer, and may be subject to some variation. A recent study [34] of installed building mounted turbines illustrated that the measured power curves matched the manufacturer's curves best at low wind speeds. As the wind speed increased, the measured power produced was somewhat lower than the manufacturer's anticipated values. This illustrates that some caution should be taken when using only the manufacturer's data, and that more research is required in obtaining either an accurate power curve, or power coefficient value for building mounted turbines. The same study [34] of installed building mounted turbines also found that on average these turbines generated about 214Wh per day. This value increased to 628Wh, if the energy produced was calculated based on the proportion of time that the turbines were on. Based on these results, these turbines are unlikely to make a significant contribution towards matching the domestic electricity demand. As a comparison, another study [33] illustrated that the energy production for a 2kW turbine, at a 7m height, in Aberdeen was 914kWh, representing a capacity factor of 5%. These two studies demonstrate that there is a great level of variability in the energy production of building mounted turbines, and that a more detailed, and reliable method for assessing the performance of building mounted turbines is required. The results also show that Aberdeen has a higher than average wind resource, making it suitable for the use of urban wind turbines.

As the modelled wind speed data in Chapter 4 represents data at a height of 10m, similar to that of a typical dwelling installation [32, 33], the calculated energy production of the 1.5kW turbine, for Aberdeen, can be compared with the previous results. The anticipated power produced by this turbine in Aberdeen, is representative of the values obtained from the cubic portion of the curve shown in Figure 6.7, which may result in an overestimation of the power produced at higher wind speeds. Again this illustrates the need for turbine power curves that accurately represent the production of turbines in urban environments. The capacity factor for this turbine was also calculated as 9.4%. This is close to the previous value obtained for Aberdeen [33], for a larger turbine. The differences in value may be due to differences in turbine height and variation in the power curves. Therefore, to be able to estimate the actual energy production of building mounted turbine, a more realistic assessment of the urban wind profile over the year is required, along with more realistic turbine power curves. However, it is not the aim of this project to provide a detailed assessment of the contribution of such building mounted turbines.

The other key issue affecting the widespread implementation of small-scale renewable systems on dwellings is the cost, especially if a number of technologies are to be combined. Considering the smallest combined system ($5m^2$ array and 1.5 kW turbine) required to meet the typical cold appliance demand, the anticipated total cost for this system is between £3700 - £7200. As both these technologies are eligible for the current feed-in tariff scheme, their potential income would be £613. This would also result in an annual energy cost saving of £250. These domestic renewable technologies could then be used in conjunction with demand-side management techniques, such as real-time pricing, to force consumers to be more energy conscious, and to help level the supply over the day. However, for these schemes to be implemented, a larger uptake of domestic renewable systems is required.

# CHAPTER 7

# CONCLUSIONS

## 7.1 SUMMARY

This project aimed to assess the potential energy contribution of small-scale renewable systems in Aberdeen. In order to quantify this contribution, detailed information about the renewable energy supply, and the domestic energy demand was required. A comparison of these two energy sets was carried out in order to estimate how much of the domestic demand could be met by small-scale wind and PV systems, and for what proportion of time. These details would also help to assess what domestic loads were suitable for certain sizes of renewable systems.

To estimate the energy available for both wind and PV systems, three model procedures were developed to generate daily sequences of global solar radiation and wind speed for Aberdeen. The use of model procedures was necessary due to the limited available data for such renewable sources, and due to the costs and time involved in measuring this data over a statistically representative time period.

The proposed model for generating solar radiation data was based on the use of Fourier series to estimate the typical underlying trend present in the daily data. The advantage of this technique was that this trend function could be generated accurately using a small number of model parameters. This technique could be applied to a number of different years and locations provided the annual mean daily solar radiation value was known. The random fluctuations within the solar radiation were modelled separately as white noise that was adjusted by a monthly set of mean and standard deviation values for Aberdeen. The results from this section of the solar model were very location dependent. However, the process outlined could be used for another location provided historical solar data was available.

The overall model procedure described in Chapter 4 generated a time series of daily solar radiation data that accurately represented the statistical properties and the structure of the actual solar data for Aberdeen. The process was quite straight forward, and could be used repeatedly to obtain a number of years of annual data that could then be used to estimate the daily energy production from a solar PV system. As some of the parameters were specific to the chosen location, the next stage in this project area would be to obtain a generalised method for obtaining the 12 sets of parameters, possibly relating them to the annual mean value. If this

relationship were to be obtained, the model could then be easily applied to any other location within the UK.

Two potential models were proposed for obtaining detailed wind speed data for the chosen location. The first procedure used a first-order autoregressive (AR(1)) model to obtain daily mean wind speed values. Although the parameters used in the model given in Chapter 4 were again specific to Aberdeen, numerous studies were reviewed that supported the use of time series techniques for modelling wind speed values. The main difference was that the model proposed in Chapter 4 used one model to generate a complete year of data, whereas the previous studies had used a number of monthly models. Once the data had been produced using this AR(1) model, it needed to be converted into data that followed the anticipated Weibull distribution for wind speeds. The parameters used for this were also dependent on the location, and on the time detail of the wind data required. There was no consistency in the value of this parameter from one year of data to the next. Due to this, the value of parameter used should be selected carefully to ensure that the wind speed data generated was statistically similar to that of the actual historic data for Aberdeen. The overall accuracy and confidence in the model procedure could be improved if a larger data set was used to build the model. These factors aside, the use of the AR(1) model had a number of advantages including its simplicity, its requirement of a small number of model parameters, and the fact that it was a quick procedure for obtaining many sets of daily wind speed data.

The second wind model stated used a combination of Fourier series and wavelet techniques. A Fourier series was proposed to model the low frequency trend function within the data, using the harmonic components present in all years of the actual data for Aberdeen. There were a number of limitations to using this method, in particular the amount of data used to build this section of the model. A longer data set of actual wind speed data for Aberdeen would provide a greater level of information about the key frequencies present in the data. Due to the variations in each year of wind speed data, this Fourier series required a much larger number of parameters than the one required for the solar model, and only accounted for about 4% of the variance in the data for any year.

The stochastic component left in the wind speed data was modelled using the Discrete Wavelet Transform (DWT). To do this, 6 sets of random data were generated as noise, to estimate the Wavelet coefficients required as the input to the DWT. These random coefficients were recombined using the Haar waveform to obtain a set of detail and approximation functions that when added together obtained a new estimation of the stochastic data component. Each of the 6 data sets was generated using three parameters – the mean, standard deviation and the number

of coefficients required for each level. This combined Fourier – Wavelet model required significantly more parameters than the AR(1) model. Again the results, and model parameters given in Chapter 4 were only applicable to Aberdeen. As the data produced from this procedure also had to be transformed to obtain the required distribution function, the same issues outlined for the choice of parameter for the AR(1) model also apply.

Although the Fourier - Wavelet model procedure maintained the key statistical properties and the distribution function of the original data, it could be improved in a number of ways. Firstly, the possibility of using a different wavelet function could be investigated. The model used here used the Haar wavelet for simplicity – another function might better match the general shape of the fluctuations in the data. Secondly, as the Fourier series was quite variable and did not represent a high proportion of the variance, it would be worth investigating the use of the DWT techniques on the complete daily wind speed data. Alternatively, if the monthly mean wind speed values were known, the annual daily trend could be estimated using a similar interpolation technique to that used in the domestic energy consumption models in Chapter 5.

Along with these resource models, a simple procedure for estimating both the electricity and heating consumption of a typical domestic building was developed. The energy consumption for a dwelling was readily available on a monthly basis, so this time scale was chosen as the input data for the first step of the model procedure. This allowed daily energy values to be obtained from 12 known parameters. This section of the procedure provided an annual approximation to the trends present in the both the electricity and gas data. However the daily fluctuations associated with both data sets also had to be accounted for. As the daily electricity demand for the chosen typical dwelling exhibited strong weekly cycles, a generalised Fourier series estimated some of these fluctuations. However the model procedure could be used for buildings that were not anticipated to have strong weekly cycles. The daily fluctuations in the gas consumption data were estimated with 12 sets of white noise that were adjusted using mean and standard deviation parameters.

Although the electricity consumption model appeared to require a significant number of parameters, most of this data could be easily obtained for a specific dwelling from energy bills, or meter readings. The same process could be applied to obtain some of the model parameters obtained for the gas model, or the monthly values could be calculated for a specific property using the process described in Chapter 5. The electricity and gas models both provided a method of generating energy consumption data that accurately maintained the statistical and structural properties of the measured data for the chosen location. As the usage pattern of energy was relatively consistent from year to year for any dwelling, the model procedures also allowed

for a way of generating multiple, representative annual profiles of energy data that could be used to assess the level of matching required by renewable system.

The main disadvantage of the model described was that the input data used was limited to a specific type of building. The next step for this area of work would be to obtain detailed demand data for a number of different dwelling types, and to assess how applicable the model procedure described was for estimating daily values. Another area to be investigated would be the use of the model for estimating the annual trend of energy consumption for office buildings. If this was carried out, a detailed assessment of some energy efficiency measure could be made on a daily basis, before the implementation of such measures. This would be beneficial in testing the feasibility and economic viability of different efficiency and waste avoidance measures. The same principle could be used for the domestic sector.

Finally, the available renewable energy data and energy demand data were compared to allow for an estimation of the sizes of small-scale renewable systems required to match the typical domestic load. As the focus of this project was on the utilisation of PV and wind systems it was assumed that the renewable systems would be connected to the grid. From the daily analysis of energy availability and demand values, it was found that at best only 10 - 30% of the domestic load could be met be either a PV system, or a small wind system on its own. This proportion of load matching was obtained using system sizes that could be realistically installed in urban environments. The analysis carried out in Chapter 6 also demonstrated that the best renewable energy supply could be obtained by using a combined PV and wind system, with the best level of demand matching achieved for a $10m^2$ array and 6kW turbine. This would result in a more constant level of supply, and match a greater proportion of the domestic load than either system could individually. This analysis could be repeated by varying the input data obtained from the resource and energy consumption models. The analysis outlined could also be used to assess the potential contribution of other sizes of renewable systems. As stated previously, these models could eventually be generalised for different dwelling types and sizes, allowing for an estimation of the level of energy matching achieved for a representative proportion of the UK housing stock.

The analysis of the energy surplus/deficits obtained for the individual PV and wind systems also demonstrated the annual distribution functions of the data. By quantifying these distribution types and parameters, it was hoped that the proportion of time that either a PV system or wind system matched its demand, and how much energy it provided, could be estimated by a set distribution function. If this could be achieved it would allow better planning of the potential contribution by small scale renewable systems without detailed knowledge of either the

resource availability or the energy demand. These distributions could also be useful in assessing the feasibility of installing small-scale community based distributed systems at specific locations around the UK. The results of this analysis, when combined with the potential use of net metering or feed-in tariff schemes would provide an estimate of the costs associated with the supply of energy from domestic buildings.

## 7.2 CONTRIBUTION TO KNOWLEDGE

In conclusion the work in this thesis can be summarised by the following contributions:

- Developed a simple model for generating synthetic daily energy consumption time series from monthly average values. This data could be easily obtained from occasional meter readings, simple load analysis and heat loss calculations, avoiding the necessity for time consuming and costly data logging. The energy models described were illustrated for one location, and could repeatedly produce a highly representative set of daily energy data.

- Investigated the application of modelling Wavelet coefficients for generating daily synthetic wind speed values, which reduced the level of detail required as an input for Wavelet decomposition. The results obtained were only applicable for Aberdeen, however similar model parameters could be obtained for other locations provided that some historical wind speed data was available. The generalisation of the technique allows many representative data sets of daily wind speed data to be obtained.

- Assessed the applicability of a number of resource models for wind and solar data in Aberdeen. The modelling techniques were chosen due to the limited level of input data required with the aim of generating synthetic resource data using limited information about a chosen location.

- Selected suitable realistic sizes of small – scale wind and PV systems and assessed their level of contribution to domestic electric loads.

- Provided a detailed method for comparing the renewable energy available with typical domestic demand profiles, using limited input data for a specific location in the UK. The results obtained were very reliable due to the strong statistical and structural commonalities between the modelled results and actual historical data.

## 7.3 FUTURE WORK

If the models could be developed further and tested for other locations within the UK, then it would be possible to optimise a renewable system design size based on the available renewable resource, a consumer's energy profile and some practical design constraints. The models developed could be used as an input in the future development of statistical energy supply and demand models for small renewable systems. These statistical models could then be generalised for any location and could allow for a detailed estimation of the costs and feasibility of distributed generation, even if only limited energy data was available. All this would be useful for the future planning of load management and power generation schemes. In order to achieve this outcome, the following key areas would need to be developed:

- Generalisation of the stochastic component of the solar radiation model with respect to the known annual average values. This would enable the realistic assessment of the available solar resource at another major city in the UK, if the only available data were the monthly average daily solar radiation value.

- Assessment of the applicability of the Fourier interpolation technique used in the energy consumption models, to monthly mean wind speed data. This data is readily available and would remove some of the location dependence in the wind model procedure. The results of this could be used as part of the Wavelet model for generating wind speed data.

- Testing of the modelling procedure for the Wavelet coefficients for a number of key locations around the UK. This could lead to the development of a database of parameters that could be used to generate accurate synthetic time series of wind speed data.

- Generalisation of the stochastic component of both the energy consumption models. The procedure for estimating the annual trend can currently be applied to any location and building in the UK. The technique used for modelling the stochastic component could be applied to other locations but more data would be required to assess its applicability.

- Develop the energy models further to obtain typical diurnal domestic load profiles. As the hourly profile of domestic electricity consumption varies both seasonally, and from weekdays to weekends, a simple procedure for estimating these different profiles should be investigated. If these profiles can be estimated based on a daily mean value, then the diurnal profiles could be related to the daily energy consumption model proposed in Chapter 5,

allowing for a more realistic estimation of the variation in the domestic electricity consumption. Once these different profiles are obtained, then a more detailed comparison between the consumption and the diurnal renewable resource availability could be carried out. This would provide a greater understanding of the potential energy matching from renewable systems, and would provide more detailed information about the proportion of the domestic load that could be met over the year.

- Development of a statistical model and distribution model from the energy surplus/deficit analysis for the PV, wind and combined PV and wind renewable energy systems. This would allow for a simple method for estimating how well numerous sizes of small – scale renewable systems match a desired domestic demand, for any location.

The procedures demonstrated in this project have the potential to be expanded for a number of other dwellings, and offices, with the aim of ultimately assessing the potential contribution of distributed generation schemes to the UK energy mix.

## REFERENCES

## CHAPTER 2 REFERENCES


1. BP.BP Statistical Review of World Energy June 2009. [Online] Available from: http://bp.com/statisticalreview
2. Department of Trade and Industry. *Energy White Paper: Meeting the Energy Challenge*. BERR. The Stationary Office; 2007
3. DEFRA. *The Environment in Your Pocket*. National Statistics; 2008
4. Solomon S, Qin D, Manning M, Chen Z, Marquis M, et al. *Contribution of Working Group I to the fourth Assessment Report of the Intergovernmental Panel on Climate Change*. Cambridge University Press; 2007
5. The Scottish Government. *Renewables Action Plan*. The Scottish Government; 2009. [Online] Available from: www.scotland.gov.uk/Publications/2009/07/06095830/0
6. Renewable Energy Statistics Database for the UK [Online] Available from: www.restats.org.uk/electricity
7. The Scottish Government. [Online] Available from: www.scotland.gov.uk/About/scotPerform/indicators/electricity
8. World Wind Energy Association. World Wind Energy Report 2008. WWEA; 2009
9. BWEA. Small Wind Systems UK Market Report 2009. BWEA; 2009
10. Sagrillo M. Apples and Oranges 2002 Choosing a Home-sized wind generator. *Home Power Magazine*. 2002; 90
11. The Energy Savings Trust [Online] Available from: www.energysavingstrust.org.uk
12. Committee on Climate Change. *Building a Low-carbon Economy The UK's Contribution to Tackling Climate Change*. CCC; 2008
13. Davidson S. *National Survey Report of PV Power Applications in United Kingdom 2007, International Energy Agency Co-operative Programme on Photovoltaic Power systems, Task 1 Exchange and Dissemination of Information on PV Power Systems*. IEA; 2008
14. Peacock S (ed.). *Small scale solar electric (photovoltaics) energy and traditional buildings*. English Heritage; 2008
15. Mustoe JE. *An Atlas of Renewable Energy Resources: In the United Kingdom and North America*. Chichester: John Wiley and Sons;
16. Sfetsos A. A comparison of various forecasting techniques applied to mean hourly wind speed time series. *Renewable Energy*. 2000; 21(1). pp 23-35
17. Lei M, Shiya L, Chuanwen J, Hongling L, Yan Z. A review on the forecasting of wind speed and generated power. *Renewable and Sustainable Energy Reviews*. 2004; 13 (4). pp 915-920

18. Jebaraj S, Iniyan S. A review of energy models. *Renewable and Sustainable Energy Reviews*. 2006; 10 (4). pp281-311
19. Commission of European Communities. *European Solar Radiation Atlas Volume 1 Global Radiation on Horizontal Surfaces*. Verlag TUV Rheinland; 1984
20. Page J, Lebens R. *Climate in the United Kingdom*. London: Her Majesty's Stationery Office; 1986
21. Manwell JF, McGowan JG, Rogers AL. *Wind Energy Explained Theory, design and Application*. Chichester: John Wiley and Sons; 2002
22. Ross SM. *Introduction to Probability Models*. 8th Edition. Location: Academic Press; 2003
23. Johnson GL. *Wind Energy Systems*. Prentice-Hall; 1985
24. Celik AN. Energy output estimation for small-scale wind power generators using weibull-representative wind data. *Journal of Wind Engineering and Industrial Aerodynamics*. 2003; 91(5). pp 693-707
25. Brett AC, Tuller S. The autocorrelation of hourly wind speed observations. *Journal of Applied Meteorology*. 1991; 30(6). pp 823-833
26. Harris RI. The macrometeorological spectrum-a preliminary study. *Journal of Wind Engineering and Industrial Aerodynamics*. 2008; 96(12). pp 2294-2307
27. Argiriou A, Lykoudis S, Kontoyiannidis S, Balaras CA et al. Comparison of methodologies for TMY generation using 20 years of data for Athens, Greece. *Solar Energy*. 1999; 66(1). pp 33-45
28. Jin Z, Yezheng W, Gang Y. Generation of typical solar radiation year for China. *Renewable Energy*. 2006; 31
29. De Miguel A, Bilbao J. Test reference year generation from meteorological and simulated solar radiation data. *Solar Energy*. 2005; 78(6). pp 695-703
30. Phillips WF. Harmonic analysis of climatic data. *Solar Energy*. 1984; 32(3). pp 319-328
31. Balling RC. Harmonic analysis of monthly insolation levels in the United States. *Solar Energy*. 1983; 31(3). pp 293-298
32. Baldasano JM, Clar J, Berna A. Fourier analysis of daily solar radiation data in Spain. *Solar Energy*. 1988; 41(4). pp 327-334
33. Dorvlo AS. Fourier analysis of meteorological data for Seeb. *Energy Conversion and Management*. 2000; 41(12). pp 327-324
34. Dorvlo AS, Ampratwum DB. Harmonic analysis of global irradiation. *Renewable Energy*. 2000; 20(4). pp 435-443
35. Salcedo AC, Baldasano JM. Fourier analysis of meteorological data to obtain a typical annual time function. *Solar Energy*. 1984; 32(4). pp 479-488
36. Zeroual A, Ankrim M, Wilkinson AJ. Stochastic modelling of daily global solar radiation measured in Marrakesh, Morocco. *Renewable Energy*. 1995; 6(7). pp 787-798

37. Sirdas S. Daily wind speed harmonic analysis for Marmara region in Turkey. *Energy Conversion and Management*. 2005; 46(7-8). pp 1267-1277
38. Shamshad A, Bawadi MA, Wan Hussin WM, Majid TA, Sanusi SA. First and second order markov chain models for synthetic generation of wind speed time series. *Energy*. 2005; 30(5). pp 693-708
39. Sahin AD, Sen Z. First order markov chain approach to wind speed modelling. *Journal of Wind Engineering and Industrial Aerodynamics*. 2001; 89. pp 263-269
40. Nfaoui H, Essiarab H, Sayigh AA. A stochastic markov chain model for simulating wind speed time series at Tangiers, Morocco. *Renewable Energy*. 2004; 29(8). pp 1407-1418
41. Brown BG, Katz RW, Murray A. Time series models to simulate and forecast wind speed and wind power. *Journal of Climate and Applied Meteorology*. 1984; 23(8). pp 1184-1195
42. Kamal L, Jafri YZ. Time series models to simulate and forecast hourly average wind speed in Quetta, Pakistan. *Solar Energy*. 1997; 61(1). pp 23-32
43. Poggi P, Muselli M, Notton G, Cristofari C, Louche A. Forecasting and simulating wind speed in Corsica by using an autoregressive model. *Energy Conversion and Management*. 2003; 44(20). pp 3177-3196
44. Torres JL, Garcia A, De Blas M, De Francisco A. Forecast of hourly average wind speed with ARMA models in Navarre (Spain). *Solar Energy*. 2005; 79(1). pp 65-77
45. Cryer JD. *Time Series Analysis*. Boston: PWS-Kent Publishing Company; 1986
46. Amato U, Andretta A, Bartoli B, Coluzzi B, Cuomo V, Fontana F, Serio C. Markov process and Fourier analysis as a tool to describe and simulate daily solar irradiance. *Solar Energy*. 1986; 37(3). pp 179-194
47. Aguiar R, Collares-Pereira M. Statistical properties of hourly global radiation. *Solar Energy*. 1992; 48(3). pp 157-167
48. Duffie JA, Beckman WA. *Solar Engineering of Thermal Processes*. 2nd Edition. New York: John Wiley and sons; 1991
49. Knight KM, Klein SA, Duffie JA. A methodology for the synthesis of hourly weather data. *Solar Energy*. 1991; 46(2). pp 109-120
50. Siddiqi AH, Khan S, Rehman S. Wind speed simulation using wavelets. *American Journal of Applied Sciences*. 2005; 2(2). pp 557-564
51. Bayazit M, Aksoy H. Using wavelets for data generation. *Journal of Applied Statistics*. 2001; 28(2). pp 157-166
52. Aksoy H, Toprak ZF, Aytek A, Erdem Ünal N. Stochastic generation of hourly mean wind speed data. *Renewable Energy*. 2004; 29(14). pp 2111-2131
53. Percival DB, Walden AT. *Wavelet Methods for Time Series Analysis*. Cambridge: Cambridge University Press; 2008

## CHAPTER 3 REFERENCES


1. Department of Trade and Industry. *Energy – Its Impact on the Environment and Society*. DECC; 2006
2. Department of Trade and Industry. *Energy Consumption in the United Kingdom*. BERR; 2002
3. Department of Energy and Climate Change. *Digest of United Kingdom Energy Statistics DUKES*. DECC. The Stationery Office; 2009
4. Shorrock LD, Utley JI. *Domestic Energy Fact File*. London: Building Research Establishment; 2003
5. Building Research Establishment. *Energy Use in Homes, A Series of Reports on Domestic Energy Use in England – Fuel Consumption*. Office of the Deputy Prime Minister; 2005
6. The Scottish Government. *Scottish Energy Study Volume 1 Energy in Scotland: Supply and Demand*; The Scottish Government; 2006 [Online] Available from: www.scotland.gov.uk/Publications/2006/01/1902748/0
7. Building Research Establishment. *Energy Use in Homes, A Series of Reports on Domestic Energy Use in England – Energy Summary*. Office of the Deputy Prime Minister; 2005
8. Scrase I. *White Collar $CO_2$, Energy Consumption in the Service Sector*. London: The Association for the Conservation of Energy; 2001
9. Energy Efficiency Best Practice Programme. *Energy Consumption Guide 19 – Energy Use in Offices*.
10. Department of Energy and Climate Change. *Maps Showing Domestic, Industrial and Commercial Consumption at local Authority Level*. Publication URN 09D/535
11. National Grid. BMRA Data, Metered half-hourly electricity demands. [Online] Available from: www.nationalgrid.com/uk/Electricity/Data/Demand+Data/
12. Al-Alawi SM, Islam SM. Principles of electricity demand forecasting part 1 methodologies. *Power Engineering Journal*. 1996; 10(3). pp 139-143
13. Hor C, Watson SJ, Majithia S. Analysing the impact of weather variables on monthly electricity demand. *IEEE Transactions on Power Systems*. 2005; 20(4). pp 2078-2085
14. Ranjan M, Jain VK. Modelling of electrical energy consumption in Delhi. *Energy*. 1999; 24(4). pp 351-361
15. Sailor DJ, Munõz JR. Sensitivity of electricity and natural gas consumption to climate in the USA – methodology and results for eight states. *Energy*. 1997; 22(10). pp 987-998
16. Valor E, Meneu V, Caselles V. Daily air temperature and electricity load in Spain. *Journal of Applied Meteorology*. 2001; 40(8). pp 1413-1421
17. Magnano L, Boland JW. Generation of synthetic sequences of electricity demand: application in South Australia. *Energy*. 2007; 32(11). pp 2230-2243

18. Dhar A, Reddy TA, Claridge DE. A Fourier series model to predict hourly heating and cooling energy use in commercial buildings with outdoor temperature as the only weather variable. *ASME Journal of Solar Engineering*. 1999; 121(1). pp 47-53
19. Bartels R, Fiebig DG. Metering and modelling residential end-use electricity load curves. *Journal of Forecasting*. 1996; 15(6). pp 415-426
20. Capasso A, Grattieri W, Lamedica R, Prudenzi A. A bottom-up approach to residential load modelling. *IEEE Transactions on Power Systems*. 1994; 9(2). pp 957-964
21. Yao R, Steemers K. A method of formulating energy load profiles for domestic buildings in the UK. *Energy and Buildings*. 2005; 37(6). pp 663-671
22. Balachandra P, Chandru V. Modelling electricity demand with representative load curves. *Energy*. 1999; 24(3). pp 219-230
23. Riddell AG, Manson K. Parameterisation of domestic load profiles. *Applied Energy*. 1996; 54(3). pp 199-210
24. Anderson BR. *BREDEM: BRE domestic energy model, background philosophy, and description.* Building Research Establishment Report. BRE; 1985
25. Larsen BM, Nesbakken R. Household electricity end-use consumption: results from econometric and engineering models. *Energy Economics*. 2004; 26(2). pp 179-200

## CHAPTER 4 REFERENCES


1. Muneer T. Lecturer. Personal Communication. 2003
2. Messenger RA, Ventre J. *Photovoltaic Systems Engineering*. 2nd Edition. London: CRC Press; 2004
3. Bracewell RN. *The Fourier Transform and its Applications*. 2nd Edition. USA: McGraw-Hill; 1986
4. Phillips WF. Harmonic analysis of climatic data. *Solar Energy*. 1984; 32(3). pp 319-328
5. Balling RC. Harmonic analysis of monthly insolation levels in the United States. *Solar Energy*. 1983; 31(3). pp 293-298
6. Baldasano JM, Clar J, Berna A. Fourier analysis of daily solar radiation data in Spain. *Solar Energy*. 1988; 41(4). pp 327-334
7. Dorvlo AS, Ampratwum DB. Harmonic analysis of global irradiation. *Renewable Energy*. 2000; 20(4). pp 435-443
8. Salcedo AC, Baldasano JM. Fourier analysis of meteorological data to obtain a typical annual time function. *Solar Energy*. 1984; 32(4). pp 479-488
9. Dorvlo AS. Fourier analysis of meteorological data for Seeb. *Energy Conversion and Management*. 2000; 41(12). pp 327-334
10. Zeroual A, Ankrim M, Wilkinson AJ. Stochastic modelling of daily global solar radiation measured in Marrakesh, Morocco. *Renewable Energy*. 1995; 6(7). pp 787-793
11. Cryer JD. *Time Series Analysis*. Boston: PWS-Kent Publishing Company; 1986
12. Jenkins GM, Watts DG. *Spectral Analysis and its Applications*. San Francisco: Holden-Day; 1968
13. Bendat JS. *Engineering Applications of Correlation and Spectral Analysis*. New York: Wiley; 1980
14. BADC. Met Office Land surface Data [Online] Available from: http://badc.nerc.ac.uk/; 2004
15. Manwell JF, McGowan JG, Rogers AL. *Wind Energy Explained Theory, Design and Application*. Chichester: John Wiley and Sons; 2002
16. Garcia A, Torres JL, Preito E, De Francisco A. Fitting wind speed distributions: a case study. *Solar Energy*. 1998; 62(2). pp 139-144
17. Celik AN. Weibull representative compressed wind speed data for energy and performance calculations of wind energy systems. *Energy Conversion and Management*. 2003; 44(19). pp 3057-3072
18. Johnson GL. *Wind Energy Systems*. Prentice-Hall; 1985
19. Box G. *Statistics for Experimenters: An Introduction to Design, Data Analysis and Model Building*. New York: Wiley; 1978

20. Yaffee RA. McGee M. *An Introduction to Time Series Analysis and Forecasting*. Elsevier; 2000
21. Aksoy H, Toprak ZF, Aytek A, Erden Unal N. Stochastic generation of hourly mean wind speed data. *Renewable Energy*. 2004; 29(14). pp 2111-2131
22. Bayazit M, Aksoy H. Using wavelets for data generation. *Journal of Applied Statistics*. 2001: 28(2). pp 157-166
23. Jensen A, la Cour-Harbo A. *Ripples in Mathematics The Discrete Wavelet Transform*. Berlin: Springer; 2001
24. Walker JS. *A Primer on Wavelets and their Scientific Applications*. London: Chapman and Hall/CRC; 1999
25. Percival DB, Walden AT. *Wavelet Methods for Time Series Analysis*. Cambridge: Cambridge University Press; 2008
26. Weiss NA. *Introductory Statistics.* 7th Edition. London: Pearson, Addison Wesley; 2005

## CHAPTER 5 REFERENCES


1. Robinson A. Personal Communication; 2006
2. Department of Trade and Industry. *Energy Consumption in the United Kingdom*. BERR; 2002
3. Shorrock LD, Utley JI. *Domestic Energy Fact File*. London: Building Research Establishment; 2003
4. Sellers D. *Using utility bills and average daily energy consumption to target commissioning efforts and track building performance. Proceedings of the First International Conference for Enhanced Building Operations, 2001, Jul 16-19; Texas, USA*. Energy Systems Laboratory, Texas A & M University; 2001
5. The Office of National Statistics. The UK 2000 Time Use Survey. 2002 [Online] Available from: www.statistics.gov.uk/TimeUse/
6. Sailor DJ, Munõz JR. Sensitivity of electricity and natural gas consumption to climate in the USA – methodology and results for eight states. *Energy*. 1997; 22(10). pp 987-998
7. Valor E, Meneu V, Caselles V. Daily air temperature and electricity load in Spain. *Journal of Applied Meteorology*. 2001; 40(8). pp 1413-1421
8. Weron R, Kozlowska B, Nowicka-Zagrajek J. Modelling electricity loads in California: A continuous-time approach. *Physica A: Statistical Mechanics and its Applications*. 2001; 299(1-2). pp 344-350
9. Beggs C. *Energy: Management, Supply and Conservation*. Oxford: Butterworth-Heinemann; 2002
10. Moss KJ. *Energy Management and Operating Costs in Buildings*. London: E & FN Spon; 1997
11. Uglow CE. The calculation of energy use in dwellings. *Building Services Engineering Research and Technology*. 1981; 2(1). pp 1-14
12. Riddell AG, Manson K. Parameterisation of domestic load profiles. Applied Energy. 1996; 54(3). pp 199-210
13. Epstein ES. On obtaining daily climatological values from monthly means. *Journal of Climate*. 1991; 4. pp 365-368
14. Rymes MD, Myers DR. Mean preserving algorithm for smoothly interpolating averaged data. *Solar Energy*. 2001; 71(4). pp 225-231
15. Cryer JD. *Time Series Analysis*. Boston: PWS-Kent Publishing Company. 1986
16. Yannos S. *Solar Energy and Housing Design Volume 1: Principles, Objectives, Guidelines*. Architectural Association Publications, DTI; 1994

17. Chartered Institute of Building Services Engineers. *CIBSE Guide Volume A: Design Data*. London: The Chartered Institute of Building Services Engineers; 1986

## CHAPTER 6 REFERENCES


1. Iqbal M. *An Introduction to Solar Radiation*. New York: Academic Press; 1983
2. Duffie JA, Beckman WA. *Solar Engineering of Thermal Processes*. 2nd Edition. New York: John Wiley and sons; 1991
3. Sukhatme SP, Nayak JK. Solar Energy: Principles of Thermal Collection and Storage. 3rd Edition. Dehli: Tata-McGraw Hill; 2008
4. Noorian AM, Moradi I, Kamali GA. Evaluation of 12 models to estimate hourly diffuse irradiation on inclined surface. *Renewable Energy*. 2008; 33(6). pp 1406-1412
5. Nijmeh S, Mamlook R. Testing of two models for computing global solar radiation on tilted surface. *Renewable Energy*. 2000; 20(1). pp 75-81
6. Zeroual A, Ankirm M, Wilkinson AJ. The diffuse-global correlation: its application to estimating solar radiation on tilted surfaces in Marrakesh, Morocco. *Renewable Energy*. 1996; 7(1). pp 1-13
7. Department of Trade and Industry. *Photovoltaics in Buildings A Design Guide*. DT1; 1999
8. Strong SJ, Scheller WG. *The Solar Electric House*. Massachusetts: Sustainability Press; 1993
9. Eiffert P, Kiss GJ. *Building-Integrated Photovoltaic Designs for Commercial and Institutional Structures: A Sourcebook for Architects and Engineers*. DOE; 2000
10. Manwell JF, McGowan JG, Rogers AL. *Wind Energy Explained Theory, Design and Application*. Chichester: John Wiley and Sons; 2002
11. Gipe P. *Wind Energy Basics A Guide to Small and Micro Wind Systems*. USA: Chelsea Green Publishing Company; 1999
12. BWEA. *Small Wind Systems UK Market Report 2009*. BWEA; 2009
13. Twidell J, Weir T. *Renewable Energy Resources*. 2nd Edition. Oxon: Taylor and Francis; 2006
14. Deshmukh MK, Deshmukh SS. Modeling of hybrid renewable energy systems. *Renewable and Sustainable Energy Reviews*. 2008; 12(1). pp 235-249
15. Sagrillo M. Apples and Oranges 2002 Choosing a Home-sized wind generator. *Home Power Magazine*. 2002; 90
16. Owen P. *The Rise of the Machines A review of energy using products in the home from the 1970's to today*. Energy Savings Trust; 2006
17. Mansouri I, Newborough M, Probert D. Energy Consumption in UK households: impact of domestic electrical appliances. *Applied Energy*. 1996; 54(3). pp 211-285
18. Department of Trade and Industry. *Energy Consumption in the United Kingdom*. BERR; 2002

19. Fawcett T, University of Oxford, Environmental Change Institute, Energy and Environment Programme. *Lower Carbon Futures for European Households*. Oxford: Environmental Change Institute; 2000
20. Household Energy Consumption. [Online] Available from: www.carbonfootprint.com/energyconsumption/html
21. UK Energy Research Centre. Electricity user load profiles by profile class. Energy Data Centre, UKERC [Online] Available from: http://data.ukedc.rl.ac.uk/browse/edc/Electricity/LoadProfile/data
22. The Office of National Statistics. The UK 2000 Time Use Survey. 2002. [Online] Available from: www.statistics.gov.uk/TimeUse/
23. de Almedia A, Fonseca P, Schlomann B, Feilberg N, Ferreira. *Residential Monitoring to Decrease Energy Use and Carbon Emissions in Europe*. Project REMODECE, EIE; 2009
24. Anderson BR. *BREDEM: BRE domestic energy model, background philosophy, and description.* Building Research Establishment Report. BRE; 1985
25. Sidler O. *Demand-side Management End-use Metering Campaign in the Residential Sector. European Community SAVE Programme*. Contract No. 4.1031/93.58. Final Report. 1995
26. EURECO. *End-use Metering campaign in 400 Households of the European Community. Project EURECO*. European Commission; 2002
27. Feed-in Tariffs. [Online] Available from: www.fitariff.co.uk
28. Davidson S. *National Survey Report of PV Power Applications in United Kingdom 2008, International Energy Agency Co-operative Programme on Photovoltaic Power systems, Task 1 Exchange and Dissemination of Information on PV Power Systems*. IEA; 2009
29. Chapman PF. A Geometrical model of dwellings for use in simple energy calculations. *Energy and Buildings*. 1994; 21. pp83-91
30. House Condition Surveys Team Communities Scotland. *Scottish House Condition Survey 2002*. Scottish Executive; 2002
31. The Carbon Trust. *Small-scale Wind Energy Policy Insights and Practical Guidances*. The Carbon Trust. 2008
32. Dutton AG, Halliday JA, Blanch MJ. *The Feasibility of Building-Mounted/Integrated Wind Turbines (BUWTs): Achieving their potential for carbon reduction*. Energy Research Centre, CCLRC. The Carbon Trust. 2005
33. Peacock AD, Jenkins D, Ahadzi M, Berry A, Turan S. Micro wind turbines in the UK domestic sector. *Energy and Buildings*. 2008; 40. pp 1324-1333
34. Encraft. Warwick Field Trials 2009; Encraft; 2009

# APPENDICES

## APPENDIX A1

## COMPARISON OF SOLAR RADIATION TYPICAL ANNUAL TIME FUNCTION STATISTICAL PARAMETERS

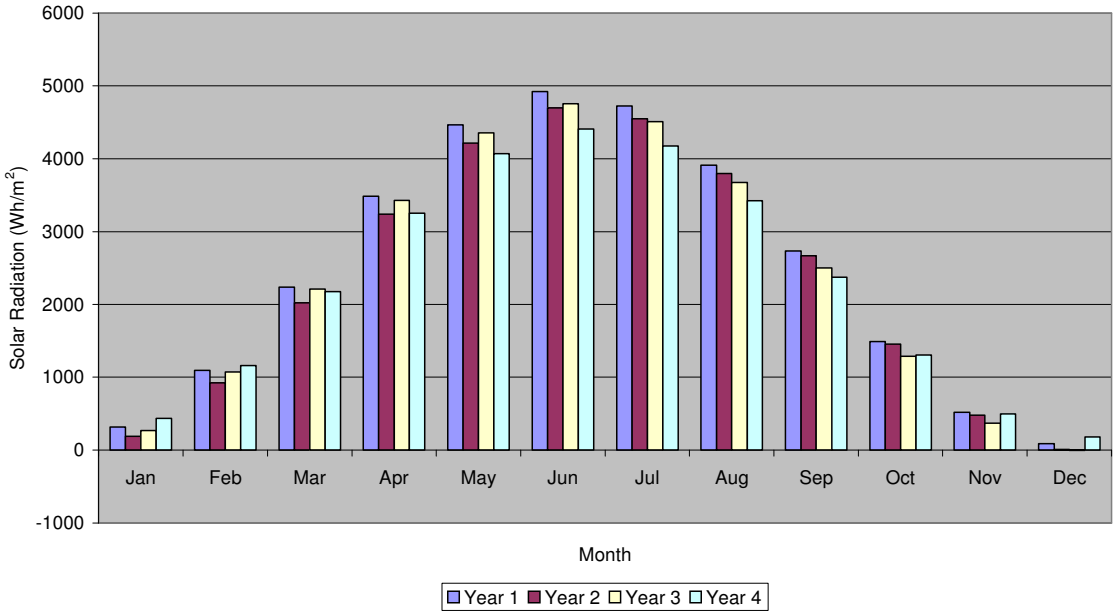


Figure A1.1: Comparison of Monthly Mean Values for Solar Radiation TAF'S

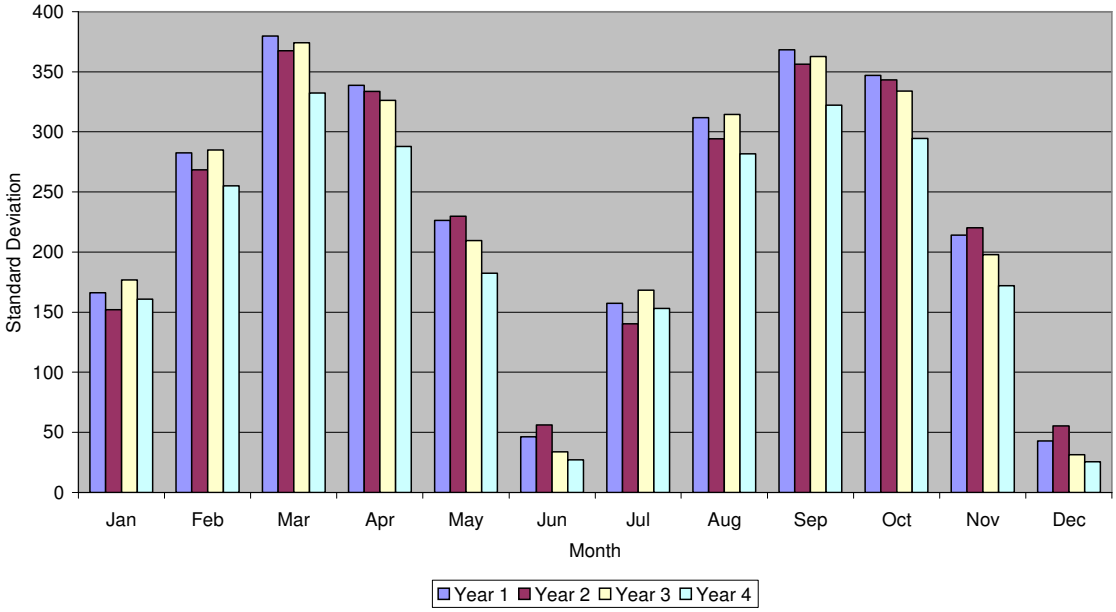


Figure A1.2: Comparison of Monthly Standard Deviation Values for Solar Radiation TAF'S

## APPENDIX A2

## MONTHLY WEIBULL PARAMETERS OBTAINED FROM HOURLY WIND SPEED DATA

| | Year 1 | | Year 2 | | Year 3 | | Year 4 | | Year 5 | |
|---|---|---|---|---|---|---|---|---|---|---|
| **Month** | k | c | k | c | k | c | k | c | k | c |
| Jan | 2.143 | 7.761 | 1.964 | 6.793 | 2.492 | 5.239 | 1.905 | 5.445 | 2.078 | 5.458 |
| Feb | 2.178 | 5.993 | 2.204 | 5.493 | 1.816 | 3.358 | 1.781 | 4.079 | 2.463 | 5.502 |
| Mar | 2.366 | 6.362 | 1.988 | 7.029 | 2.028 | 6.839 | 2.515 | 6.473 | 2.285 | 7.390 |
| Apr | 1.996 | 6.629 | 1.891 | 5.441 | 1.946 | 6.671 | 2.205 | 4.728 | 2.076 | 5.606 |
| May | 2.757 | 7.162 | 2.126 | 5.350 | 1.956 | 4.361 | 1.828 | 4.181 | 2.034 | 5.018 |
| Jun | 2.526 | 5.725 | 2.893 | 4.059 | 2.004 | 5.603 | 1.942 | 5.136 | 1.897 | 4.546 |
| Jul | 3.216 | 4.737 | 2.532 | 3.583 | 2.217 | 4.599 | 1.946 | 5.398 | 1.943 | 3.934 |
| Aug | 2.927 | 4.378 | 2.124 | 3.327 | 1.591 | 4.106 | 2.064 | 4.387 | 1.981 | 4.189 |
| Sep | 2.157 | 6.128 | 1.969 | 5.441 | 2.353 | 6.195 | 2.022 | 5.598 | 2.066 | 6.049 |
| Oct | 1.833 | 5.048 | 1.866 | 4.925 | 1.781 | 6.359 | 2.057 | 4.567 | 2.383 | 5.683 |
| Nov | 2.067 | 6.435 | 1.810 | 4.605 | 1.663 | 6.385 | 2.042 | 6.849 | 1.935 | 5.695 |
| Dec | 2.366 | 6.362 | 2.167 | 4.185 | 1.936 | 5.947 | 2.112 | 6.376 | 1.781 | 6.017 |

## APPENDIX A3

## COMPARISON OF AVERAGE DAILY GAS CONSUMPTION VALUES PER MONTH

The following table of values contains the three-year average daily gas consumption values for the dwelling example used in this project. The calculated average consumption values were calculated assuming an average base temperature of 16°C over the year, and a average heat loss coefficient of 276W/°C.

| Month | Actual Average Consumption (kWh/day) | Calculated Average Consumption (kWh/day) |
|---|---|---|
| Jan | 135.265 | 139.612 |
| Feb | 137.353 | 139.748 |
| Mar | 127.812 | 119.231 |
| Apr | 99.411 | 109.040 |
| May | 70.522 | 78.461 |
| Jun | 49.503 | 47.895 |
| Jul | 36.866 | 27.513 |
| Aug | 39.024 | 37.705 |
| Sep | 44.718 | 58.086 |
| Oct | 74.480 | 88.658 |
| Nov | 116.955 | 115.672 |
| Dec | 135.800 | 139.748 |

The average daily gas consumption values can also be calculated using degree-day data for the location of the dwelling. The average consumption, $E_m$, for any month can be calculated from:

$$E_m = \frac{H \times \text{Degree}-\text{days}}{\eta}$$

where H is the average design heat loss coefficient. Assuming a value of 276W/°C for the design heat loss, a 20 year average degree-day value for January of 356, and a boiler efficiency of 70%, the average gas consumption is:

$$E_m = \frac{276 \times 356}{0.7} = 140.366 \quad \text{kWh}/\text{day}$$

This procedure can be repeated for the remaining months.

## APPENDIX A4

## COMPARISON OF DAILY WIND ENERGY ESTIMATION

| Wind Speed (m/s) | Energy Available (kWh/m$^2$) |
|---|---|
| 4.231 | 0.0093 |
| 4.197 | 0.0091 |
| 4.230 | 0.0092 |
| 4.148 | 0.0087 |
| 4.227 | 0.0093 |
| 4.268 | 0.0095 |
| 4.338 | 0.0104 |
| 4.492 | 0.0111 |
| 4.767 | 0.0132 |
| 5.049 | 0.0157 |
| 5.316 | 0.0184 |
| 5.490 | 0.0202 |
| 5.635 | 0.0219 |
| 5.769 | 0.0235 |
| 5.693 | 0.0226 |
| 5.495 | 0.0203 |
| 5.461 | 0.0199 |
| 5.157 | 0.0168 |
| 5.031 | 0.0156 |
| 4.773 | 0.0133 |
| 4.478 | 0.0110 |
| 4.327 | 0.0099 |
| 4.213 | 0.0092 |
| 4.170 | 0.0089 |
| | **$\sum$ 0.337kWh/m$^2$** |

Assuming a mean wind speed of 4.629m/s, the daily energy available per unit area (based on eq. (6.6)) for a small wind turbine is:

$$E = 12 \times 1.225 \times 0.2 \times (4.629)^3 = 0.292 \text{kWh/m}^2$$

Demonstrating that the energy calculated using the daily mean wind speed is lower than the amount calculated over the typical day.